2018

Identification of Cancer Stem Cells: Applications for a Spy1 Clinical Trial

Ellen Marie Laurie
University of Windsor

Identification of Cancer Stem Cells: Applications for a Spy1 Clinical Trial

By

Ellen M. Laurie

A Thesis
Submitted to the Faculty of Graduate Studies
through the Department of Biological Sciences
in Partial Fulfillment of the Requirements for
the Degree of Master of Science
at the University of Windsor

Windsor, Ontario, Canada

2018

Identification of Cancer Stem Cells:
Applications for a Spy1 Clinical Trial

by

Ellen M. Laurie

APPROVED BY:

_____

L. Freeman
Faculty of Nursing

_____

J. Hudson
Department of Biological Sciences

_____

L. Porter, Advisor
Department of Biological Sciences

February 7, 2018

DECLARATION OF CO-AUTHORSHIP

I hereby declare that this thesis incorporates material that is result of joint research, as follows:

This thesis incorporates the outcome of a joint research undertaken in collaboration with Dr. Rosa Ferraiuolo, Anne Semaan, and Dr. Mohammed Bourouh under the supervision of Dr. Lisa Porter. This collaboration is covered in Figures 2 and 3 of this thesis. The data analysis, statistical analysis, graphing results, interpretation, and writing were performed by the author. The contribution of Dr. Rosa Ferraiuolo was primarily through the determination of drug concentrations, covered in Figures 2 and 3, and determination and provision of key ideas, primary contributions, experimental designs, and technical assays for Figure 3. Anne Semaan contributed to the technical assays in Figure 3. Dr. Mohammed Bourouh contributed to the design and key ideas of the ALDH reporter constructs.

I am aware of the University of Windsor Senate Policy on Authorship and I certify that I have properly acknowledged the contribution of other researchers to my thesis, and have obtained written permission from each of the co-author(s) to include the above material(s) in my thesis.

I certify that, with the above qualification, this thesis, and the research to which it refers, is the product of my own work.

I declare that, to the best of my knowledge, my thesis does not infringe upon anyone's copyright nor violate any proprietary rights and that any ideas, techniques, quotations, or any other material from the work of other people included in my thesis, published or otherwise, are fully acknowledged in accordance with the standard referencing practices. Furthermore, to the extent that I have included copyrighted material that surpasses the bounds of fair dealing within the meaning of the Canada Copyright Act, I certify that I have obtained a written permission from the copyright owner(s) to include such material(s) in my thesis.

I declare that this is a true copy of my thesis, including any final revisions, as approved by my thesis committee and the Graduate Studies office, and that this thesis has not been submitted for a higher degree to any other University or Institution.

ABSTRACT

Triple-negative breast cancer is considered the most aggressive subtype of breast cancer; while patients respond well to initial treatment the tumour relapse rate in patients is approximately 1 in 3. There is increasing evidence for a small population of cells that are able to evade treatment and repopulate the tumour after treatment, called cancer stem cells. Understanding key factors in cancer stem cell resistance is important to decrease tumour relapse. In a Spy1 clinical trial, responses to treatment and *in vitro* and *in vivo* to a standard of care treatment are investigated. Spy1 is an atypical cyclin-like regulator that enhances cellular proliferation. Spy1 overexpression has been implicated in cancer stem cell population and drug resistance, in other forms of cancer. The role of Spy1 in resistance to treatment has yet to be elucidated in triple-negative breast cancer (TNBC) cells; however, we have established the knockdown of Spy1 sensitizes cells to treatment. The current standard of care for TNBC is a combination of AC/T. When mimicking clinical treatment *in vitro* and *in vivo*, with standard of care with or without carboplatin, a population of cells remain viable after treatment. Detoxification enzymes, like aldehyde dehydrogenase (ALDH), have enhanced expression in cancer stem cell populations; thereby, ALDH can be used as a marker to identify and isolate cancer stem cells. This study outlines the creation and validation of an ALDH reporter system to identify cancer stem cells in heterogeneous triple-negative breast cancer cell lines. Elucidating characteristic of drug-resistant populations, such as expression of Spy1 and ALDH, can provide insight into drug-resistance and tumour relapse.

ACKNOWLEDGEMENTS

I would like to extend my gratitude to Dr. Lisa Porter, my supervisor, for providing me this opportunity. I have gained many valuable skills, and enhanced others, that I would not be able to elsewhere. I thank you for your patience and understanding all through-out this degree. Your interest in all the facets of science is truly inspiring.

Thank you to my committee members, Dr. John Hudson and Dr. Laurie Freeman, for your time, guidance and input.

Thank you to Dr. Andrew Swan for support during my degree, allowing me to use lab space for cloning and use of antibodies. It's my pleasure to be an honourary member of the Swan lab.

Thank you to Linda Sterling, Melissa Gabrieau, Des Overdulve, Ingrid Churchill, Rodica Leu, Bob Hodge, and Nancy Barkley – you truly are the foundation of the biology building and we couldn't do anything without your hard work.

Thank you to Ingrid Qemo for virus production, Dr. Elizabeth Fidalgo da Silva for running flow cytometry/cell sorting experiments, Dr. Rosa Ferraiuolo for *in vivo* collaborations and thesis review, Annie Semaan for *in vivo* collaborations, Dr. Bre-Anne Fifield for help troubleshooting the ALDELFUOR™ kit and thesis review and Dr. Mohammed Bourouh for assistance with all cloning and thesis review. Thank you to the rest of the Porter Lab members, your support through this degree is appreciated.

Big thanks goes out to my lab families, BioFamily and LabTings, for making everyday of my degree brighter. It's amazing to have such a supportive group of friends; I truly thank you for all the laughs and fun times together.

Lastly, thank you to Redha Mohammed Bourouh and Ingrid Qemo. The two of you have helped me endlessly through this degree. I cannot express my gratitude to you for your kindness, guidance and empathy. I come out of this degree with two amazing friends, whom I will always cherish.

TABLE OF CONTENTS

LIST OF TABLES

LIST OF FIGURES

LIST OF ABBREVIATIONS/SYMBOLS

ABC…..…… ATP-binding cassette

AC……doxorubicin plus cyclophosphamide

AC/T….……...paclitaxel after doxorubicin plus cyclophosphamide

ALDH…….aldehyde dehydrogenase

ALDH1A1-dTomato……pHIV- ALDH1A1- dTomato

ALDH1A1-eGFP…….....pHIV- ALDH1A1-eGFP

ALDH1A3-eGFP ……...pHIV-ALDH1A3-eGFP

BCSC…….breast cancer stem cell

BCL-2……..……B-cell lymphoma 2

Ca…….carboplatin

CD……...cluster of differentiation

Cdk...…….……..cyclin-dependent kinase

CKI…….. cyclin-dependent kinase inhibitor

CSC……..cancer stem cell

DDR……..DNA-damage repair

DEAB……diethylaminobenzaledehyde

DFS……...disease-free survival

dpf……..……..days post-fertilization

DMEM……..Dulbecco's modified Eagle's medium

DMSO……..dimethyl sulfoxide

EF-1α.…….elongation factor-1α

(e)GFP…….(enhanced) green-fluorescent protein

ER……..estrogen receptor

ESA……...epithelial specific antigen

FACS……...fluorescence-activated cell sorting

HER2……..…….… human epidermal growth factor 2

IC50 ……..……...…….…….inhibitory concentration of 50%

Lin…….lineage markers

Mammocult™ media ……Mammocult™ Basal Medium Human

MaSC……..mammary stem cell

OS…… overall survival

PBS…..……...phosphate buffered solution

pCR……..pathological complete response

PCR…….. ……...polymerase chain reaction

PR……progesterone receptor

qRT-PCR……..…….Quantitative Real-Time polymerase chain reaction

RA……..retinoic acid

RAR…….retinoic acid receptor

RQ……..relative quantification

shRNA……..short hairpin RNA

siRNA…….short interfering RNA

Spy1……Spy1A

SOC……..standard of care

T±Ca……..paclitaxel with/without carboplatin

TNBC……triple-negative breast cancer

wt……wild-type

INTRODUCTION

I. Prevalence of Breast Cancer

Breast cancers are the most common cancers in Canadian women and the 3rd most common overall (Canadian Cancer Statistics Advisory Committee, 2017). Canadian females are more likely to develop breast cancer than any other type of cancer, with 1 in 8 females developing breast cancer at some point in their lifetime (Canadian Cancer Statistics Advisory Committee, 2017). Breast cancer accounts for approximately 25.8% of all new cancer cases in women, approximately 25,700 females in Canada alone (Canadian Cancer Statistics Advisory Committee, 2017). Women comprise approximately 99% of all breast cancer cases; suggesting a link between the development of the mammary gland and breast cancer incidence (Canadian Cancer Statistics Advisory Committee, 2017). In both Canada and the United States of America, breast cancer incidence rates declined around 2002, with numbers stabilizing from 2004-2010 (Canadian Cancer Statistics Advisory Committee, 2017; Edwards et al., 2014). Breast cancer deaths have continued to decline due to breast cancer screening, decrease use of hormone therapies and advances in breast cancer treatment (Autier et al., 2011; Bleyer and Welch, 2012; Kricker et al., 1995). The five-year relative survival rate for breast cancer has increased reaching 79-87% in 2016, with survival rates increasing with decreasing grade (Canadian Cancer Statistics Advisory Committee, 2017). Research into factors important in cancer initiation, progression and response to treatment will continue to improve breast cancer statistics.

II. An Overview of the Mammary Gland

Given that breast cancer is a predominantly female disease (Canadian Cancer Statistics Advisory Committee, 2017), the unique features of mammary development of the female gland may provide critical insight for the initiation and progression of breast cancer. Mammalian female breasts, or mammary glands, are very dynamic and undergo the majority of growth and development postnatally. The mammary gland is a network of epithelial cells, connective tissue, adipocytes, fibroblasts, and extracellular matrix that undergo changes in response to hormonal cues and growth factors (Malhotra et al., 2010). Within the mammary gland network, there are important morphological features that are necessary to produce milk (Malhotra et al., 2010; Visvader and Stingl, 2014). A mature gland contains alveoli, hollow spherical structures comprised of epithelial cells, that produce and secrete milk into the lumen (Malhotra et al., 2010; Visvader and Stingl, 2014). Several alveoli group together form lobules; lobules connect to a shared lactiferous duct which transports produced milk to the nipple, by way of contractile myoepithelial cells (Malhotra et al., 2010; Visvader, 2009). These types of mammary cells are thought to be organized in a hierarchy where the initial mammary gland develops from a single multipotent fetal mammary stem cell (MaSC) (Spike et al., 2012; Visvader and Stingl, 2014).

The concept of MaSCs was introduced when random fragments of the mammary gland were serially transplanted into a cleared fat pad of mice and rats and the functional gland reformed, indicating regenerative potential (Daniel et al., 1968). MaSCs are important in establishing the mature gland at puberty and for maintenance of the gland and expansion during pregnancy (Dontu et al., 2003; Liu et al., 2005). MaSCs are found

within highly heterogeneous populations of long and short-term populating cells (Asselin-Labat et al., 2010; Visvader and Lindeman, 2006). More differentiated progenitor cells are sometimes described as an intermediate cell between stem cells and the differentiated target cell; they are able to form one or more types of cells down a specific cell lineage, but cannot divide indefinitely (Malhotra et al., 2010; McDermott and Wicha, 2010). The type and number of stem and progenitor cell populations within the mammary gland is still under investigation and requires further research; however, there are established luminal and myoepithelial progenitor populations (Visvader and Lindeman, 2006; Visvader and Stingl, 2014). Differentiated myoepithelial progenitor cells form mature myoepithelial cells that produce the basement membrane surrounding the gland and contractile cells for milk expulsion (Visvader and Lindeman, 2006; Visvader and Stingl, 2014). Mature ductal and alveolar cells are formed from myoepithelial progenitor cells. Interestingly, when luminal progenitor cells were transplanted into the cleared fat pad of mice, they were able to reconstitute the entire gland showing that the hierarchy of cells is not necessarily a unidirectional progression from MaSC to mature differentiated cell (Visvader and Stingl, 2014). It is important to note, however, that not all cells have the capacity to form a functioning mammary gland, specifically more differentiated cells (Neville et al., 1998). Progression down the hierarchy of MaSC results in cells with less potency.

III. Adult Stem Cell Characteristics

Stem cells possess many qualities that allow for their longevity: the capacity for self-renewal and differentiation, increased anti-apoptotic and detoxification mechanisms, and the ability to enter a temporary dormant state. To be considered an adult stem cell, a cell

must possess the ability to self-renew and differentiate into multiple progeny lineages (Morrison and Kimble, 2006). Tissue homeostasis is highly dependent on stem cell populations that balance asymmetric and symmetric cell division. Asymmetrical division results in two daughter cells of two different fates that allow for tissue maintenance throughout the lifespan of the organism (Morrison and Kimble, 2006). Symmetric cell division results in two daughter cells that are genetically identical to the parent, thereby expanding the stem cell pool, also known as self-renewal (He et al., 2009; Morrison and Kimble, 2006). Both modes of division are essential for maintaining a pool of stem cells that can divide during the wound repair process or at important developmental times (Prockop et al., 2003; Rojas et al., 2005; Slack, 2008). Due to their necessity in tissue maintenance, stem cells require mechanisms, such as anti-apoptotic factors and enhanced telomerase activity, to evade cell death through their lifetime (Allsopp et al., 1992; Blalock et al., 1999; Reya et al., 2001; Yui et al., 1998). Over time, stem cells can be exposed to and resist many forms of endogenous and exogenous stressors including, alcohols, vitamins, lipids, and environmental toxins and agents, respectively (Bettinardi et al., 2012; Dontu et al., 2003; Reya et al., 2001; Tu et al., 2002). To prevent accumulation of dangerous agents, detoxification mechanisms are important to decrease the risk of mutations. Additionally, stem cells are able to evade damage through a temporary reversible exit of the cell cycle, termed quiescence. Quiescence is a mechanism that allows stem cells to exit the cell cycle, not incurring damage as a result of cellular division.

Numerous assays are utilized to examine the functional characteristics of stem cells. Stem cells are primarily isolated by using known stem cells markers, alone or in

combination with each other. Further validation of these stem cell populations has been highlighted using lineage tracing, transplantation assays and mammosphere formation assays. Lineage tracing is a method of using fluorescent detection used to monitor the fate of a potential stem cell; daughter cells retain the label from the marked parent cell, allowing identification of progeny (described in (Hayakawa et al., 2015; Schepers et al., 2012)). Lineage tracing can be used in combination with transplantation assays, where one, or a population, of potential stem cells are injected *in vivo* to assess tumour-formation potential (Illa-Bochaca et al., 2010). Originally modelled in the brain using 'neurosphere formation assays' (Weiss et al., 1996), sphere-formation assays utilize anchorage-independent conditions to select for or expand populations of stem and progenitor cells *in vitro* (Louis et al., 2008). Differentiated normal epithelial cells undergo apoptosis when in anchorage-independent conditions, as they require adhesion to survive and proliferate (Askari et al., 2003; Krause et al., 2001; Reynolds and Weiss, 1996; Simian et al., 2001; Weiss et al., 1996). Stem and progenitor cells will remain viable and form 3-dimensional spheres of cells. Details within these assays differ depending on the tissue of study, speaking to differences in the biology of adult stem cell populations, an area of science that requires much more work.

IV. Cancer Stem Cells

Similar to adult stem cells, a small population of malignant cells with stem-like characteristics exist within many forms of cancer (Heppner, 1984). The cancer stem cell (CSC) model supports the hypothesis that this small population of stem-like cells can generate a heterogeneous tumour. This hierarchical model suggests CSCs give rise to all malignant cells comprising a tumour (Sleeman et al., 2006; Stingl et al., 2001, 2005;

Villadsen et al., 2007; Wicha et al., 2006). This model is supported by data demonstrating that not all cells have the ability to form a tumour; however, a single CSC transplanted into immunodeficient mouse recapitulated an entire heterogeneous tumour (Shackleton et al., 2006; Sleeman et al., 2006; Stingl et al., 2006). Evidence for differentiation capacity was demonstrated when CSCs cued to differentiate produced cells with varying proliferative potential and phenotypes (Kleinsmith and Pierce, 1964). Additionally, self-renewal potential was evaluated when single CSCs or colonies were selected and placed into micro-wells and they were able to repopulate the well (Buick et al., 1979). CSCs are highly implicated in tumour recurrence as in driving tumourigenesis; protection of the population is critical for the long-term survival of a tumour.

Similar to normal stem cells, CSCs have several mechanisms of protection that mimic those in adult stem cells. Quiescent CSCs resist cytotoxic agents and may repopulate a tumour after treatment, whereas actively dividing CSCs drives progression of cancer (Chen et al., 2012). Ishikawa et al. found dormant human leukemia cancer cells in the bone marrow of transplanted mice (Ishikawa et al., 2007). CSCs have increased expression of anti-apoptotic proteins and drug pumps that protect the integrity of the cell (reviewed in (Clevers, 2011)). CSC populations vary within the different forms of cancer and have implications for treatment, prognosis, and tumour relapse.

V. Breast Cancer Stem Cell Populations in Genetic Subtypes

While initially discovered in the blood (Spangrude et al., 1988), CSCs have been described in many solid cancers including, but not limited to, brain, colon, head and neck, lung, and breast (reviewed in (O'Brien et al., 2009)). In the breast, data supports that breast cancer can be initiated by the malignant transformation of normal mammary stem

cells or progenitor populations (Dontu et al., 2003). Malignant stem-like cells specific to the breast were isolated and verified for the first time in 2003, termed breast cancer stem cells (BCSC) (Al-Hajj et al., 2003). Like other CSCs, BCSCs and progenitor cells show resistance to therapies – chemotherapy, targeted therapies, radiation therapy; a proposed mechanism for cancer relapse post-treatment (Dontu et al., 2003; Li et al., 2008; Phillips et al., 2006; Reya et al., 2001; Tu et al., 2002; Zielske et al., 2011).

Differences in the cell of origin of the subtypes of breast cancer is a possible explanation for variation in gene expression profiles and overall prognosis. Gene expression profiles eluted to at least five distinct subtypes of breast cancer: luminal A or B, human epidermal growth factor receptor 2 (HER2)-overexpressing, basal-like, and claudin-low (Perou et al., 2000). Debate exists for a potential 6^{th} type of breast cancer, called normal-like breast cancer, that accounts for less than 10% of all breast cancer cases (Fan et al., 2006; Perou et al., 2000). The inclusion of additional data, like single nucleotide polymorphisms and copy number variants have resulted in the further subdivision of classes to upward of 10 distinct forms of breast cancer (Curtis et al., 2012).

Normal-like breast cancers have a much more favourable prognosis for patients compared to all other subtypes (Perou et al., 2000). Luminal A breast cancers have a favourable prognosis for patients in initial responses to treatment; whereas luminal B breast cancers respond well to treatment but are at a higher risk for relapse (Dontu et al., 2004; Sørlie et al., 2001). A third type of luminal cancer exists, luminal C, however, is considered a subtype of luminal A and luminal B due to expression of genes, whose function is not yet known (Sørlie et al., 2001). HER2-overexpressing breast cancers have elevated levels of the HER2 receptor, are highly proliferative, have a poor prognosis for

patients with an overall lower survival rate (Sørlie et al., 2001). Basal-like breast cancers represent approximately 10-15% of all breast cancer cases and are difficult to treat (Gusterson, 2009). Basal-like cancers are often affiliated with an aggressive form of breast cancer that is classified on receptor status, triple-negative breast cancers (TNBC). It is important to note that not all basal-like breast cancers are triple-negative and not all TNBC are basal-like. TNBC is characterized by the absence or extremely low levels of estrogen receptor (ER), progesterone receptor (PR), and HER2 receptors. TNBCs are very aggressive and patients are at a high risk for tumour relapse (Perou et al., 2000). TNBC encompasses several subtypes, most commonly in basal-like breast cancers, but also normal-like and claudin-low (Kumar and Aggarwal, 2016). Lastly, claudin-low breast cancers have low levels of claudins involved in cell-cell and cell-membrane adhesion (Gusterson, 2009). Claudin-low breast cancers are associated with poor prognosis as evidence suggests they are relatively resistant to conventional chemotherapies (Prat et al., 2010).

Differences in the stem cell population may provide information about the origin of these different subtypes of breast cancer. It is reasonable that luminal B, HER2-overexpressing, and basal-like breast cancers, some of the more difficult to treat, are derived from similar progenitor populations, as they have common gene alterations (Dontu et al., 2004; Liu et al., 2016). Luminal B breast cancers had signatures most like bipotent-enriched progenitor cells (Liu et al., 2016). CSCs in HER2-overexpressing cancers most resembles bipotent-enriched progenitor cells (Liu et al., 2016). Basal-like breast cancer gene signatures are most similar to bipotent-enriched progenitor cells or mature luminal cells (Liu et al., 2016). Luminal A breast cancers have gene signatures

similar to luminal progenitor or mature luminal cells, of which it is thought to be derived (Liu et al., 2016). Claudin-low breast cancers are thought to be derived from the mammary stem cell population; making these heterogeneous tumours difficult to treat (Prat et al., 2010). The aforementioned subtypes have varying levels of established stem cell and progenitor populations (Ricardo et al., 2011). Isolation of stem cells and progenitor cells are routinely performed via fluorescence active cell sorting (FACS) using known markers of stem/progenitor cells: cluster of differentiation (CD) proteins (CD44, CD24, CD133), epithelial cell adhesion molecule, lineage markers (Lin), epithelial specific antigen (ESA) and aldehyde dehydrogenase (ALDH) (Perou et al., 2000; Sotiriou et al., 2003; Stingl et al., 1998, 2001).

VI. Cluster of Differentiation Proteins as Markers of CSC

Presence, low or high, or absence of different markers of stemness are used to isolate desired subpopulations, based on previously established markers. CD proteins have been used extensively for the identification and isolation of subpopulations of cells. This has been particularly useful to analyze stem/progenitor populations that are fewer in number than the bulk of a tumour. CD44, a trans-membrane glycoprotein involved in cell adhesion, and CD24, a phosphatidylinositol-anchored glycoprotein, have been widely used in the literature in combination with other markers of stemness to isolate CSCs/progenitor cells (Aigner et al., 1997; Aruffo et al., 1990). When progenitor luminal B cells and differentiated luminal C cells from a heterogeneous population were sorted for $CD44^{high}$ and $CD24^{low}$ populations, both formed mammospheres; however, luminal B had greater forming efficiency, suggesting increased potency (Ghebeh et al., 2013). In another experiment, reduced CD44 expression with short-interfering RNA (siRNA) and

short hairpin RNA (shRNA) enhanced differentiation of the progenitor population (Pham et al., 2011).

The functional application of sorting with stem cell markers was examined when serial dilutions of human breast cancer cells, with the marker combination $ESA^{+}CD44^{+}CD24^{-/low}Lin^{-}$, was injected into immunocompromised mice; as few as 200 injected cells were able to form tumours on a consistent basis after 5-6 months (Al-Hajj et al., 2003). Cells sorted for $ESA^{-}CD44^{+}CD24^{-/low}Lin^{-}$ failed to form tumours even when 20,000 cells were injected (Al-Hajj et al., 2003). When secondary tumours were analyzed via flow cytometry ESA, CD44 and CD24 expression resembled the tumour from which they were derived (Al-Hajj et al., 2003). $ESA^{+}CD44^{+}CD24^{-/low}Lin^{-}$ cells passaged through four rounds of tumour formation had no decrease in their tumourigenicity (Al-Hajj et al., 2003), suggesting that their tumourigenic capacity is similar to that of normal stem cells (Al-Hajj et al., 2003). Clinically, Lin et al. showed that the cell surface markers $CD44^{high}$ and $CD24^{-/low}$ negative correlated with disease-free survival (DFS) and overall survival (OS), and positively correlated with cancer recurrence (Lin et al., 2012). While evidence demonstrated that for $CD44^{high}$ and $CD24^{-/low}$ selects for a tumourigenic subpopulation of cells, others found that they are better indicators of relapse when used with a marker of stemness (Zhong et al., 2014).

VII. Aldehyde Dehydrogenase –A Marker of Stemness

ALDHs are a family of $NAD(P)^{+}$-dependent enzymes. The family of 19 isoenzymes are ubiquitously distributed in adult tissues to protect cells by catalyzing aldehyde oxidation to carboxylic acids (Bettinardi et al., 2012; Chen et al., 2013; Kiefer et al., 2012). Several isoforms of ALDH (notably ALDH1A1, ALDH1A2, ALDH1A3 and ALDH8A1)

function in the retinoic acid (RA) signalling pathway (Collins and Watt, 2008; Marcato et al., 2011a; Rexer et al., 2001). Through a series of stages retinol (vitamin A1) is oxidized to RA, with ALDH1 facilitating the final oxidation step (Duester et al., 2003; Marchitti et al., 2008). RA can bind to the retinoic acid receptor (RAR) and mediate gene expression and cellular differentiation (Figure 1) (Duester et al., 2003; Elizondo et al., 2009). A negative feedback mechanism controls ALDH expression. Due to its ability to detoxify harmful agents, it is not surprising ALDH expression is present in both normal and cancerous tissues.

Originally used as a marker of normal stem/progenitor cells in neural stem cells, ALDH became useful in identification of CSC populations in a disease like multiple myeloma and acute myeloid leukemia (Hess et al., 2004, 2006; Matsui et al., 2004). ALDH became an important enzyme in several clinical applications; where high expression of ALDH had value in predicting metastasis, prognosis and was correlated with poor patient outcome (Balicki, 2007; Charafe-Jauffret et al., 2010; Ginestier et al., 2007; Liu et al., 2014; Marcato et al., 2011b). Interestingly, suppression of specific isoforms of ALDH found in blood cancers by all-*trans* retinoic acid showed that drove differentiation of CSCs and increased sensitivity to cyclophosphamide (Fenaux et al., 1992; Sanz and Lo-Coco, 2011). This demonstrated that targeting specific isoforms of ALDH could increase sensitivity to drugs, to which CSCs are highly resistant.

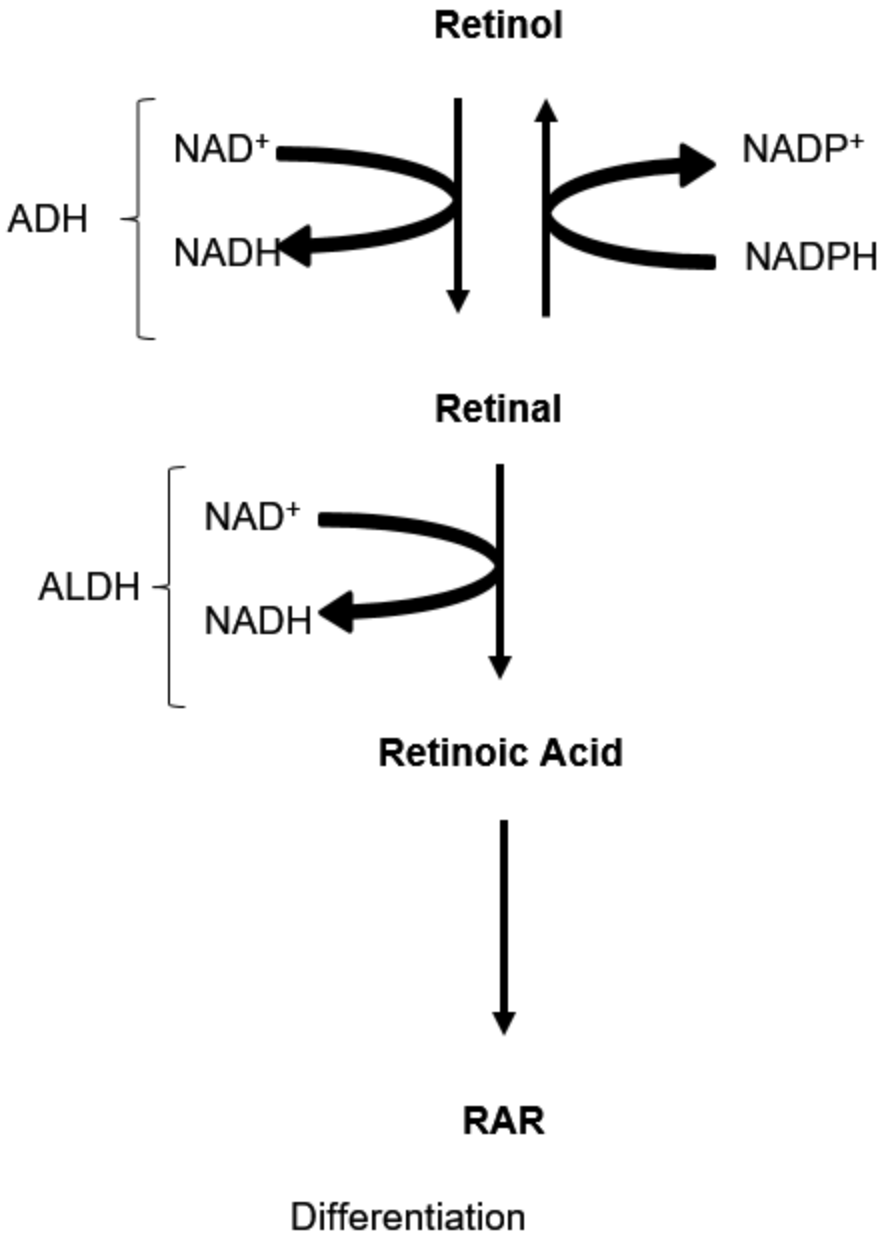

Figure 1: Retinol oxidation to retinoic acid. Retinol is reversibly oxidized by alcohol dehydrogenase (ADH) to retinal. Retinal is irreversibly oxidized by aldehyde dehydrogenase (ALDH) to retinoic acid.

The role of ALDH1 in breast cancers was identified in 2007 by Ginestier et al. when they established ALDH1 as a marker of normal and cancerous human MaSC (Ginestier et al., 2007). ALDH expression varied in different subtypes of breast cancers where drug-sensitive subtypes had the lowest expression and drug-resistant subtypes had the highest expression (Ricardo et al., 2011). A clinical role for ALDH was established when ALDH1 expression in patient tissues positively correlated with poor clinical outcome and prognosis, supported by several additional studies (Charafe-Jauffret et al., 2010; Ginestier et al., 2007; Marcato et al., 2011a; Morimoto et al., 2009; Neumeister et al., 2010; Resetkova et al., 2010; Sophos and Vasiliou, 2003; Zhou et al., 2010). Additionally, all-*trans* retinoic acid used in breast cancer treatment with chemotherapy, but not on its own, was effective in regulating apoptosis, cell growth and differentiation (Elizondo et al., 2000; Moreb et al., 2005). Numerous other studies confirmed that ALDH1 expression in tumour cells is associated with stem-like characteristics, clonal capacity, and drug resistance (Ginestier et al., 2007; Ikawa et al., 1983; Magni et al., 1996). Specific isoforms ALDH1A1 and ALDH1A3 play an important role in RA production in the breast (Collins and Watt, 2008). To determine the effects of ALDH1 isozyme expression on characteristics of cancer, Croker et al. used siRNAs targeted against ALDH1A1 and ALDH1A3. Knockdown of ALDH1A3 demonstrated no variation in proliferation or chemotherapy/radiation sensitivity but decreased cell adhesion and migration *in vivo*, suggesting importance in metastasis (Croker et al., 2017). The knockdown of ALDH1A1 decreased cellular proliferation, adhesion, migration *in vivo* and increased sensitivity to multiple classes of chemotherapy drugs and radiation (Croker et al., 2017). These findings suggest that ALDH1A1 is important in therapy resistance in

breast cancer cells, supporting clinical data where ALDH1A1 correlated with poor prognosis in breast cancers (Charafe-Jauffret et al., 2010; Ginestier et al., 2007; Khoury et al., 2012; Morimoto et al., 2009). Studies of ALDH1A1 and ALDH1A3 suggest their different, but important, roles to consider for patient prognosis.

To identify ALDH expression in cells, Storms et al. developed the ALDEFLUOR™ Assay (Storms et al., 1999). BODIPY-aminoacetaldehyde diffused into viable cells is converted by ALDH to a fluorescing BODIPY-aminoacetate substrate and trapped inside the cell (Figure 2A). Highly fluorescent cells are indicative of high expression of ALDH (Storms et al., 1999). Populations are sorted via (FACS) and compared to a control containing diethylaminobenzaldehyde (DEAB), an inhibitor of many ALDH isoenzymes (Figure 2B) (Alexa et al., 2009; Bunting and Townsend, 1996; Moreb et al., 2008; Storms et al., 1999). It is presumed that the ALDEFLUOR™ assay measures activity from the ALDH1 family (STEMCELL Technologies, 2009). Based on several studies, the ALDEFLUOR™ assay recognizes other ALDH isoenzymes (Moreb et al., 2008; Morgan et al., 2015; Wu et al., 2016).

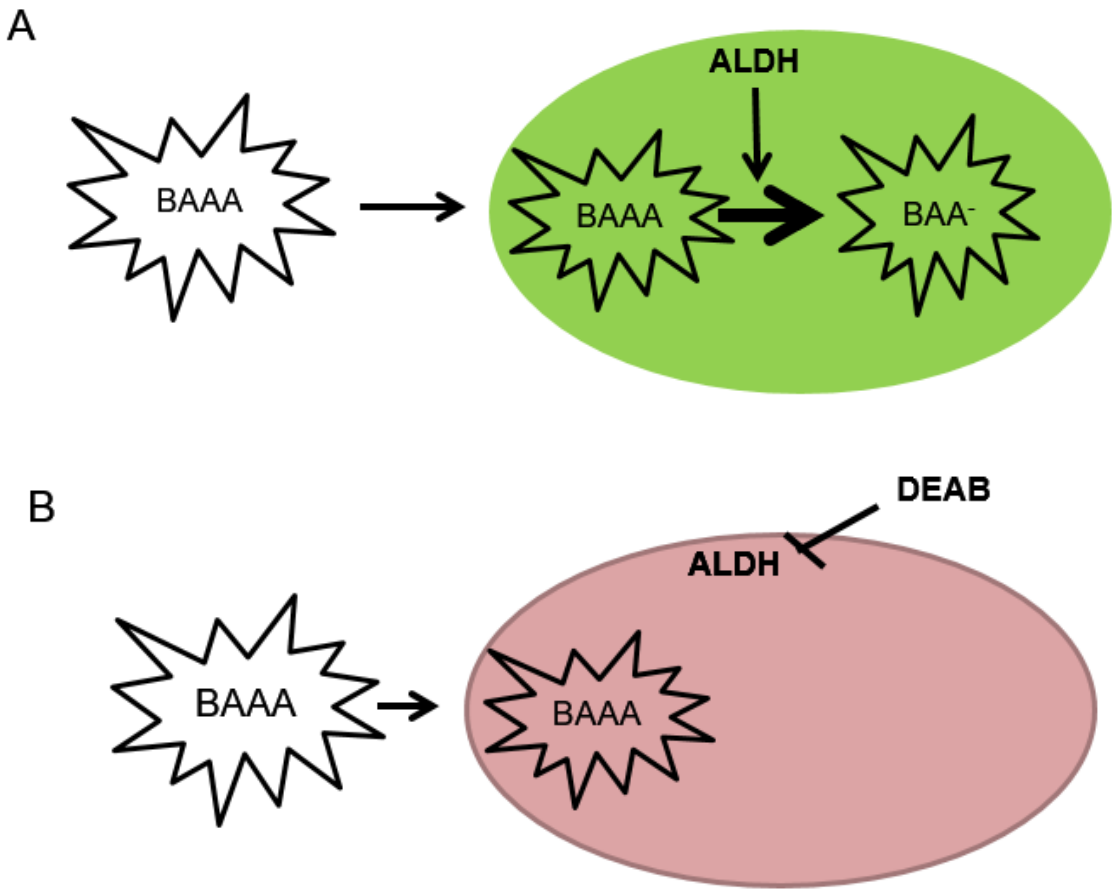

Figure 2: Schematic of ALDEFLUOR™ Assay. (A) ALDH acts to breakdown BAAA into substrate BAA^- that fluoresces. (B) DEAD inhibits the breakdown of BAAA to BAA^- by inhibiting ALDH.

VIII. Drug Resistance in CSCs and Tumour-Initiating Populations

Drug resistance is thought to develop as an adaptive response to DNA-damage repair (DDR) or mutations. Clinically, the presence of drug-evading cells, namely CSCs, may result in an increased risk of recurrence, serving as a prognostic indicator for patient disease-free survival and prognosis for patients (André and Zielinski, 2012). Improvements in treatment can be made to decrease the risk of recurrence of cancers as mechanisms of drug-resistance are better understood. CSCs can resist the action of many drugs due to modifications of cellular mechanisms – drug transport modification, detoxification, pro-survival proteins, and alternative DNA damage responses (Dontu et al., 2003; Reya et al., 2001; Tu et al., 2002). Mechanisms to protect the cell from damage are necessary for the longevity of the CSC pool.

Expression of membrane proteins has been implicated in playing a role in drug resistance. ATP-binding cassette (ABC) transport proteins are involved in molecule transport across a plasma membrane and have been implicated in resistance by ejecting drugs from the cell (Fletcher et al., 2010). Acquired resistance models suggest that CSCs express drug transporters to survive chemotherapy, while differentiated cells are killed (Dean, 2009).

Additionally, detoxification enzymes are important in normal cells to protect against toxins; however, they play a negative role in breaking-down toxins that kill dangerous cells. CSCs have increased expression of detoxification enzymes to decrease the effectiveness of drugs within these populations (Manolitsas et al., 1997; Townsend and Tew, 2003). For example, ALDH is a detoxification agent and is highly expressed in

CSC populations of many tumour types (Clay et al., 2010; Duong et al., 2012; Dylla et al., 2008; Friedman et al., 1992; Hellsten et al., 2011; Sreerama and Sladek, 1997; Sullivan et al., 2010). Specific inhibitors of ALDH, for example, DEAB, sensitize $ALDH^{high}CD44^{+}$ populations to radiation and chemotherapy (Croker and Allan, 2012; Wickström et al., 2007). Detoxification mechanisms are supported by enhanced expression of pro-survival genes, where DNA can be repaired if damage occurred.

Pro-survival genes play an integral function in damaged cells and can lead to drug-resistance in CSC populations. BCL-2 expression, a protein involved in the balance of cell survival and apoptosis, impairs the ability to release pro-apoptotic proteins (Madjd et al., 2009; Verrier et al., 2004). In numerous cancers BCL-2 was overexpressed in CSC/progenitor populations and resulted in resistance to anti-cancer drugs; where the knockdown of BCL-2 in CSC/progenitor populations increased sensitivity to drugs (Konopleva et al., 2002; Madjd et al., 2009; Pham et al., 2011; Verrier et al., 2004). Enhanced pro-survival genes decreased apoptosis in CSC/progenitor populations; however, some damage to their DNA was present (Bao et al., 2006). DDR mechanisms allow for the cell to efficiently repair the damage allowing for cells to re-enter the cell cycle (Bao et al., 2006).

Inflicting significant amount of DNA damage to a cell to elicit an apoptotic response is the basis of anti-cancer treatments (Raguz and Yagüe, 2008). Cells have mechanisms to repair damaged DNA thereby decreasing the effectiveness of treatment. Many chemotherapies damage DNA through intra-strand, inter-strand, single-stranded, and double-stranded breaks (Deans and West, 2011). CSC and progenitor populations, in several cancers like breast and glioma, are known to have efficient DDR machinery (Bao

et al., 2006; Diehn et al., 2009). When CSCs were isolated from a breast tumour, transcriptome analysis shows upregulation of DDR-related genes indicating that CSCs have enhanced capacity to repair damage (Zhang et al., 2008). Treatments aim to inflict enough damage to the DNA to elicit a cell death response, as opposed to activation of DDR mechanisms.

IX. Current Strategies for Treating Breast Cancers

Strategies surrounding treatment of breast cancer is highly based on the subtype of breast cancer, proliferation status and receptor status. Surgery, radiation, chemotherapies and/or hormone therapies are often used in combination with each other to remove tumours and any remaining cancer cells (Al-Ejeh et al., 2011; Raguz and Yagüe, 2008). Targeted therapies are designed to block ERs and/or PRs, whose activation is known to stimulate transcription or pro-proliferative signal transduction pathways (Goldhirsch et al., 2011; Migliaccio et al., 1998; Prat et al., 2011). ER+ breast cancers, in general, are treated with selective estrogen receptor modulations and aromatase inhibitors to inhibit estrogen signalling (Dowsett and Haynes, 2003; Lumachi et al., 2013). Similarly, breast cancers that overexpress HER2 are targeted through direct binding to the HER2 receptor or suppression of HER2 kinase activity (Spector et al., 2005).

Breast cancers with the triple-negative phenotype are treated with combinations of surgery, radiation, and chemotherapy as they lack targets that are traditionally used in endocrine targeted therapies (Al-Ejeh et al., 2011; Raguz and Yagüe, 2008). TNBCs are very aggressive and have a higher risk of recurrence and death than non-TNBC (Burnell et al., 2008; Dent et al., 2007; Stockmans et al., 2008). Cytotoxic chemotherapies are

used to induce large amounts of DNA damage and activate apoptotic pathways in rapidly dividing cells (Raguz and Yagüe, 2008). Additional chemotherapies are often tested with standard treatments, also referred to as the standard of care (SOC), as an effort to increase efficacy. With these rigorous courses of treatment, many patients with TNBC exhibit peak tumour relapse within a 3-year period as opposed to other subtypes of breast cancer (Dent et al., 2007; Jatoi et al., 2011; Kennecke et al., 2010; Perou et al., 2000).

X. Current Treatment Options in TNBC

There are many areas of research working to improve treatments for patients with TNBC. Research emphasizing alternative targeted therapies for TNBC patients often fall short in clinical trials (Bonner et al., 2010; Heinemann et al., 2014; Pirker et al., 2009). Targeted therapies would be beneficial; however, TNBC patients significantly benefit from high dose chemotherapies in terms of event-free survival (Carey et al., 2012; Diallo-Danebrock et al., 2007; Gluz et al., 2008; Lang et al., 2013; Miller et al., 2007). Cell cycle dependence of some cytotoxic drugs highlights the importance of drug dose and timing of administration in the overall effectiveness of treatment.

Currently, many types of chemotherapeutic drugs are used independently or in combination with each other for treatment. Anthracyclines induce cell cycle arrest and apoptosis by binding to topoisomerase II-alpha and stabilizing DNA double-stranded breaks (Pommier et al., 2010; Weiss, 1992). Additionally, taxane drugs such as paclitaxel, in combination with anthracyclines, result in a higher pathological complete response (pCR), in TNBC, than anthracyclines alone (Liedtke et al., 2008; Rouzier et al., 2005; Sánchez-Muñoz et al., 2008). A common anthracycline-containing chemotherapy regimen first became popular by a National Surgical Adjuvant Breast and Bowel Project

for patients with node-positive TNBC; treatment is comprised of doxorubicin plus cyclophosphamide (AC) that is administered every 14-21 days (Fisher et al., 1990). AC treatment became the regimen standard due to its benefits of a decreased number of patient visits while still maintaining the effectiveness of other therapies (Fisher et al., 1990). A clinical trial by Mamounas et al., with 3060 patients, the addition of paclitaxel after AC treatment (AC/T) increased the 5-year DFS events to 76% ±2%, from 72% ±2% with only AC treatment, in node-positive breast cancers (Mamounas et al., 2005). Results from previous studies with the addition of paclitaxel, improved the standard of care (SOC) to an AC/T regimen; becoming an acceptable treatment for node-positive TNBC (Henderson et al., 2003; Mackey et al., 2013; Mamounas et al., 2005). In a follow-up stage III clinical trial, 234 TNBC patients received the full treatment of AC/T (doxorubicin 60mg/m^2 + cyclophosphamide 600mg/m^2 administered at 3-week intervals followed by weekly paclitaxel 80mg/m^2 for 12 weeks); beginning 3 weeks after the 4^{th} AC administration (Yardley et al., 2017); the 2- and 5-year DFS rates were high at 88.8 and 84.7%, respectively, and OS rates were 93.8 and 89.6%, respectively for patients receiving AC/T treatment (Yardley et al., 2017). Moreover, patients that exhibit lower pCR to anthracycline and/or taxane regimens have a high risk for relapse and a decrease in OS 3-5 years post-treatment (Cheang et al., 2009; Dent et al., 2007).

Current trials are exploring different combinations of drugs in addition to SOC chemotherapies in hopes of increasing pCR and DFS, which remains an important goal to be addressed. One category of drugs that have gained interest in treating TNBCs are platinum drugs. Platinum agents directly induce DNA damage by cross-linking DNA, preventing synthesis and are not metabolized into harmful by-products (Pruefer et al.,

2008; Rosenberg et al., 1969; Siddik, 2003; Wang and Lippard, 2005). For patients with a mutation in the BRCA1 gene, it has been demonstrated that platinum drugs increased pCR; cellular mechanisms involved in repairing double-strand breaks, created by platinum drugs, are compromised (Byrski et al., 2012; Tutt et al., 2001). Additionally, platinum drugs are effective in further increasing pCR when administered sequentially with anthracycline-/taxane-based chemotherapy regimens; studies show pCR up to 75% when cisplatin or carboplatin (Ca) was combined with anthracycline-/taxane-base neoadjuvant chemotherapy (Hurley et al., 2013; Sikov et al., 2009). Platinum-based therapies represent an option for TNBC patients to use in addition to SOC treatments and a possible strategy for overcoming drug resistance.

Current chemotherapies target actively dividing cells by damaging DNA at various stages in the cell cycle (Bharadwaj and Yu, 2004; Emadi et al., 2009; Hall and Tilby, 1992; Jordan and Wilson, 2004; Minotti et al., 2004). In the event of DNA damage a cell enters a state of repair and is unable to be targeted until it begins actively dividing again; therefore, ensuring there is enough time between chemotherapy cycles is necessary. It is essential to understand the role of cell cycle regulators and how these mechanisms may affect the efficacy of chemotherapy.

XI. Cell Cycle Regulation

The process of cellular division is outlined by distinct phases whose proper completion will result in two cells. The cell cycle has four stages: a phase of growth coined gap phase 1 (G1), a phase of DNA synthesis (S phase), a second gap phase (G2) and mitosis (M). Progression through phases of the cell-cycle is promoted by cyclin-dependent kinases (Cdks); whose activity level is altered during different phases of the cell cycle (Arellano

and Moreno, 1997; Nurse, 2002). Cdk protein levels remain constant throughout the cell cycle while their binding partners, cyclins, vary in protein levels, controlling Cdk-cyclin activity (Evans et al., 1983; Pines and Hunter, 1991). Cyclins interact with Cdks through binding at conserved regions of amino acids termed as the "cyclin-box" (Noble et al., 1997). In the absence of cyclins, active sites of Cdks are blocked by the T-loop resulting in an inactive form (Russo et al., 1996). Typically, Cdk catalytic domains remain inactive until bound by a cyclin that induces a conformational change but does not result in full activation of the Cdk (Kim and Sharpless, 2006; Malumbres and Barbacid, 2009; Sherr, 1996). Full activation is dependent on Cdk activating kinase that acts on the Cdk to phosphorylate a threonine residue found on the T-loop of the Cdk and dephosphorylation of inhibitory residues (Jeffrey et al., 1995; Paulovich and Hartwell, 1995). Various cyclin-Cdk complexes form throughout cell cycle and aid in its progression. For example, cyclin E binds with Cdk2 at the G1/S transition and cyclin A binds with Cdks 2 in S phase (Girard et al., 1991; Ohtsubo et al., 1995; Walker and Maller, 1991). Mechanisms are in place throughout the cell cycle to ensure proper Cdk activation. Cdk activity can be counteracted by Cdk kinase inhibitors (CKIs) proteins that act to regulate cyclin-Cdk complexes or Cdk activity alone through inhibition (Sherr and Roberts, 1999). CKIs block the adenosine triphosphate region on the Cdk; thereby, controlling the activity of cyclin-Cdk complexes and cellular division at specific stages in the cell cycle (Sherr and Roberts, 1999). Tumour cells acquire genetic mutations that alter expression of Cdks, cyclins, CKIs, Cdk substrates, activating enzymes and checkpoint proteins are implicated in the misregulation of the cell cycle (Malumbres and Barbacid, 2009; McDonald and El-Deiry, 2000; Sherr, 1996; Sherr and Roberts, 1999). Currently, therapies are being

developed that act in the same manner as CKIs, inhibiting the cell cycle. Since several noncanonical protein regulators are important in normal and cancer cell proliferation, further investigation into typical and atypical cyclin-Cdk complexes are needed, to increase the effectiveness of CKIs and cell-cycle targeting drugs for patients (Nebreda, 2006).

XII. Spy1 – An Atypical Cell Cycle Regulator

Spy1A1 (also called Speedy, RINGO, Spy1A; herein referred to as Spy1) was originally discovered in a cDNA screen to identify genes to rescue a *rad1* resistant strain of *Schizosaccharomyces pombe* when subjected to UV or gamma irradiation (Lenormand et al., 1999). *Xenopus* Speedy and the human homolog Spy1A1 possess 40% homology (Porter et al., 2002). In humans, Spy1 is encoded by the SPDYA gene on chromosome 2 and is a member of the Speedy/RINGO family of proteins (Cheng et al., 2005). The Speedy/RINGO family of proteins all have a conserved Speedy/RINGO box that facilitates interactions with Cdk 2 at the G1/S phase transition as well as Cdk1 at G2/M (Cheng et al., 2005). Spy1 also does not display sequence homology to cyclin proteins, displaying a unique role in the progression of the cell cycle (Karaiskou et al., 2001). Spy1 binds and fully activates Cdk1 and Cdk2 independent of classic phosphorylation on the T-loop (Karaiskou et al., 2001). Spy1 has been shown to phosphorylate $p27^{Kip1}$ at Thr187 and tags it for degradation allowing the cell cycle to progress (Karaiskou et al., 2001). Spy1 enhances cellular proliferation and inhibits checkpoint activation, allowing for cell cycle progression even in the presence of DNA damage (Gastwirt et al., 2006).

Spy1 overexpression leads to resistant phenotypes and decreased sensitivity to many agents utilized in cancer therapies (Barnes et al., 2003). In glioblastoma multiforme, a very aggressive form of brain cancer, there was positive staining for Spy1 in 72.8% of patient glioma samples (n=70) (Lubanska and Porter, 2017). Patient samples with elevated levels of Spy1 had an overall lower survival rate than those without elevated Spy1 (Lubanska and Porter, 2017). A multivariate analysis presented Spy1 as one of the highest independent predictor of survival, second to tumour grade (Lubanska and Porter, 2017). Additionally, Spy1 plays a role in maintaining stemness in glioma tumour-initiating populations (Lubanska et al., 2014). The knockdown of Spy1 in glioma cell lines shows a reduction in proliferation, stem cell marker CD133, and other stemness properties (Lubanska et al., 2014). The role of Spy1 in brain cancers leads to speculation about its role in other Spy1-elevated cancers.

In human breast cancer cell lines, Spy1 protein levels were found to be elevated (Al Sorkhy et al., 2012). Overexpression of Spy1 was also implicated in accelerated tumour formation *in vivo* (Golipour et al., 2008). Additionally, in a study where ER+ Spy1-overexpressing breast cancer cells were treated with tamoxifen cell numbers increased where their control counterpart failed to proliferate (Ferraiuolo et al., 2017). An *in vivo* xenograft model using *Danio rerio,* herein referred to as zebrafish, demonstrated Spy1s importance in treatment resistance. Spy1-overexpressing cells had decreased sensitivity to tamoxifen treatment in comparison to their control counterparts, when treated *in vivo* (Ferraiuolo et al., 2017). The role of Spy1 in breast cancer stem cells needs to be further investigated, specifically in more aggressive forms like TNBC.

XIII. *In vitro* and *In vivo* Model Systems to Study Breast Cancer

Breast cancer cell lines are a valuable tool for assessing the molecular and biological similarities between breast cancer subtypes (Charafe-Jauffret et al., 2009a; Neve et al., 2006). Currently, there are 51 cells lines and primary breast tumours whose karyotypes remain quite stable throughout many divisions in cell culture (Neve et al., 2006). Several studies have used gene expression data to outline that breast cancer cell lines can be molecularly classified into the 5 classic genomic subtypes of breast cancer discussed previously (Hollestelle et al., 2010; Kao et al., 2009; Neve et al., 2006). Cell lines contain functional CSCs that are capable of forming mammospheres in culture and tumours when injected into mice (Charafe-Jauffret et al., 2009b). While the mouse is the classical model for cancer studies, the zebrafish has gained traction in the last few decades as an alternative system for drug screens and translational medicine (Blackburn and Langenau, 2014; Veinotte et al., 2014). Approximately 70% of human genes have a zebrafish orthologue and 70% of zebrafish genes have a human orthologue (Howe et al., 2013; Vilella et al., 2009). Cost of starting and maintaining colonies are much cheaper than mouse counterparts due to less equipment needed, a large number of offspring, quick maturity to adulthood and decreased maintenance costs (Lieschke and Currie, 2007; White et al., 2013). Human cells are also able to be injected without rejection as the zebrafish acquired immune system is not active until approximately 21-30 days post fertilization (dpf) when B cells and T cells begin to form (Lam et al., 2004; Willett et al., 1999). In addition to these advantages, zebrafish embryos are transparent, making imaging easy until pigmentation inhibits such imaging. Zebrafish have been of interest in translational medicine as a method of drug screening of patient tissues, where tissues are

transplanted and drugs are added directly to the water and absorbed by the fish (Veinotte et al., 2014). Xenotransplantation of human tumours and the study of them is, therefore, increasingly feasible.

XIV. Summary of Research

A clinical trial investigating the role of Spy1 in triple-negative breast cancers in patient overall survival and tumour relapse is underway at Windsor Regional Hospital (Hamm, 2011). The study will accrue 90 patients with TNBC where they will undergo surgery then combination chemotherapy treatment in an adjuvant setting using a SOC regimen. Protein and mRNA will be analyzed from patient tumours by utilizing proteomics, microarray analysis and immunohistochemistry. Patients receive treatment with AC/T+Ca. Spy1 trial patients will receive dose-dense AC for 4 cycles followed by T±Ca with Ca administration on even-numbered cycles (Figure 1A). A portion of the extracted tumour will be embedded in paraffin for a tissue microarray assay. The fresh tissue will be sent for genomic profiling and lab analysis. Data from multiple *in vitro* and *in vivo* models, genomic profiling, tissue microarray data will be correlated to 5-year survival data (Figure 1B). Optimization of dose and timing of drug administration *in vitro* and *in vivo* is essential in determining the validity of these tools to act as pre-treatment indicators of response to a chemotherapy regimen in TNBC cells. Manipulation of the levels of Spy1 prior to treatment will also elucidate its implication in treatment resistance. The study hypothesizes that amplification of Spy1 will correlate with clinical resistance, and that manipulation of Spy1 will sensitize CSC populations to treatment *in vitro* and *in vivo*.

Objective 1: Establish a treatment protocol to best mimic patient treatment, *in vitro* and *in vivo*. The cell line, MDA-MB-231, was utilized as a model of TNBC. Cell response to AC/T+Ca will be analyzed in a heterogeneous population of TNBC cells, by assessing cell viability *in vitro.* Cells were also injected into zebrafish, and treated with the AC/T+Ca. A measure of tumour burden before and after AC/T+Ca treatment with MDA-MB-231 cells will establish a protocol of treatment for future patient samples. Spy1 is implicated in resistance to standard of care treatment as we know it plays a role in resistance to tamoxifen treatment in ER+ breast cancers (Ferraiuolo et al., 2017).

Objective 2: Validation of a reporter based system for ALDH detection for CSC identification. Using TNBC breast cancer cell line, MDA-MB-231 cells, drug-sensitive/resistant standards must be established for use *in vitro* and *in vivo* in which to compare patient samples. While the use of the ALDEFLUOR™ assay is optimum for assessing patient samples, variability in results demonstrate that it requires further optimization. To validate results from the ALDEFLUOR™ assay, a reporter-based system for the stem cell marker ALDH1 was designed and is currently being validated to answer questions about resistance to treatment in CSC populations.

The CSC model of initiation and progression of breast cancer carries significant implications for resistance in TNBCs. The CSC model suggests that tumour-initiating populations have mechanisms that allow them to evade apoptosis in response to treatment. Identification and isolation of CSCs are vital in determining their current standard of care treatments; which may explain the high relapse rate in TNBCs. Since ALDH is a marker of CSCs, expression data of specific isoforms of ALDH may result in

a greater understanding of drug resistance and cancer characteristics, with greater reproducibility than that of an enzymatic-based assay.

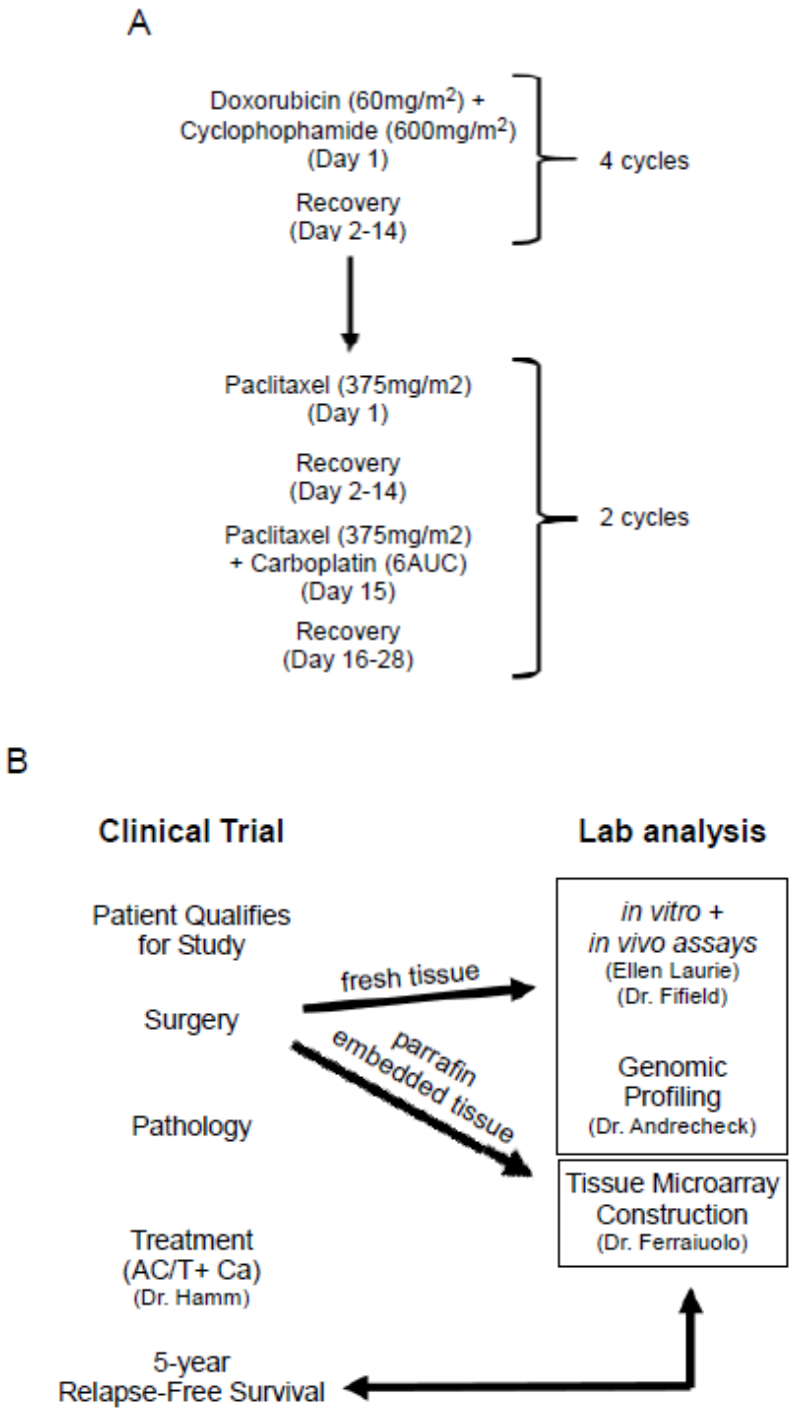

Figure 3: Schematic of Spy1 clinical trial. A) Schematic of chemotherapy administration to patients. (B) Schematic of collaboration for Spy1 trial.

MATERIALS & METHODS

I. Cell Lines Utilized

MDA-MB-231 wild-type (wt) cells were maintained in growth media containing Dulbecco's modified Eagle's medium (DMEM) (HyClone SH30022.01) supplemented with 10% fetal bovine serum (Gibco 10437028) and 1% penicillin and streptomycin (Invitrogen 15140148). Once cells reached 80-90% confluency, plates were washed with sterile 1X phosphate buffered solution (PBS) and collected by gentle pipetting. Cells were cultured in a 5% CO_2 environment.

MCF-7wt cells were maintained in DMEM supplemented with 10% fetal bovine serum and 1% penicillin and streptomycin. Once cells reached 80-90% confluency, plates were washed with sterile 1XPBS and 1mL of 0.05% trypsin in 1X PBS (Hyclone SH3023601) was added to the plate and incubated at 37°C for 3-4 minutes. Cells were cultured in a 5% CO_2 environment.

SK-BR-3 cells were maintained in McCoy's 5A media (ATCC 30-2007) supplemented with 10% fetal bovine serum and 1% penicillin and streptomycin. Once cells reached 60-70% confluency, plates were washed with sterile 1XPBS and 1mL of 1XPBS + 0.05% trypsin was as added to the plate and incubated at 37°C for 3-4 minutes. Cells were cultured in a 5% CO_2 environment.

II. Cell Viability Assay

MDA-MB-231wt cells were collected by centrifugation for 5 minutes at 1000rpm. Cells were counted using a hemocytometer and resuspended in 1mL of DMEM growth media.

Eight-thousand cells were seeded in a 12 well plate with 500µL of DMEM growth media. Twenty-four hours after seeding the growth media was removed and replaced with serum-free media reflecting the inhibitory concentration(s) of 50% (IC50) of the cells of doxorubicin plus cyclophosphamide (AC) was added to the wells. Twenty-four hours later, media containing AC was removed and DMEM growth media was added. Twenty-four hours later, growth media was removed and media reflecting the IC50s of paclitaxel and with or without carboplatin (T±Ca) was added for 24 hours. The same regimen was done with equal volumes of dimethyl sulfoxide/distilled water (DMSO)/diH_2O, to the drug counterpart, as a vehicle control. The vehicle control was controlling for the addition of carboplatin. The doses of each drug, the IC50s, are outlined in Table 1. Upon completion of the treatment regimen, cells were washed 3 times with 1XPBS and collected in 1mL of DMEM growth media. Cells were suspended and 50µL was transferred to a tube with 50µL of trypan blue and mixed well. Ten microliters of the cell/trypan blue suspension were added to a hemocytometer and viable cells were counted.

III. Zebrafish Drug Screening

i. Cell Labelling for use in Zebrafish Injection

Cells with knock-down Spy1 and its vector control were collected by centrifugation for 5 minutes at 1000rpm. Cells were counted using a hemocytometer and resuspended in serum-free DMEM to a final concentration of 500,000cells/ 500µL. 5µL of Vybrant™ Dil cell-labelling solution (ThermoFisher TV22885) was added to a concentration of 8µL/mL. Cells were mixed then incubated at 37°C for 45 minutes, mixing every 5-10 minutes. Fluorescence was confirmed via Leica CTR6500 microscope using AF software.

Table 1: Chemotherapeutic drugs utilized

Anti-cancer drug (Vehicle)	Doses used in treatment *(in vitro/in vivo*)	Product Number
Doxorubicin hydrochloride (DMSO)	0.025µM/0.25µM	D1515 Sigma-Aldrich
Cyclophosphamide monohydrate (DMSO)	6000µM/4mM	C0768 Sigma-Aldrich
Paclitaxel (DMSO)	0.1µM/1µM	T7402 Sigma-Aldrich
Carboplatin (diH_2O)	1250µM/500 µM	C2538 Sigma-Aldrich

Cells with a labelling efficiency of 85-90% were deemed sufficient for injection. If less than 85% of cells were successfully labelled, cells were incubated further and efficiency was checked again. Cells were washed, collected via centrifugation and resuspended in 50µL of serum-free DMEM media to a final concentration of 500,000 cells/50µL. Cells were incubated at 37°C until the injector is prepared. While injecting cells were kept on ice and resuspended prior to aspiration of media.

ii. Zebrafish Injection Protocol

Eggs were collected 2 hours post fertilization. Dead eggs, opaque in transparency, were removed from the rest. Healthy viable eggs were rinsed with 1X Hank's Buffered Saline Solution and stored in embryo media at 28°C. Dead fish were removed promptly. Three dpf healthy embryos –no skeletal abnormalities, steady pulse, and maintain homeostasis– were used for experiments. Any dishes containing protozoan that can harm embryos were not used in experiments. Embryos were anesthetized with 0.168mg/mL of ethyl 3-aminobenzoate methanesulfonate (Sigma-Aldrich E10521). In a blinded trial, colleagues Dr. Rosa Ferraiuolo and Annie Semaan injected labelled cells that were infected with knock-down Spy1 or its vector control. Cells at a concentration of 1000cells/µL were aspirated into a microinjection needle that has been tapered, for ease of injection. The cut site of the needle was standardized between every experiment to ensure consistency. Two nanolitres of labelled cell suspension were injected into the yolk sac of the zebrafish using a Nanoject II (Fisher Scientific) at 3dpf. Cells were given 24 hours to invade before treatment began. Treatment with AC/T+Ca was completed over 7 days and fish were imaged to assess tumour burden. Embryos were then imaged under a Leica fluorescence

stereo microscope (Leica MZ10 F) to confirm injection and placed into a single well of a 96-well plate containing embryo water for recovery.

iii. Drug Screening and Analysis in Zebrafish

Twenty-four hours post-injection fluorescent images of each embryo were taken for a pre-treatment measure of tumour burden (Day 0). After initial imaging (Day 0) embryo water containing AC was added to the wells. Twenty-four hours later, drug-containing water was removed and replaced with embryo water for 24 hours. Treatment with AC was repeated over the next 48 hours. Embryo water was removed and replace with embryo water containing T+Ca. Twenty-four hours later drug-containing water was replaced with equal volumes of embryo water. Treatment with T+Ca was repeated over the next 48 hours (Summarized in Figure 3A). DMSO/diH_2O treated fish acted as vehicle controls for each treatment Post-treatment fluorescent images were taken immediately after the final treatment (Day 7). Experimental fish received the chemotherapy regimen in embryo media and control fish received an equal concentration of the vehicle control, DMSO/diH_2O, in embryo media. Concentrations of drugs are outlined in Table 1.

Images captured were imported into ImageJ software. The image was cropped to include the entire embryo but to limit background fluorescence. The image was converted to a 32-bit grayscale and the threshold was adjusted to eliminate background pixels. The total area of fluorescence was measured to reflect tumour burden. The difference in tumour burden between pre-treatment and post-treatment in each individual was recorded and results were reflected in overall fold change. Prior to treatment unhealthy fish with skeletal/cardiac abnormalities, slow or rapid pulse, and inability to maintain homeostasis

were removed from the trial. Individuals were considered outliers if their fold change was 3 or more times the standard deviation.

IV. ALDEFLUOR® Assay

Aldehyde dehydrogenase (ALDH), primarily ALDH1 isoforms, were detected using the ALDEFLUOR™ Assay (STEMCELL Technologies 01700). Multiple dilutions of MDA-MB-231wt and MCF-7wt cells were collected and resuspended in 1mL of cold ALDEFLUOR™ assay buffer in a 15mL conical tube. Two methods of staining were utilized. 5µL of activated ALDEFLUOR™ reagent was added to the cell suspension and mixed well by pipetting. 500µL of the sample was transferred to a tube containing an inhibitor of ALDH, DEAB, to act as the negative control for each sample. Alternatively, samples were evenly split into two 15mL conical tubes one of which contains 5µL of DEAB. 5µL of activated ALDEFLUOR™ reagent was then added to all cell suspension and mixed well by pipetting. Importantly, in both methods buffers and all samples were kept on ice. All cell suspensions were incubated for 35-45 minutes in the dark at 37°C. After incubation, cells were centrifuged at 1000rpm minutes to collect cells. Cells were resuspended in 500µL of cold ALDEFLUOR™ assay buffer, filtered through a 70µm filter, and analyzed via BD FACSAria Fusion™ 5-Laser 18-Colour with ACDU. Wild-type unstained cells were used for cell size calibration and to gate for a fluorescence-negative population. Each inhibited sample was analyzed and gated for followed by the uninhibited sample.

V. Plasmid Construction

The following mammalian DNA plasmids were constructed by Dr. Bryan Welm and were utilized for reporter construction and confirmation of infection:

pHIV-dtomato from Bryan Welm (Addgene plasmid #21374) (unpublished)

pHIV- enhanced green fluorescent protein (eGFP)(Welm et al., 2008)

The following mammalian DNA plasmids were constructed by Ellen M. Laurie and were utilized during infection:

pHIV- ALDH1A1- dTomato (hereafter ALDH1A1-dTomato)

pHIV- ALDH1A1-eGFP (hereafter ALDH1A1-eGFP)

pHIV-ALDH1A3-eGFP (hereafter ALDH1A3-eGFP)

Lentiviral vector ALDH1A1-dTomato was constructed by amplification of the ALDH1A1 genomic promoter and enhancer regions, flanked by AgeI(BshTI) and NotI restriction sites, followed by ligation to pHIV-dTomato backbone replacing elongation factor-1α promoter (EF-1α).

Lentiviral vectors ALDH1A1-eGFP and ALDH1A3-eGFP were constructed by the amplification of the ALDH1A1 and ALDH1A3 genomic promoter and enhancer regions, flanked by AgeI(BshTI) and XbaI restriction sites, followed by ligation to the pHIV-eGFP backbone, replacing the EF-1α promoter.

VI. Infection Method

Twenty-four hours prior to infection MDA-MB-231wt and MCF-7wt cells were seeded at 20,000 cells/well in a 12-well plate format containing 1mL of growth media. Cells were grown to 70-80% confluency and growth media was changed to serum and antibiotic-free media with 8μg/mL polybrene (Santa Cruz Biotechnology sc-134220). Cells were then

incubated for 45 minutes before the addition of virus to each well. The plate was gently rocked to ensure mixing and then incubated for 16-18 hours. The multiplicity of infection was 2 and the virus titer for all lentiviral production was $1x10^7$ pfu/mL. After 16-18 hours, the virus was removed, cells were washed with 1XPBS, and 1mL of growth media was added to each well. Successfully infected cells were monitored through fluorescent microscopy.

VII. Transfection Method

SK-BR-3wt cells were transfected for the incorporation of ALDH1A1-dTomato. Cells were seeded 18-24 hours before transfection with 1mL of full growth media, growing to 60-70% confluency at the time of transfection. Transfections were completed in a 12-well plate. Before transfection, 1µg of DNA was incubated in 100µL serum-free media and 2µL of *Trans*IT-BrCa Reagent (Mirus MIR5504) for 30 minutes at room temperature. Incubated DNA was added drop-wise to each well and the plate was rocked to evenly distribute the mixture. Cells were harvested 48 hours after transfection for experimentation.

VIII. Isolation of ALDH1 low and high populations using a reporter-based system

MDA-MB-231wt, MCF-7wt or SK-BR-3wt cells were infected/transfected with ALDH1A1-dTomato or co-infected with ALDH1A1- and ALDH1A3-eGFP lentiviral constructs. Infected MCF-7 and SK-BR-3 cells were washed with 1XPBS, incubated for 3-4 minutes in 500µL 0.05% trypsin, and collected by gently washing with serum- and antibiotic-free media. Infected MDA-MB-231 cells were collected in the same fashion without the use of trypsin. Cells were washed three times with 1XPBS and resuspended

in 500µL of 1XPBS. Cells were filtered through a 70µm cell strainer and were sorted by fluorescence-activated cell sorting (FACS) via BD FACSAria Fusion™ 5-Laser 18-Colour with ACDU. Wild-type cells of each type were used for FACS to calibrate cell size and to gate fluorescence negative. When cells were collected for further experimentation, the highest and lowest 0-5% of fluorescent cells were collected from MDA-MB-231 and/or MCF-7 infected cells. Upon collection, cells were washed with 1XPBS three times and pellets were either resuspended in cell culture or stored at -20°C for later experimentation.

IX. Mammosphere assay

Infected MDA-MB-231 cells sorted for stem-like ($ALDH1^{hi}$) and non-stem-like ($ALDH1^{low}$) populations were seeded into 6-well ultra-low attachment plates at 500 cells/well. In each well, 2mL of DMEM/F-12 50/50 1X (Corning 10-092) media supplemented with 20ng/mL of epidermal growth factor (Gibco PHG0315), 20ng/mL human fibroblast growth factor (Sigma F5392), 4µg/mL heparin (Sigma H0777) and 1% penicillin/streptomycin tested against Mammocult™ Basal Medium Human (Mammocult™ media) (Stem Cell Technologies 05621) supplemented with 5ng/mL epidermal growth factor, 5ng/mL human fibroblast growth factor, 5µg/mL heparin, 2.5µg/mL isoproterenol (Sigma I6504), 0.5µg/mL hydrocortisone (Sigma H0888), and 5µg/mL insulin (Sigma I3536). Mammospheres were cultured for 7 days at 37°C with 5% CO_2. Images were taken of each well, in its entirety, using a Leica CTR6500 microscope with AF software. The mammosphere diameter (µm) was measured using ImageJ version 1.51k. Spheres ≥40µm or ≥60µm were counted in the total number of

spheres, reflected as a percent sphere formation. Calibration of the scale was performed using a slide micrometre.

X. Quantitative Real-Time polymerase chain reaction (qRT-PCR)

RNA extractions were performed using Qiagen RNeasy Plus Mini Kit (Qiagen Cat# 74104) as per manufacture's instructions. Concentration and purity of eluted RNA were measured using an ND-1000 Nanodrop Spectrophotometer (NanoDrop Technologies). cDNA synthesis was performed using qScript™ cDNA SuperMix Master Mix (Quantabio 9048) as per manufacture's protocol. cDNA was stored at -20°C for further experimentation. qRT-PCR was performed using SYBR Green detection utilizing Fast SYBR™ Green Master Mix (ThermoFisher 4385612). Reactions of 10µL were run over 40 cycles of denaturation at 95°C and primer annealing and elongation at 60°C. Each reaction contained 6.25nM of primers (see Table 2). The analysis was done using Viia7 Real-Time PCR System and software (Life Technologies). Samples were normalized to an internal control, human GAPDH. Analysis of qRT-PCR results was completed using QuantaStudio™ Real-Time PCR Software v1.3.

To normalize genes to GAPDH the difference between the Ct value of the gene of interest and the Ct value of GAPDH is calculated resulting in the ΔCt. The ΔCt of the calibrator sample is set to 0 and all samples are compared to generate ΔΔCt values (ie. $\Delta\Delta Ct_{sample} = \Delta Ct_{sample} - \Delta Ct_{calibrator}$). The relative quantification (RQ) of a sample is calculated for each sample with the equation $RQ=2^{-\Delta\Delta Ctsample}$. The $\log_{10}RQ$ represents the fold change between the sample and the calibrator. Error bars represent the standard error of the mean $\log_{10}RQ$ value.

Table 2: Primers utilized in PCR and qRT-PCR

	Primers (Forward/Reverse)
ALDH1A1 (PCR)	5'-ACCGGTCCACAATCAGAGCATCCAGAG-3' 5'-GCGGCCGCCTCCTGGAACACAGGTGACTGGCTCAG-3'
ALDH1A3 (PCR)	5'-TACCGGTGGAATGGCATGCATCAGAAGCC-3' 5'-TTCTAGACTCCTCCGCGCTCCCTGGC-3'
hGAPDH (qRT-PCR)	5'-GCACCGTCAAGGCTGAGAAC-3' 5'-GGATCTCGTCCTGGAAGATG-3'
hALDH1A1 (qRT-PCR)	5'-CTGCCGGGAAAAGCAATCTG-3' 5'-CCACAAAAATCCTGGATGCGG-3'
hALDH1A3 (qRT-PCR)	5'-ACCATCCCCACAGATGACAAC-3' 5'-ATAAAGGGCGGTGAGAGGTGTCT-3'
eGFP (qRT-PCR)	5'-ACGTAAACGGCCAAGTTC-3' 5'-CGGTGGTGCAGATGAACTTC-3'
hSpy1 (qRT-PCR)	5'-TTGTGAGGAGGTTATGGCCATT-3' 5'-GCAGCTGAACTTCATCTCTGTTGTAG-3'

XI. Immunocytochemistry

i. Immunostaining

ALDH1^{hi} and ALDH1^{low} cells were seeded on to a 12-well adherent plate containing coverslips. After 48 hours coverslips were collected. Cells were fixed with 4% paraformaldehyde in 1XPBS for 45 minutes at room temperature. After fixation, cells were stored at -20°C in a 1:1 ratio of glycerol and 1XPBS. Coverslips were then washed with 1XPBS three times. Cells were permeabilized with 0.2% Titron X-100 in 1XPBS for 30 minutes. Slips were blocked with LAP blocker (Titron X-100, glycine, FBS, and 1XPBS). Rabbit Anti-GFP (Abcam 290) was used at 1/10,000 in LAP blocker incubated in the dark for 1 hour at room temperature, followed by 3 washes with 1XPBS. Alexa conjugated antibodies (Invitrogen A-11034) and propidium iodide (ThermoFisher Scientific p3566) (a gift from Dr. A. Swan) was used at 1/1000 in LAP blocker, incubated in the dark for 30 minutes, followed by 3 washes with 1XPBS. Slide coverslips were mounted to slides using mounting solution (Ibidi 50001), then sealed with nail polish.

ii. Confocal Microscopy

Immunostained cells were imaged using an Olympus FluoView FV1000 laser scanning confocal microscope. Images were analyzed in Olympus FluoView software version 1.5.

RESULTS

I. Treatment with AC/T±Ca decreased the viability of TNBC *in vitro* and *in vivo*.

To examine the effects of carboplatin (Ca) on cell viability when combined with doxorubicin (A) plus cyclophosphamide (C) then paclitaxel (T), MDA-MB-231 triple negative breast cancer cells were treated with a regimen of AC/T ± Ca or their vehicle control counterparts (outlined in Figure 2A). Cell viability was assessed using a trypan blue exclusion assay. The vehicle control shows no effect on cell viability. Treatment of AC/T significantly decreased the viability of cells compared to control, to under 18% viability and the addition of carboplatin further decreased viability, significantly, to under 9% (Figure 2B). Therefore, carboplatin further decreases cell viability in MDA-MB-231wt cells, when combined with AC/T.

To elucidate the role of Spy1 in treatment resistance MDA-MB-231 cells were infected with shSpy1 or its control empty vector (plko) then injected into zebrafish and treated with AC/T+Ca over a 7-day treatment (outlined in Figure 3A). Zebrafish were imaged before (Day 0) and after (Day 7) treatment. Treatment with AC/T+Ca decreased the area of fluorescence in both shSpy1 and control populations, compared to the vehicle control. The knockdown of Spy1 significantly decreased the area of fluorescence when combined with AC/T+Ca treatments, suggesting that the knockdown of Spy1 sensitizes cells to treatment *in vivo* (Figure 3B).

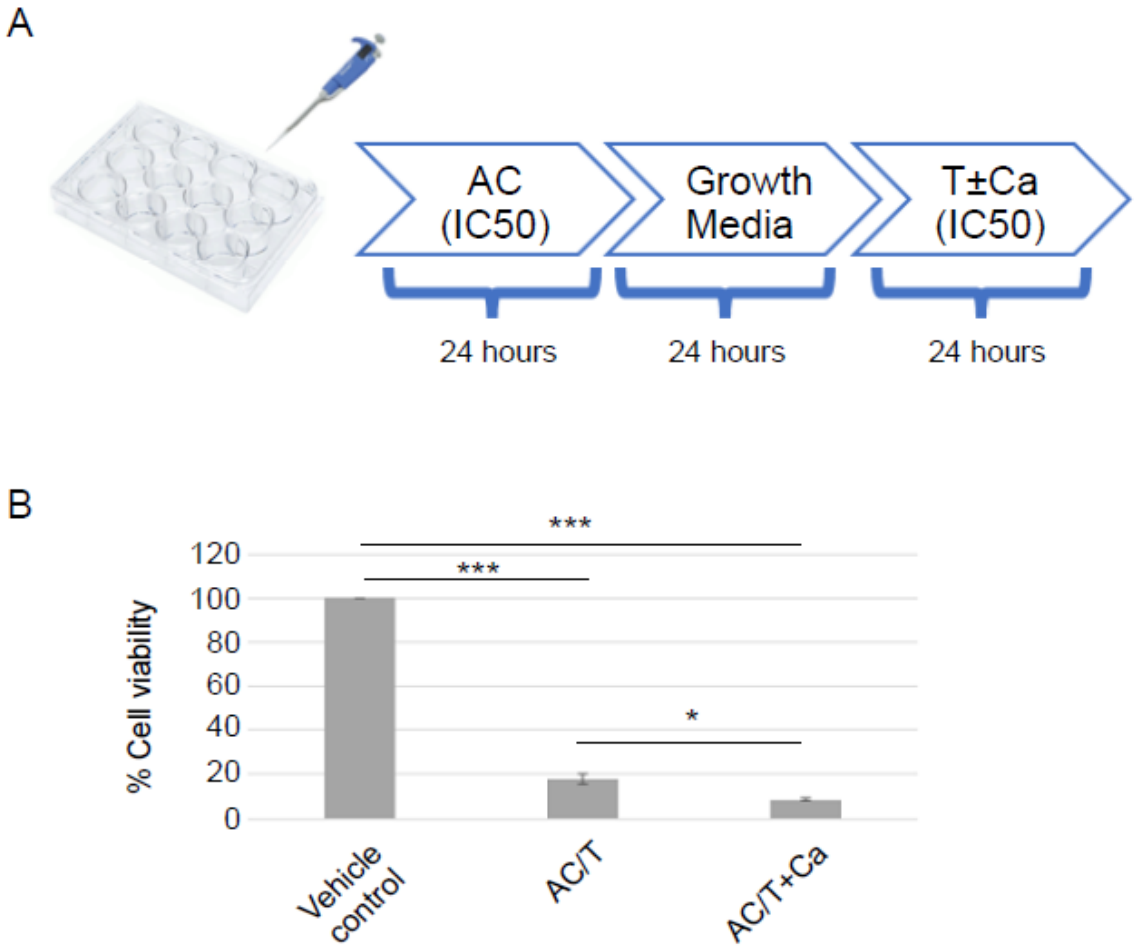

Figure 4: Treatment of TNBC cells *in vitro* with AC/T ± Ca decreases cell viability. A) Schematic of treatment with doxorubicin (A), cyclophosphamide (C), paclitaxel (T), and/or carboplatin (Ca) MDA-MB-231wt cells were treated with the inhibitory concentration of 50% of the cells (IC50) (IC50s provided by Dr. R. Ferraiuolo). (B) Percent cell viability of cells treated with AC/T ± Ca determined through the trypan blue exclusion assay. Error bars represent standard error of the mean of three samples counted in triplicate. *p<0.05, ***p<0.001. Statistical significance was analyzed using a Student's paired t-test.

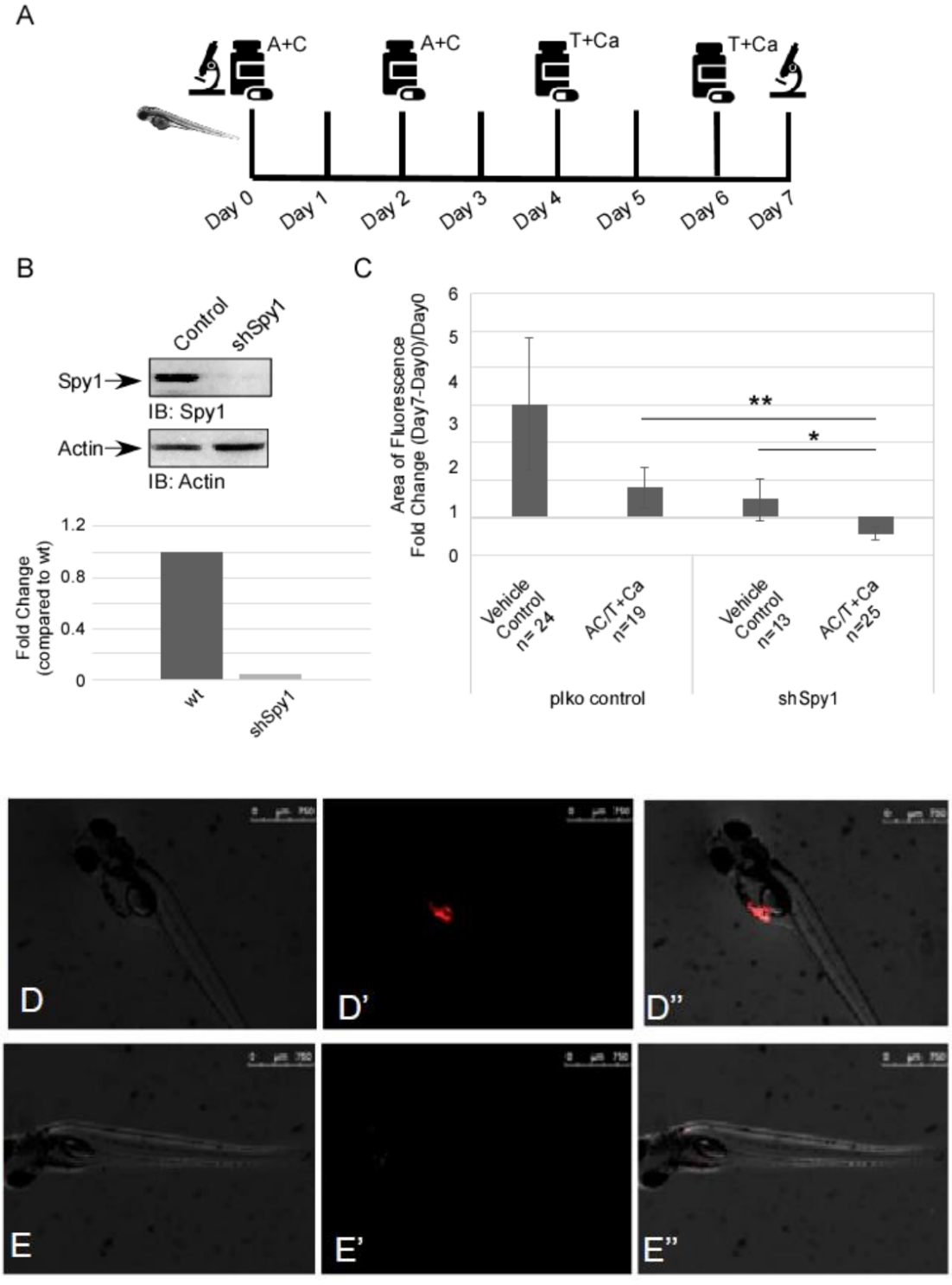
A
A+C
A+C
T+Ca
T+Ca
Day 0
Day 1
Day 2
Day 3
Day 4
Day 5
Day 6
Day 7
B
Control
shSpy1
Spy1
IB: Spy1
Actin
IB: Actin
Fold Change (compared to wt)
1.2
0.8
0.4
0
wt
shSpy1
C
Area of Fluorescence
Fold Change (Day7-Day0)/Day0
6
5
4
3
2
1
0
**
*
Vehicle Control n= 24
AC/T+Ca n=19
Vehicle Control n=13
AC/T+Ca n=25
plko control
shSpy1
Day 0
D
D'
D''
Day 7
E
E'
E''

Figure 5: Knock-down of Spy1 *in vivo* sensitizes TNBC cells to treatment with AC/T+Ca. (A) Schematic of zebrafish treatment regimen with drugs doxorubicin (A), cyclophosphamide (C), paclitaxel (P), and carboplatin (Ca) where the pill icon represents days where drugs were added and the microscope represents days of imaging. (Completed by Dr. R. Ferraiuolo and Anne Semaan) (B) Western blot showing Spy1 knockdown with actin as a loading control (Completed by Dr. R. Ferraiuolo). Densitometry of 1 experiment below. (C) Fold change in the area of fluorescence between treatment with AC/ T ± Ca or vehicle control (plko), with or without the knockdown of Spy1. Error bars represent standard error of the mean. p*<0.05, p**<0.01. Statistical significance was analyzed using a 1-tailed homoscedastic t-test. (D-D'') Representative images before treatment. (E-E'') Representative images after treatment. Images were provided by Dr. R. Ferraiuolo for quantification. Bright-field (left), fluorescent images detecting Vybrant™ dye (middle), and merge images (right) were taken at 3.75X zoom.

II. STEMCELL™ Technologies' ALDEFLUOR™ kit shows variable results for TNBC

To assess the effectiveness of the ALDEFLUOR™ kit in detecting ALDH-high vs. ALDH-low cells, the staining conditions for cell lines MDA-MB-231 and MCF-7s were determined. MCF-7s are reported to have a low frequency of stem cells comprising <1% of the population (Charafe-Jauffret et al., 2009b; Croker et al., 2009), whereas

MDA-MB-231wt cells are reported to contain a stem cell population of approximately 10% and hence were used to initially optimize the ALDEFLUOR™ assay (Ginestier et al., 2007; Kong et al., 2015). Unstained MDA-MB-231wt cells were used as a fluorescent-negative control (Figure 4B: gate P2). MDA-MB-231 cells were stained with ALDEFLUOR™ reagent and an inhibitor of ALDH activity, DEAB, was added to half the sample to serve as a control for specificity. All samples were incubated at 37°C for 35 minutes. Inhibited samples followed the same trend as unstained samples, with only 0.4% of cells staining positively (Figure 4C: P3). ALDEFLUOR™ stained cells showed cells with an increased ALDEFLUOR™ signal (Figure 4D: P3). Results supported that ~36% of the MDA-MB-231 population was ALDEFLUOR™ positive.

In a repeat experiment, unstained MDA-MB-231wt cells were used to set the gates for an $ALDH^-$ population (Figure 5B: P3). To increase the staining efficiency of the ALDEFLUOR™ kit the incubation times were increased from 35 minutes to 45 minutes, as suggested by STEMCELL™ Technologies (STEMCELL Technologies, 2011). Increasing the time of incubation altered the spread of signal intensity, shifting towards higher intensity (Figure 5D: P2), however, treatment with the DEAB inhibitor resulted in

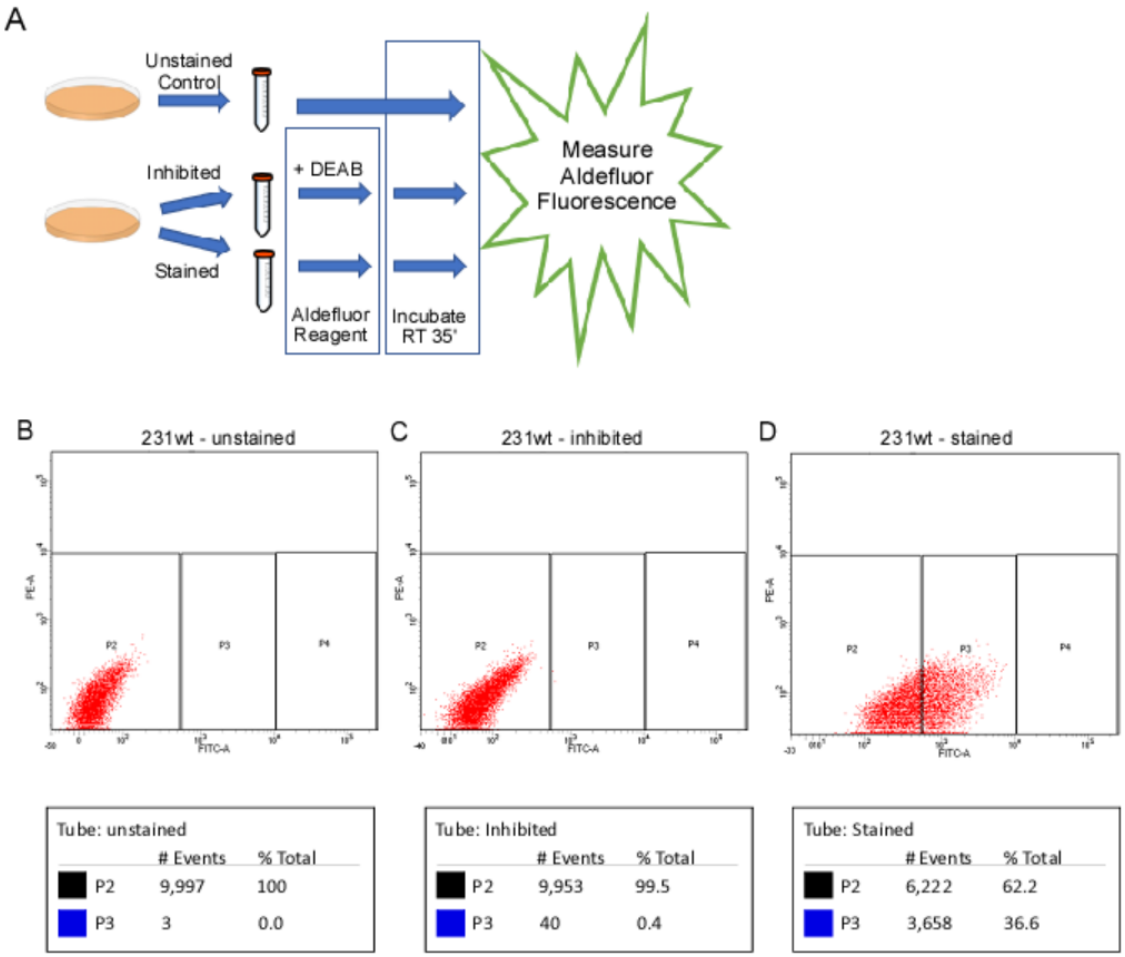

Figure 6: Optimization of ALDEFLUOR™ assay with TNBC cells. A) Schematic of experimental design for panels B-D. (B-D) Flow cytometry was conducted to measure ALDEFLUOR™ eGFP fluorescence (FITC: x-axis) and light emitted from phycoerythrin (PE: Y axis). (B) Unstained MDA-MB-231wt cells were used to gate for a fluorescence-negative population (P2). (C) Fluorescence intensity of ALDEFLUOR™ stained MDA-MB-231wt cells inhibited by DEAB. (D) Fluorescence intensity of ALDEFLUOR™ stained MDA-MB-231wt cells. P3/P4 representing positive ALDEFLUOR™ fluorescence. Quantification, in percent, of cells within each gate are below each plot.

A

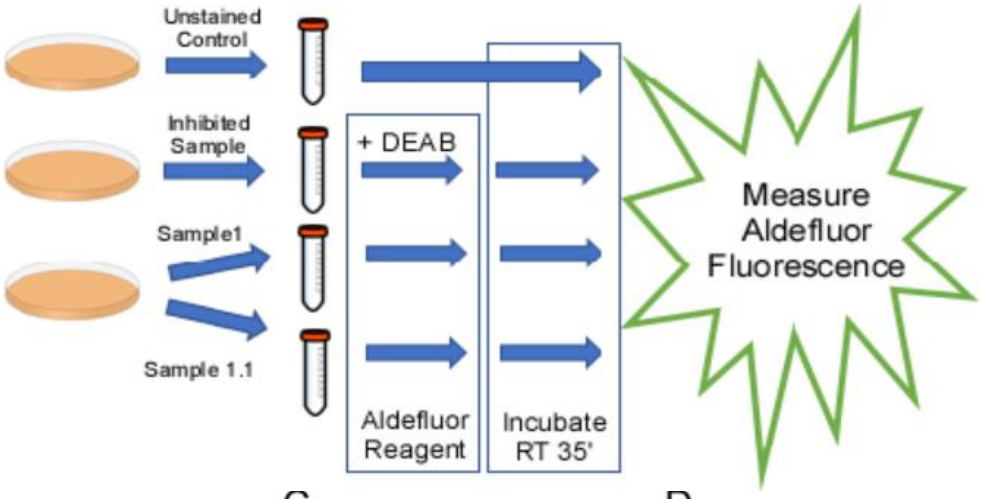

B

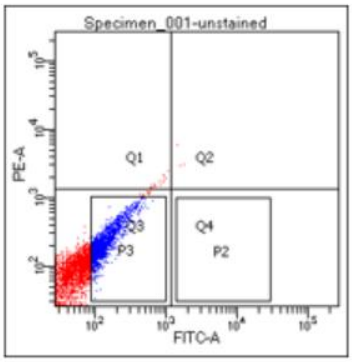

C

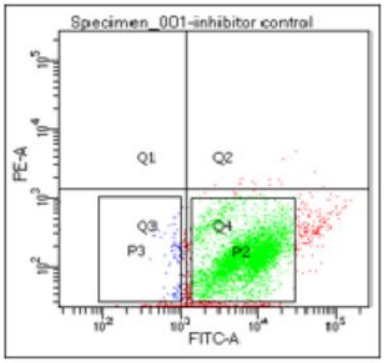

D

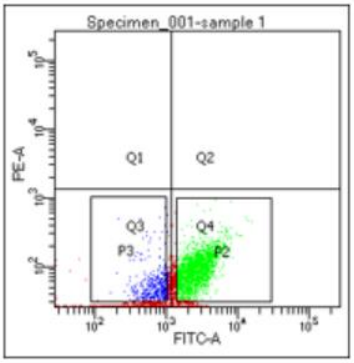

Tube: Unstained	# Events	% Total
P3	1,455	14.5
P2	0	0.0

Tube: Inhibited	# Events	% Total
P3	82	0.8
P2	4,221	42.2

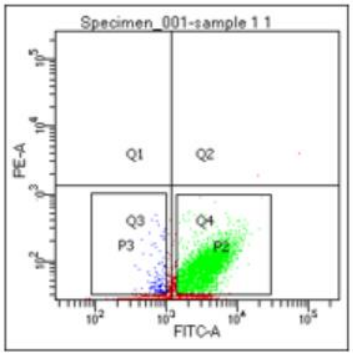

E

Tube: Sample 1	# Events	% Total
P3	491	4.9
P2	2,277	22.8

Tube: Sample 2	# Events	% Total
P3	383	3.8
P2	3,204	32.0

Tube: Sample 3	# Events	% Total
P3	184	1.8
P2	4,123	41.2

Tube: Sample 1.1	# Events	% Total
P3	137	1.4
P2	3,819	38.2

Tube: Sample 2.1	# Events	% Total
P3	359	3.6
P2	3,468	34.7

Tube: Sample 3.1	# Events	% Total
P3	74	0.7
P2	4,390	43.9

Figure 7: ALDEFLUOR™ fluorescence is variable within samples. A) Schematic of experimental design where 1 sample was split evenly and analyzed as 2 samples. (B-D) Flow cytometry was conducted to measure ALDEFLUOR™ eGFP fluorescence (FITC: x-axis) and light emitted from phycoerythrin (PE: Y axis). (B) Unstained MDA-MB-231wt cells were used to gate for a fluorescence-negative population (P2). (C) Fluorescence intensity of ALDEFLUOR™ stained MDA-MB-231wt cells inhibited by DEAB. Quantification, in percent, of cells within each gate are below each plot. (D) Fluorescence intensity of ALDEFLUOR™ stained cells from the same culture. (E) Quantification, in percent for 3 repetitions of the experiment within each gate. P3/P4 representing positive ALDEFLUOR™ fluorescence.

cells with higher fluorescence than ‘samples’ at 42.4% (Figure 5C: P2). Cells collected from a single plate of cells were divided into 2 samples and analyzed separately, as an example sample 1 and 1.1. Interestingly, flow cytometry results from samples collected from the same plate of cells (Figure 5E) showed variability in some samples of up to 15.4%. Variability increased further between samples, with $ALDH^+$ populations (P2), ranging from 22.8- 43.9%.

To better understand the variability seen with DEAB inhibition between experiments (Figures 4B and 5C), new DEAB inhibitor was purchased and added to inhibited samples prior to the addition of ALDELUOR™ reagent (STEMCELL Technologies, 2011). In MDA-MB-231 and MCF-7 cell lines, the early addition of DEAB did not show results similar to the unstained control (Figure 6A: top/middle and 6B: top/middle). Additionally, high level of staining at 98.4 and 37.8% in both 231 and MCF7 cells, respectively, was particularly discerning (Figure 6A, 6B: middle/far right panels). Overall, these results show that the ALDEFLUOR™ assay may not be a reliable method to detect ALDH fluorescence in MDA-MB-231wt and MCF-7wt cells.

III. Transcriptional Reporter System ALDH1A1 and ALDH1A3

As an alternative to STEMCELL™ Technologies’ ALDEFLUOR™ kit, we set out to derive a transcriptional based system for the isoforms of ALDH, to identify $ALDH^+$ populations. An expression reporter construct/system that expresses dTomato under the ALDH1A1 enhancer was used to assay ALDH1A1 expression in successfully infected cells (Figure 7A). MDA-MB-231wt and SK-BR-3wt cells were infected or transfected,

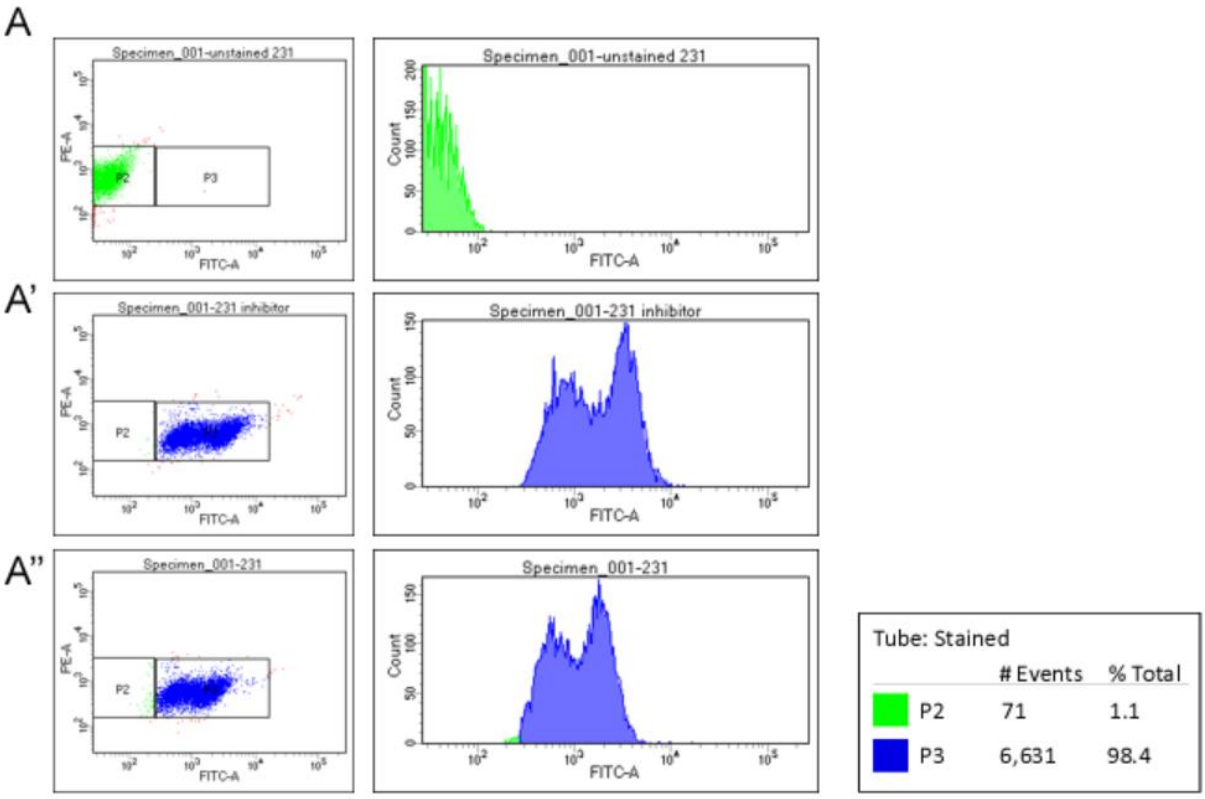
A
Specimen_001-unstained 231
PE-A
FITC-A
P2
P3
Count
A'
Specimen_001-231 inhibitor
A''
Specimen_001-231
Tube: Stained
Events
% Total
P2 71 1.1
P3 6,631 98.4

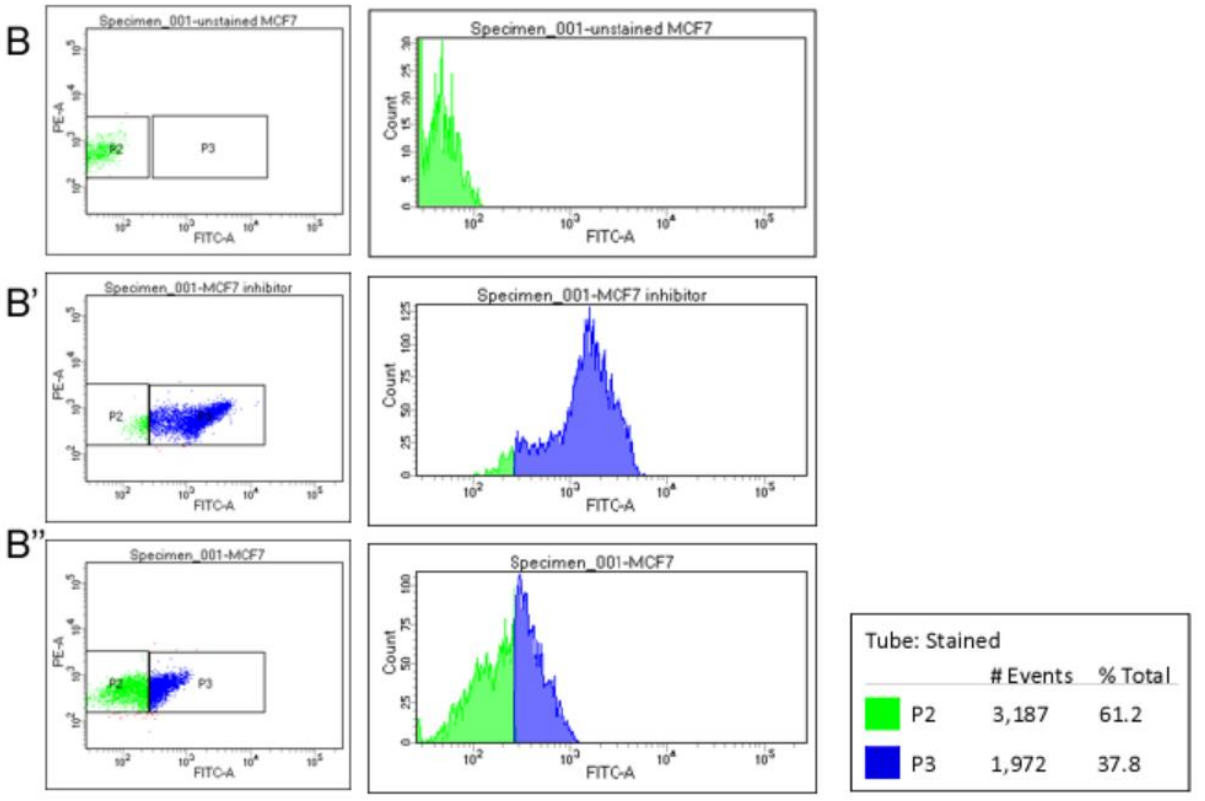
B
Specimen_001-unstained MCF7
PE-A
FITC-A
P2
P3
Count
B'
Specimen_001-MCF7 inhibitor
B''
Specimen_001-MCF7
Tube: Stained
Events
% Total
P2 3,187 61.2
P3 1,972 37.8

Figure 8: ALDEFLUOR™ fluorescence in triple-negative and luminal breast cancer cells. MDA-MB-231wt and MCF-7wt cells were analyzed via flow cytometry to measure ALDEFLUOR™ fluorescence (FITC: x-axis) and light emitted from phycoerythrin (PE: y-axis). Quantification of each gated population, in percent, is on the far right. (A) Unstained MDA-MB-231wt cells were used to gate for a fluorescence-negative population (P2). (A') Fluorescence intensity of ALDEFLUOR™ stained MDA-MB-231wt cells inhibited by DEAB. (A'') Fluorescence intensity of ALDEFLUOR™ stained MDA-MB-231wt cells. (B) Unstained MCF-7wt cells were used to gate for a fluorescence-negative population (P2). (B') Fluorescence intensity of ALDEFLUOR™ stained MCF-7wt cells inhibited by DEAB. (B'') Fluorescence intensity of ALDEFLUOR™ stained MCF-7wt cells.

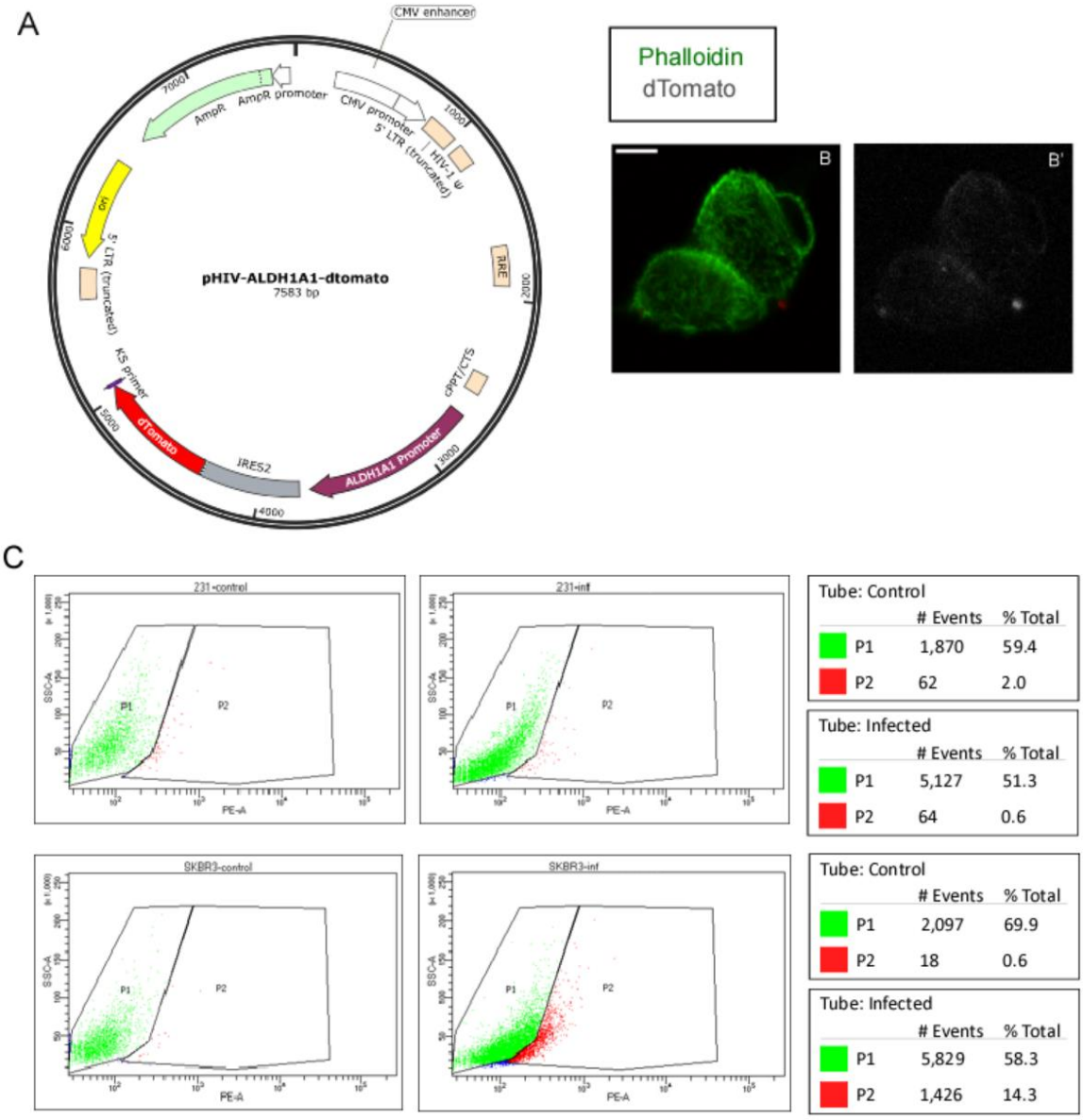
A
CMV enhancer
AmpR
AmpR promoter
CMV promoter
5' LTR (truncated)
HIV-1 ψ
RRE
cPPT/CTS
ALDH1A1 Promoter
IRES2
dTomato
KS primer
5' LTR (truncated)
gag
pHIV-ALDH1A1-dtomato
7583 bp
Phalloidin
dTomato
B
B'
C
231-control
231-inf
SKBR3-control
SKBR3-inf
SSC-A
PE-A
P1
P2
Tube: Control
Events
% Total
P1 1,870 59.4
P2 62 2.0
Tube: Infected
Events
% Total
P1 5,127 51.3
P2 64 0.6
Tube: Control
Events
% Total
P1 2,097 69.9
P2 18 0.6
Tube: Infected
Events
% Total
P1 5,829 58.3
P2 1,426 14.3

Figure 9: The dTomato-ALDH1A1 reporter has low positive staining. A) Vector map of pHIV-ALDH1A1-dTomato. (B-B') Representative confocal image of MDA-MB-231 cell stained to detect Phalloidin (green) and dTomato fluorescence (B': show in grayscale). 60X magnification. The scale bar measures 10μm. (C) MDA-MB-231wt and SK-BR-3wt cells infected or transfected, respectively, with pHIV-dTomato (control) or pHIV-ALDH1A1-dTomato, as indicated. Flow cytometry was conducted to measure reporter dTomato signal (PE-A: x-axis) and side scatter (SSC-A: Y axis) to measure cell granularity. P1 gates for negative fluorescence and background and P2 gates for positive fluorescence. Each repetition represents an independent infection.

respectively, with pHIV-dTomato control or ALDH1A1-dTomato and detection of dTomato was performed through fluorescence detection. Infection/transfection of the control plasmid in MDA-MB-231 and SK-BR-3 cells did not show any increase fluorescence compared to uninfected cells (wt control not shown). There was only a marginal increase, of 1.8%, in fluorescence in SK-BR-3wt cells and no increase in MDA-MB-231wt cells; both lines were specifically chosen for their high ALDH-expression (Ginestier et al., 2007; Kong et al., 2015; STEMCELL Technologies, 2009). These results suggest that that the live signal of ALDH1A1-dTomato, alone, is not sufficient for FACS.

It is reported that ALDH1A3 is the isoform of ALDH mostly responsible for ALDEFLUOR™ fluorescence in stem cell populations (Ikawa et al., 1983; Rexer et al., 2001); however, after the construction of a pHIV-ALDH1A3-dTomato reporter construct, technical issues halted progress with this vector. As an alternate approach, ALDH1A1-eGFP and ALDH1A3-eGFP reporters were constructed (Figure 8).

IV. Transcript levels of eGFP, ALDH1A1, ALDH1A3 and hSpy1 are increased in ALDH1^{high} populations

The live signal of co-infected cells expressing eGFP was sufficient for FACS. To validate the reporter, transcript levels were analyzed to determine whether ALDH1A1 and 1A3 levels were elevated as indicated by fluorescence. ALDH1A1 and ALDH1A3 (ALDH1, for brevity)^{low} and ALDH1^{high} cells were sorted based on eGFP intensity via FACS (as summarized in Figure 9A). As performed in other studies, the 0-4% lowest and highest fluorescing cells were selected as ALDH1^{low} and ALDH1^{high} (Figure 9B). Quantification,

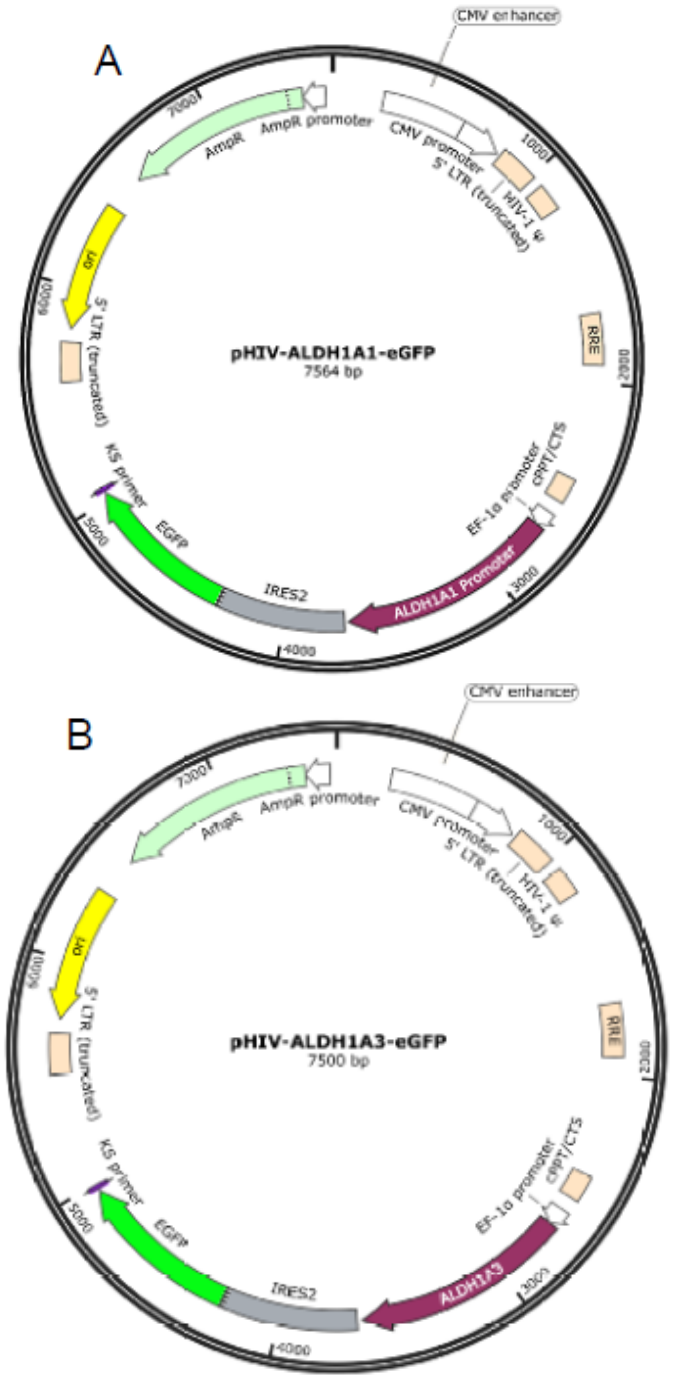

Figure 10: Vector maps of eGFP reporters. A) Vector map of pHIV-ALDH1A1-eGFP. (B) Vector map of pHIV-ALDH1A3-eGFP.

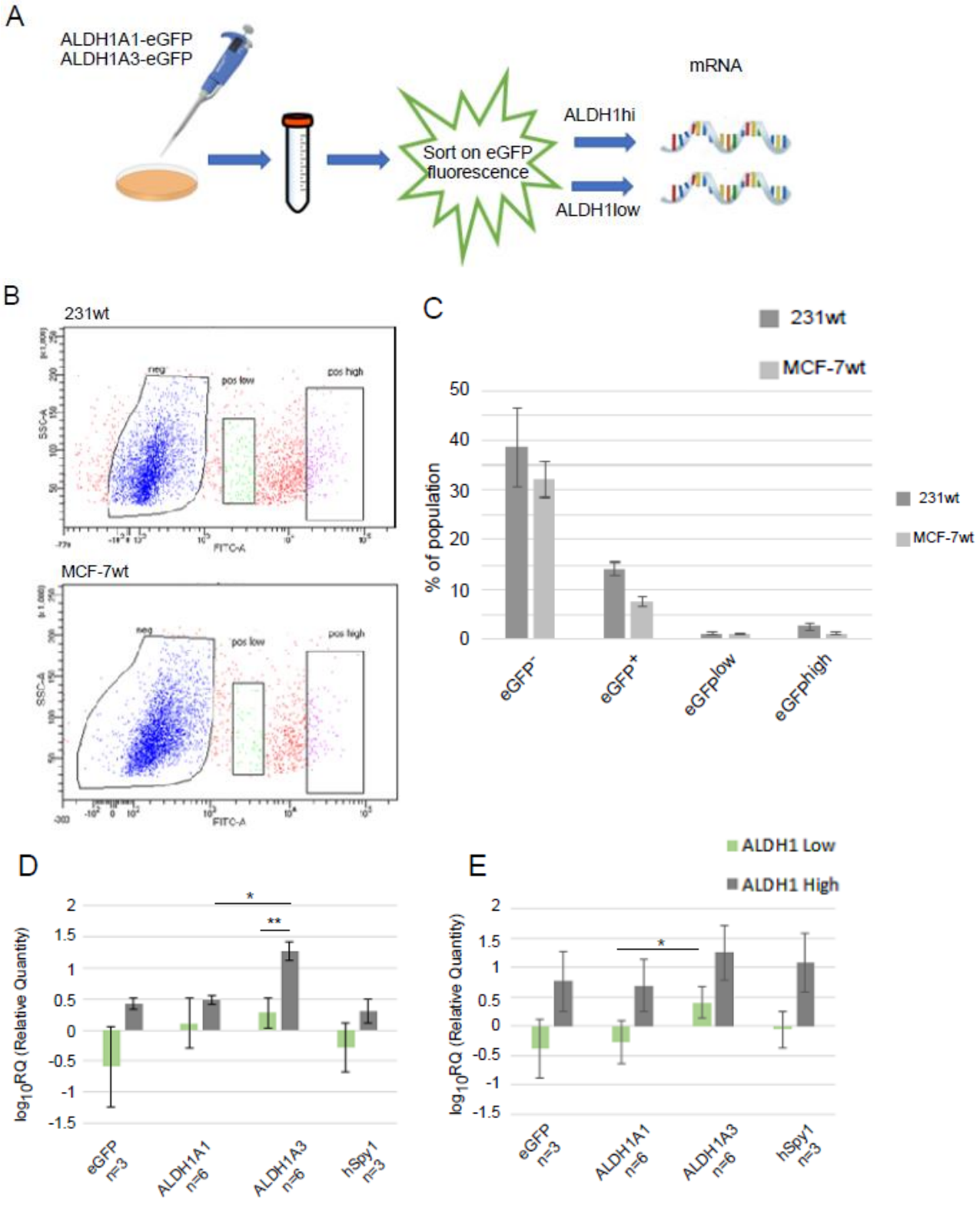
A
ALDH1A1-eGFP
ALDH1A3-eGFP
Sort on eGFP fluorescence
ALDH1hi
ALDH1low
mRNA
B
231wt
MCF-7wt
neg
pos low
pos high
SSC-A
FITC-A
C
231wt
MCF-7wt
% of population
eGFP-
eGFP+
eGFPlow
eGFPhigh
D
log10RQ (Relative Quantity)
eGFP n=3
ALDH1A1 n=6
ALDH1A3 n=6
hSpy1 n=3
E
ALDH1 Low
ALDH1 High
log10RQ (Relative Quantity)
eGFP n=3
ALDH1A1 n=6
ALDH1A3 n=6
hSpy1 n=3

Figure 11: ALDH1^{high} populations have increase transcript levels of hSpy1, eGFP, ALDH1A1 and ALDH1A3. A) Schematic demonstrating the protocol for ALDH1^{low} and ALDH1^{high} transcript analysis. (B) FACS was conducted to measure reporter eGFP signal (FITC-A: x-axis) and side-scattered light (SSC-A: y-axis) was measuring cell granularity. (C) Quantification of three independent sorts, in percent, of gated populations eGFP^{-} (neg), eGFP^{+}, eGFP^{low} (pos low) and eGFP^{high} (pos high) cells in MDA-MB-231wt and MCF-7. (D) Log_{10} Relative Quantity (RQ) of transcript levels of eGFP, ALDH1A1, ALDH1A3 and hSpy1 in MDA-MB-231 cells. (E) Log_{10} Relative Quantity (RQ) of transcript levels of eGFP, ALDH1A1, ALDH1A3 and hSpy1 in MCF-7wt cells. Error bars represent the standard error of the mean of three independent infections, run in triplicate qRT-PCR reactions. p*<0.05, p**<0.01.

in percent, of the average $eGFP^-$, $eGFP^+$, $eGFP^{low}$, $eGFP^{high}$ cells between MDA-MB-231 and MCF-7 populations (Figure 9C). We found an average 13.9% of the population reflecting an eGFP positive population, in three separately infected samples with a range of 12.3-16.8%. Uninfected cells provide a distinct population of fluorescence-negative cells (wt control not shown). MCF-7 infected cells showed an average 7.6% eGFP positive cells with a range of 6.3-9.9% over three separately infected samples (Figure 9C). Relative quantification of mRNA, normalized to GAPDH, showed an increase in eGFP, ALDH1A1 and ALDH1A3 in $ALDH1^{high}$ populations compared to $ALDH1^{low}$ in both triple-negative MDA-MB-231 cells (Figure 9D) and luminal MCF-7 cells (Figure 9E). The increase in ALDH1A3 transcript levels was statistically higher in the $ALDH1^{high}$ population of triple-negative cells. Additionally, there was an increase in hSpy1 in $ALDH1^{high}$ populations, suggesting that Spy1 may play a role in stemness. While the reporter needs further validation, preliminary results show that hSpy1 may be increased in CSC populations in MDA-MB-231wt cells.

V. Mammosphere formation is enhanced in $ALDH1^{high}$ triple negative populations

To validate the reporter through functional assays, MDA-MB-231wt cells were co-infected with ALDH1A1-eGFP and ALDH1A3-eGFP reporters, collected, and sorted by low and high eGFP intensity ($ALDH1^{low}$ and $ALDH1^{high}$ respectively). Mammosphere forming capacity was in $ALDH1^{low}$ and $ALDH1^{high}$ sorted populations (summarized in Figure 10A). Uninfected cells from infected population provide a distinct population of fluorescence-negative cells (wt control not shown). The selected lowest and highest 1.5-2% of fluorescing cells were collected for mammosphere formation analysis (Figure

10B). Sorted populations were each put into two different mammosphere conditions that favour growth of stem-like cells (Dontu et al., 2003). Mammospheres that measured greater or equal to 40µm (Figure 10C) or 60µm (Figure 10C') were counted. ALDH1^{high} cells had more mammospheres in all types of media and cell sizes, significantly in DMEM F-12 supplemented media and mammospheres equal or greater to 40 µm in Mammocult™ supplemented media (Figure10 D & E: left panel). ALDH1^{high} cells show an increased ability to form spheres compared to ALDH1^{low} cells. These results also indicate that MDA-MB-231 cells with low expression of ALDH1A1 and ALDH1A3 are still capable of sphere formation, but not as efficiently as those with higher expression. These results suggest that identification of stem-like cells through reporters for ALDH1A1 and ALDH1A3 is functionally relevant, and further supports the functionality of our transcriptional reporter system.

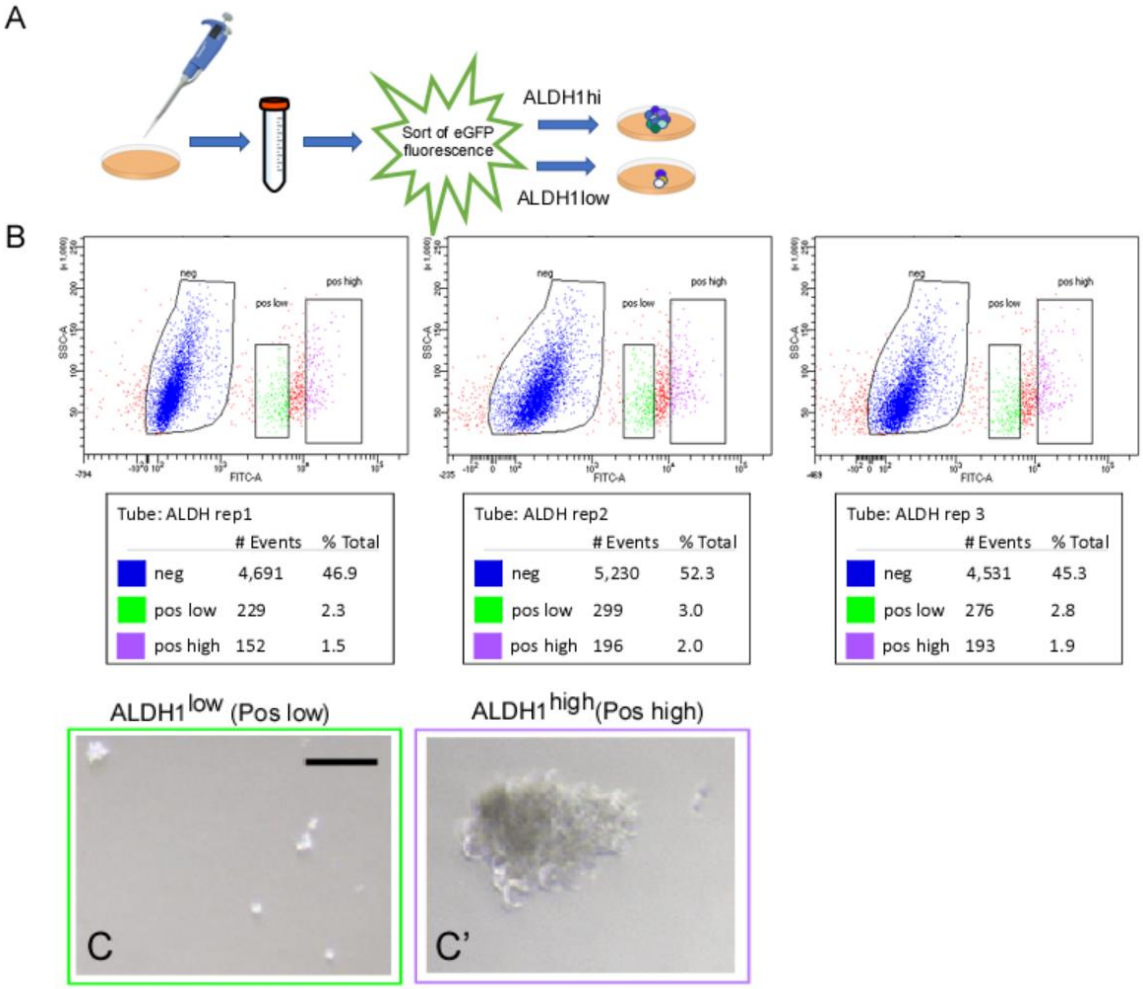
A
ALDH1hi
Sort of eGFP fluorescence
ALDH1low
B
neg
pos low
pos high
SSC-A
FITC-A
Tube: ALDH rep1
Events
% Total
neg 4,691 46.9
pos low 229 2.3
pos high 152 1.5
Tube: ALDH rep2
Events
% Total
neg 5,230 52.3
pos low 299 3.0
pos high 196 2.0
Tube: ALDH rep 3
Events
% Total
neg 4,531 45.3
pos low 276 2.8
pos high 193 1.9
ALDH1low (Pos low)
ALDH1high(Pos high)
C
C'

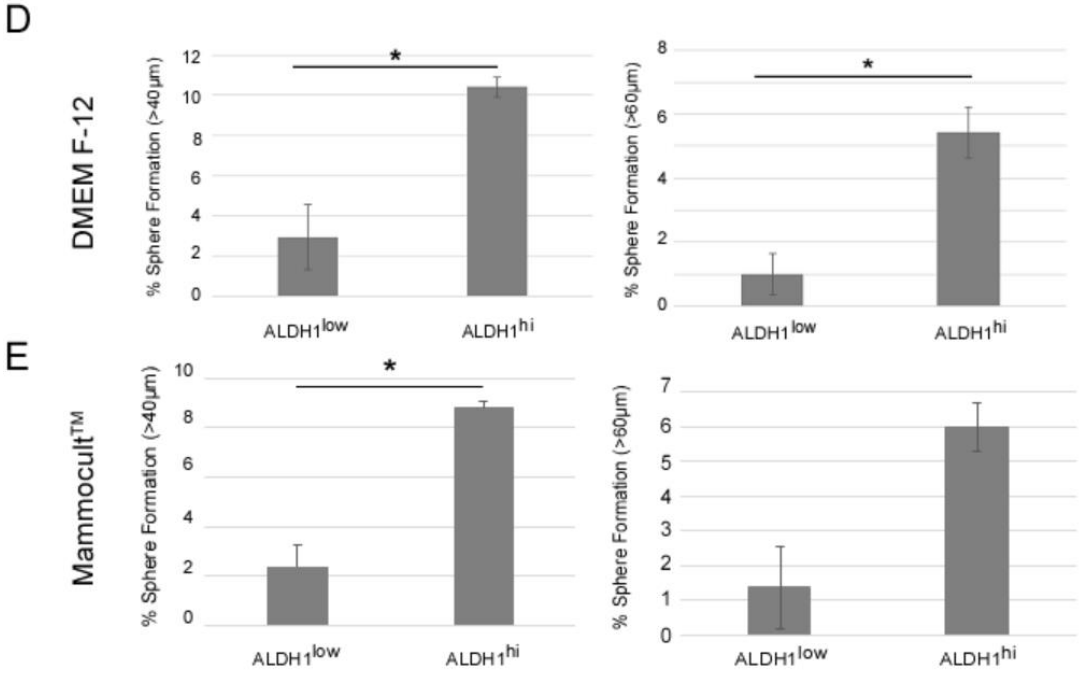
D
DMEM F-12
% Sphere Formation (>40µm)
% Sphere Formation (>60µm)
ALDH1low
ALDH1hi
E
Mammocult™
% Sphere Formation (>40µm)
% Sphere Formation (>60µm)
ALDH1low
ALDH1hi

Figure 12: The number of mammospheres formed in ALDH1^{high} cells are greater than ALDH1^{low} cells. A) Schematic of experimental design for mammosphere formation assay with ALDH1^{low} and ALDH1^{high} sorted cells. (B) FASC was conducted to measure eGFP signal (FITC: x-axis) and side-scattered light (SSC-A: y-axis) measured cell granularity in MDA-MB-231 cells. Gated populations negative/ background fluorescence (neg), ALDH1-positive low-fluorescing (pos low) and ALDH1-positive high-fluorescing (pos high). Each repetition represents an independent infection. (C) Representative mammosphere images in bright-field from ALDH1^{low} and ALDH1^{high} cells. (D) Quantification, in percent, of mammospheres ≥40 μm and ≥60 μm formed from ALDH1^{low} and ALDH1^{high} cells in DMEM F-12 media. (E) Quantification, in percent, of mammospheres ≥40 μm and ≥60 μm formed from ALDH1^{low} and ALDH1^{high} cells in Mammocult™ media. Error bars represent standard error of the mean percentage of three independent co-infections. *$p<0.05$. Statistical significance was analyzed using a Student's paired t-test. Scale bar measures 40μm.

DISCUSSION

Approximately one-third of patients with triple-negative breast cancer (TNBC) will experience tumour relapse within the first 3 years after treatment (Dent et al., 2007). Compared to other subtypes of breast cancer, TNBC has a higher rate of cerebral metastases, visceral metastases, and local relapse (Rodriguez et al., 2006). Pre-clinical drug screening has become a focus in translational biology to better understand individual patient responses to various treatments. TNBCs are known to be made up of a heterogeneous population of cells that add to the complexity of a tumour (Heppner, 1984). Furthermore, subpopulations of cells in TNBCs are known to respond differently to treatment (Visvader and Lindeman, 2006). Targeting the bulk of a tumour and targeting subpopulations of cells that evade treatment is a central focus in resolving factors contributing to relapse.

Recently, platinum agents have shown success in further enhancing chemotherapy regimens and patient responses (Hurley et al., 2013; Sikov et al., 2009). Currently, there is no data in the literature that test the addition of platinum agent carboplatin (Ca) to test responses imitating the timing of administration in the clinic, in TNBC cell lines. To mimic a clinical setting the platinum drug, carboplatin, was used in combination with standard of care (SOC) doxorubicin plus cyclophosphamide the paclitaxel (AC/T) treatment (Figure 1A) using the TNBC cell line MDA-MB-231wt (Figure 2A). We found that approximately 8% of MDA-MB-231 cells remained viable after treatment with AC/T+Ca, a decrease of approximately 9% compared to AC/T alone. The further decrease in cell viability with the addition of carboplatin to chemotherapy regimens is consistent with the literature (Wang and Lippard, 2005).

While preliminary results from drug screens are often determined through the *in vitro* techniques, the use of zebrafish, with an intact microenvironment, provided a more translational model for drug-response. Using zebrafish to determine drug responses in cells has gained reputability as a pre-clinical model in which survival data from patients can later be compared. Labelled cells were injected into zebrafish, followed by addition of chemotherapy drugs to determine the resistance of these cells to treatment. Using this method, tumour burden was measured, as area of fluorescence, before and after treatment to determine the effectiveness of treatment on decreasing tumour burden. The knockdown of Spy1, an atypical cell cycle regulator implicated in breast cancer, further sensitized cells to AC/T+Ca treatment (Figure 3C). While findings are preliminary, they suggest that zebrafish can be utilized as *in vivo* model to elucidate Spy1's role in resistance to treatment in TNBCs. These findings support similar published data in which the knock-down of Spy1 sensitizes ER+ breast cancer cells to tamoxifen treatment (Ferraiuolo et al., 2017).

While there was a statistically significant difference in the area of fluorescence, a large amount of variability was found within groups. Standardization of treatment involves many technical aspects leaving several possible explanations for the large deviation. One experimental procedure that needs better standardization is the number of cells injected. Even though the injection needle is tapered to the same length, it is difficult to ensure that the same number of suspended cells are injected every time, especially if trials are completed over multiple days. Standardizing the number of cells injected will allow greater comparability of replicates and data sets. Assuming the same number of cells are injected, the staining of cells is not entirely optimal and can result in

an inaccurate measure of tumour burden. The area of fluorescence was compared within fish, before and after treatment, and presented as fold change to mitigate variability between individuals. The zebrafish are stored in the same well during the duration of their treatment with the addition and removal of embryo water, with or without drugs, completed by manual pipetting. The removal or addition of embryo water to the well is a stressful event for the embryo. If the embryo becomes stressed it may be necessary to leave some embryo water in the well prior to the addition of new embryo water. If all the embryo water containing drugs cannot be removed it is possible that drugs remaining in the well of the plate could affect cell viability. Though it's unlikely that it would have a large impact at such dilute concentrations the possibility of enhancing treatment cannot be discounted. Lastly, what cannot be controlled for is variability in metabolism between zebrafish. Variation in the metabolism of each fish means that some fish may be affected by drugs to a larger or lesser extent. Since the breakdown of drugs into their functional components are necessary, a decrease in fish metabolism would reduce the availability of drugs to act on the cancer cells. Varying metabolism of drugs between fish can create variability in the overall area of fluorescence if drugs are not broken down at the same rate. To mitigate these issues, White et al., suggests the use of statistical methods that accounts for signal variability using power and significance values to account for false-call rates (White et al., 2016), though this is geared toward high-throughput samples (White et al., 2013). Sample size of 40-50 fish are common in low- to mid-throughput screening, however sizes up to 100-200 have been recommended (Veinotte et al., 2014). Increasing the number of individuals will increase the accuracy of fold change quantification and decrease standard deviation.

If *in vitro* data is an indication, it is conceivable that a resistant population of cells will remain in the zebrafish. Previous *in vitro* studies found that MDA-MB-231 cells that survived treatment with paclitaxel had high expression of stemness markers – Sox2, OCT3/4, c-Myc, Nanog – compared to untreated populations (Jeong et al., 2016). Therefore, it is reasonable to believe that the drug-resistant population would possess stem-like characteristics that may allow them to evade cell death mechanisms. A critical step after treatment would be the isolation and characterization of the drug-resistant populations. Hypothesizing that drug-resistant cells have some stem-like qualities, determining whether the drug-resistant populations display markers of cancer stem/progenitor cells – ALDH, $CD44^+$, $CD24^-$– would provide an excellent characterization of these drug-resistant cells.

In preparation for the use of patient samples in the Spy1 trial, drug-sensitive and drug-resistant standards are necessary to establish, to which patient samples will be compared. Since the knockdown of Spy1 sensitized TNBC cells to AC/T+Ca treatment, knockdown and overexpression of Spy1 are important standards for patient sample comparison. Additionally, since CSCs are highly drug-resistant compared to more differentiated cells, $ALDH^{+/high}$ and $ALDH^-$ cells, as well as $CD44^+/CD24^-$ and $CD44^-/CD24^+$ cells would provide an excellent standard for drug-resistant and drug-sensitive populations. Protocols for isolation of $CD44^+CD24^-$ populations are currently being optimized. Isolation of $ALDH^{+/high}$ populations is routinely completed by use of the ALDEFLUOR™ assay. The ALDEFLUOR™ kit has been used in numerous studies as a method for identifying ALDH expression in cells using fluorophore GFP, as a marker for BCSCs. Optimization of this assay involved a number of steps. STEMCELL™

Technologies, used the SK-BR-3 cell line as a positive control for ALDH expression as it has a substantial $ALDH^+$ expression (STEMCELL Technologies, 2009, 2011). MCF-7 cells were used as a negative control as studies examined a low ALDH population of <1% (Croker et al., 2009; Ginestier et al., 2007). TNBC cell line MDA-MB-231 cells are known to have an $ALDH^+$ population of approximately 10% (Ginestier et al., 2007; Kong et al., 2015). Unfortunately, the SK-BR-3 cell line was not available at that time and would have provided an excellent positive control. Inhibitor of ALDH, DEAB, was used as a control for non-specific staining and an unstained control provided a control for background fluorescence (Figure 4B-C). Interestingly, there was a higher percent of $ALDH^+$ cells than what has been reported in the literature (Figure 4D) (Croker and Allan, 2012). Furthermore, it has been reported that MDA-MB-231 populations have high levels of transcript variation (Nguyen et al., 2016), which may explain an increased $ALDH^+$ population. To validate these findings, cells were incubated longer as recommended by STEMCELL™ Technologies (STEMCELL Technologies, 2011) and samples were split and analyzed as 2 (ie. sample 1 and 1.1). Interestingly, the inhibited sample showed positive staining for ALDH (Figure 5C) which could be a result of multiple possibilities: the inhibitor did not work to inhibit ALDH and/or there is non-specific staining allowing for enriched detection of fluorescence. Equally as concerning was the high degree of variability between samples derived from the same plate of cells; this suggests that the enhanced $ALDH^+$ fluorescence in the prior experiment was not a result of transcript variation within the MDA-MB-231 population (Figure 5E). To test for non-specific staining, ALDEFLUOR™ fluorescence of MCF-7 cells were compared to MDA-MB-231 cells. Similar to the previous experiment, the DEAB inhibitor, showed increased

fluorescence compared to the unstained control, even though it was added before the additional of ALDEFLUOR™ reagent to ensure inhibition of enzymatic activity. Additionally, in MCF-7 cells there were a large amount of ALDEFLUOR$^+$ cells, which is inconsistent with previous findings (Figure 6B'') (STEMCELL Technologies, 2009). This suggests that the inhibitor DEAB and non-specific staining could both be possibilities in the variability of results shown. Future work with the ALDEFLUOR™ kit will utilize SK-BR-3s as a positive control for ALDEFLUOR™ and MCF-7s as a negative control. Further troubleshooting with the STEMCELL™ Technologies is required.

In addition to the technical issues with the ALDEFLUOR™ kit, it is known that this kit does not distinguish between isoforms of ALDH (STEMCELL Technologies, 2009). The identification of individual isoforms would serve as a powerful tool to enhance consistency of results while serving as a tool to further identify characteristics of specific isoforms. ALDH1A1 and ALDH1A3 are two important isoforms of ALDH1 that have been identified in BCSC populations (Croker et al., 2017; Marcato et al., 2011b). It has been demonstrated that ALDH1A1 expression is an important predictor of metastasis but does not greatly contribute to the expression of ALDH detected by the ALDEFLUOR™ kit (Croker et al., 2017). Inversely, ALDH1A3 is important in the overall detection of ALDH levels in the ALDEFLUOR™ assay but its expression has not demonstrated importance in predicting metastasis (Croker et al., 2017). For these reasons, the creation of reporters to detect expression of ALDH1A1 and ALDH1A3 are valuable tools for BCSC identification and are good candidates for verifying results from the ALDEFLUOR™ assay.

To investigate the validity of constructed reporter systems in the identification of breast cancer cells, MB-MDA-231s, MCF-7s and SK-BR-3s were infected or transfected, respectively, with ALDH1A1-dTomato or coinfected with ALDH1A1-eGFP and ALDH1A3-eGFP. Reporter systems were modelled after the development of a fluorescent reporter for CSC pluripotency gene, Nanog (Thiagarajan et al., 2015). From ALDEFLUOR™ data we know that MDA-MB-231 cells show 2 distinct populations when sorted, one similar to an inhibited sample and one with enhanced ALDH activity (Croker et al., 2009). MCF-7 cells were utilized because their ALDH activity is extremely low (Croker et al., 2009; Nie et al., 2015). Since many important vectors in our lab contain eGFP fluorescent reporters, dTomato was chosen as it would be beneficial for expression experiments. Our preliminary results using flow cytometry showed MB-MDA-231 and SK-BR-3 cells infected or transfected, respectively, however, ALDH1A1-dTomato exhibited lower expression, as indicated by low detection of a live signal in both cell lines (Figure 7C). The empty vector, expressing dTomato under the control of the eukaryotic translation EF-1α enhancer also showed very low or no fluorescence. Detection of dTomato by confocal microscopy confirmed these results as the dTomato signal was present, but very low, in MDA-MB-231 cells (Figure 7B-B'). These results were presumably not a result due to infection/transfection efficiency, as utilization of the same protocol resulted in other experiments resulted in successfully infected/transfected cells. While others have reported a strong signal with dTomato (Lee et al., 2012), there is no published material, using this vector, to directly compare results. Future work, using an antibody against dTomato could verify that the low signal is a true reflection

ALDH1A1 activity; however, would limit further experimentation and downstream applications due to fixation of the cells.

Due to the fact that ALDH1A3 is important in overall expression in the ALDEFLUOR™ assay, and technical issues prevented the construction of an ALDH1A3-dTomato reporter, eGFP containing reporters were constructed. The fluorophore eGFP was chosen as many have used in reporter-based systems (Kain et al., 1995), an antibody was readily available, and the live signal was strong enough to detect for FACS. Co-infection with ALDH1A1-eGFP and ALDH1A3-eGFP reporter constructs allowed us to quantify expression of important isoforms in the ALDH1 family. Co-infected MDA-MB-231 were sorted via FACS after gating for the 2% of lowest and highest fluorescence of the population. Gating was modelled after Croker et al., where the lowest and highest 20% of fluorescing cells represented $ALDH^{low}$ and $ALDH^{high}$ populations, respectively (Croker and Allan, 2012). Gates were unchanged for MCF-7 populations where there was a decreased percent of cells collected; this is not surprising considering MCF-7 have an extremely low stem cell population (STEMCELL Technologies, 2009). It is surprising, however, that a notable percentage of MCF-7 cells were $eGFP^{+}$, contrary to findings from the ALDEFLUOR™ kit (STEMCELL Technologies, 2009), however this population represents a smaller proportion of cells compared to $eGFP^{+}$ cells in MDA-MB-231 cells. Therefore, these results support the functionality of the reporter system designed.

Previous literature suggests that Spy1 plays an important role in maintaining stem-like characteristics in CSC of glioblastoma multiforme (Lubanska and Porter, 2017). Additionally, Spy1 is known to contribute to tamoxifen resistance in a breast cancer cell line (Ferraiuolo et al., 2017). The increase in transcript levels from $ALDH1^{low}$

to ALDH1^{high} cells, in both MDA-MB-231 and MCF-7 cells, indicated that Spy1 may contribute to BCSC properties, including drug-resistance. To investigate the role of Spy1 in BCSC, the ALDH1^{low} and ALDH1^{high} populations were isolated using our reporter system, and hSpy1, ALDH1A1, ALDH1A3 and eGFP transcript levels were quantified by qRT-PCR (Figure 9D-E). Levels of all transcripts were elevated in ALDH1^{high} populations compared to ALDH1^{low} populations, in both cell lines. It is interesting that eGFP mRNA levels in either cell line were not statistically significant, considering cells were sorted eGFP on protein expression, comparison to eGFP negative populations is a future experiment.

Ideally, protein levels of ALDH would be quantified in addition to mRNA expression, however with gates established as the lowest and highest 2% of fluorescence, scaling to the number of cells required for protein would be a challenge. An alternative would involve gating to include a larger percentage of cells in low and high-fluorescent populations; however, as gates become close together, mRNA and protein differences between low and high-fluorescing populations would be less obvious. An alternative would be to generate GFP tagged ALDH1 isoforms, expressed under its endogenous enhancers to distinguish post-translational regulatory mechanisms of ALDH1 in different cell lines. This would provide an easier detection method by western blotting, using anti-GFP antibodies, if enough cells can be collected, and would determine whether there are translational mechanisms that regulate ALDH1 activity. Transcript levels of ALDH1A3 increased in ALDH1^{high} population of MDA-MB-231 cells and MCF-7 cells. This data supports the literature demonstrating that the majority of fluorescence in the ALDEFLUOR™ assay is a result of the ALDH1A3 expression (Marcato et al., 2011b).

Mammosphere formation assays provide a functional representation of the percentage of CSCs in a given population (Grimshaw et al., 2008). $ALDH1^{low}$ and $ALDH1^{high}$ were collected from MDA-MB-231 cells co-infected with ALDH1A1-eGFP and ALDH1A3-eGFP. Sorted cells were put in two different media conditions. Supplements and growth factors are known to have a large impact on cellular proliferation and mammosphere formation (Dontu et al., 2003; Wang et al., 2014), mammospheres were cultured in 2 types of mammosphere media. $ALDH1^{high}$ cells had a greater capacity for sphere formation when spheres were ≥40μm and ≥60μm. In all media types and cell sizes, mammosphere formation was still possible in approximately 1-3% of $ALDH1^{low}$ cells (Figure 10D). There are many isoforms within the ALDH family, many of which have applications in various cancers. While ALDH1A1 and ALDH1A3 are important in the identification of the CSC population in TNBCs, ALDH expression is not limited to those isoforms (STEMCELL Technologies, 2009). Further construction of reporters of relevant ALDH isoforms, such as ALDH3A1, are important in understanding what specific isoforms contribute to different characteristics of CSC, both alone and together. Due to the specific roles of select isoforms, fluorescent reporters of select isoforms may provide further insight into select isoforms important in drug-resistance, and other clinically relevant applications.

Future experiments regarding validation of these ALDH1A1-eGFP and ALDH1A3-eGFP reporters are necessary. To better understand the role of each individual isoform, described experiments should be repeated assessing 1 isoform at a time. Assays involving co-infection with ALDH1A1-eGFP and ALDH1A3-eGFP was initially used as a tool to answer questions of ALDH's role in stemness, as an alternative

to the ALDELFUOR™ kit while it was being optimized. When results from the ALDEFLUOR™ assay are reproducible, an issue currently being addressed by a colleague, co-infected populations with ALDH1A1-eGFP and ALDH1A3-eGFP can validate eGFP fluorescence in the ALDEFLUOR™ assay. These preliminary results suggest that co-infection of ALDH1A1-eGFP and ALDH1A3-eGFP may be an effective tool in isolating CSC, as suggested by the mammosphere assay. Validation using transplantation assays and lineage tracing assays *in vivo* would be importing in supporting evidence for these reporters as tools for CSC isolation. In the event these reporter constructs are effective in isolating CSC populations, drug testing with AC/T+Ca *in vitro* and *in vivo* could establish standards for drug-sensitive ($ALDH1^{-/low}$) and drug-resistant ($ALDH1^{high}$) for the Spy1 clinical trial.

This thesis set out to investigate relapse in TNBC patients. Data from *in vitro* and *in vivo* models suggest that the addition of carboplatin to SOC AC/T treatment sensitizes cells to treatment using clinically relevant drug regimens. Technical tools were developed to study CSC populations, which have major implications in relapse and remains a major barrier. While these reporter constructs need further validation, they have many applications moving forward. CSC and more differentiated populations can be examined for viability after AC/T±Ca *in vitro*. Additionally, reporter-based fluorescence can allow for long-term treatment *in vivo* of CSC populations. Since CSC are known to be resistant to chemotherapies, these reporters may provide insight into TNBC drug-resistant populations. Insight into treating and identifying drug-resistant populations is critical to enhance the predictability of TNBC recurrence, which remains a real concern for many patients after treatment.

REFERENCES

Aigner, S., Sthoeger, Z.M., Fogel, M., Weber, E., Zarn, J., Ruppert, M., Zeller, Y., Vestweber, D., Stahel, R., Sammar, M., et al. (1997). CD24, a mucin-type glycoprotein, is a ligand for P-selectin on human tumor cells. Blood *89*, 3385–3395.

Al Sorkhy, M., Ferraiuolo, R.-M., Jalili, E., Malysa, A., Fratiloiu, A.R., Sloane, B.F., and Porter, L.A. (2012). The cyclin-like protein Spy1/RINGO promotes mammary transformation and is elevated in human breast cancer. BMC Cancer *12*.

Al-Ejeh, F., Smart, C.E., Morrison, B.J., Chenevix-Trench, G., López, J.A., Lakhani, S.R., Brown, M.P., and Khanna, K.K. (2011). Breast cancer stem cells: treatment resistance and therapeutic opportunities. Carcinogenesis *32*, 650–658.

Alexa, K., Choe, S.-K., Hirsch, N., Etheridge, L., Laver, E., and Sagerström, C.G. (2009). Maternal and Zygotic aldh1a2 Activity Is Required for Pancreas Development in Zebrafish. PLoS ONE *4*.

Al-Hajj, M., Wicha, M.S., Benito-Hernandez, A., Morrison, S.J., and Clarke, M.F. (2003). Prospective identification of tumorigenic breast cancer cells. Proc. Natl. Acad. Sci. U. S. A. *100*, 3983–3988.

Allsopp, R.C., Vaziri, H., Patterson, C., Goldstein, S., Younglai, E.V., Futcher, A.B., Greider, C.W., and Harley, C.B. (1992). Telomere Length Predicts Replicative Capacity of Human Fibroblasts. Proc. Natl. Acad. Sci. U. S. A. *89*, 10114–10118.

André, F., and Zielinski, C.C. (2012). Optimal strategies for the treatment of metastatic triple-negative breast cancer with currently approved agents. Ann. Oncol. Off. J. Eur. Soc. Med. Oncol. *23 Suppl 6*, vi46-51.

Arellano, M., and Moreno, S. (1997). Regulation of CDK/cyclin complexes during the cell cycle. Int. J. Biochem. Cell Biol. *29*, 559–573.

Aruffo, A., Stamenkovic, I., Melnick, M., Underhill, C.B., and Seed, B. (1990). CD44 is the principal cell surface receptor for hyaluronate. Cell *61*, 1303–1313.

Askari, A.T., Unzek, S., Popovic, Z.B., Goldman, C.K., Forudi, F., Kiedrowski, M., Rovner, A., Ellis, S.G., Thomas, J.D., DiCorleto, P.E., et al. (2003). Effect of stromal-cell-derived factor 1 on stem-cell homing and tissue regeneration in ischaemic cardiomyopathy. Lancet Lond. Engl. *362*, 697–703.

Asselin-Labat, M.-L., Vaillant, F., Sheridan, J.M., Pal, B., Wu, D., Simpson, E.R., Yasuda, H., Smyth, G.K., Martin, T.J., Lindeman, G.J., et al. (2010). Control of mammary stem cell function by steroid hormone signalling. Nature *465*, 798.

Autier, P., Boniol, M., Gavin, A., and Vatten, L.J. (2011). Breast cancer mortality in neighbouring European countries with different levels of screening but similar access to treatment: trend analysis of WHO mortality database. The BMJ *343*.

Balicki, D. (2007). Moving Forward in Human Mammary Stem Cell Biology and Breast Cancer Prognostication Using ALDH1. Cell Stem Cell *1*, 485–487.

Bao, S., Wu, Q., McLendon, R.E., Hao, Y., Shi, Q., Hjelmeland, A.B., Dewhirst, M.W., Bigner, D.D., and Rich, J.N. (2006). Glioma stem cells promote radioresistance by preferential activation of the DNA damage response. Nature *444*, 756–760.

Barnes, E.A., Porter, L.A., Lenormand, J.-L., Dellinger, R.W., and Donoghue, D.J. (2003). Human Spy1 promotes survival of mammalian cells following DNA damage. Cancer Res. *63*, 3701–3707.

Bettinardi, V., Picchio, M., Di Muzio, N., and Gilardi, M.C. (2012). Motion Management in Positron Emission Tomography/Computed Tomography for Radiation Treatment Planning. Semin. Nucl. Med. *42*, 289–307.

Bharadwaj, R., and Yu, H. (2004). The spindle checkpoint, aneuploidy, and cancer. Oncogene *23*, 2016–2027.

Blackburn, J.S., and Langenau, D.M. (2014). Zebrafish as a model to assess cancer heterogeneity, progression and relapse. Dis. Model. Mech. *7*, 755–762.

Blalock, W.L., Weinstein-Oppenheimer, C., Chang, F., Hoyle, P.E., Wang, X.-Y., Algate, P.A., Franklin, R.A., Oberhaus, S.M., Steelman, L.S., and McCubrey, J.A. (1999). Signal transduction, cell cycle regulatory, and anti-apoptotic pathways regulated by IL-3 in hematopoietic cells: possible sites for intervention with anti-neoplastic drugs. Leuk. 08876924 *13*, 1109–1166.

Bleyer, A., and Welch, H.G. (2012). Effect of Three Decades of Screening Mammography on Breast-Cancer Incidence. N. Engl. J. Med. *367*, 1998–2005.

Bonner, J.A., Harari, P.M., Giralt, J., Cohen, R.B., Jones, C.U., Sur, R.K., Raben, D., Baselga, J., Spencer, S.A., Zhu, J., et al. (2010). Radiotherapy plus cetuximab for locoregionally advanced head and neck cancer: 5-year survival data from a phase 3 randomised trial, and relation between cetuximab-induced rash and survival. Lancet Oncol. *11*, 21–28.

Buick, R.N., Minden, M.D., and McCulloch, E.A. (1979). Self-renewal in culture of proliferative blast progenitor cells in acute myeloblastic leukemia. Blood *54*, 95–104.

Bunting, K.D., and Townsend, A.J. (1996). Protection by Transfected Rat or Human Class 3 Aldehyde Dehydrogenases against the Cytotoxic Effects of Oxazaphosphorine Alkylating Agents in Hamster V79 Cell Lines DEMONSTRATION OF ALDOPHOSPHAMIDE METABOLISM BY THE HUMAN CYTOSOLIC CLASS 3 ISOZYME. J. Biol. Chem. *271*, 11891–11896.

Burnell, M.J., O'Connor, E.M., Chapman, J.W., Levine, M.N., Pritchard, K.I., O'Brien, P.S., Howarth, K.J., Ding, Z., Whelan, T.J., and Shepherd, L.E. (2008). Triple-negative receptor status and prognosis in the NCIC CTG MA. 21 adjuvant breast cancer trial. J. Clin. Oncol. *26*, 550–550.

Byrski, T., Dent, R., Blecharz, P., Foszczynska-Kloda, M., Gronwald, J., Huzarski, T., Cybulski, C., Marczyk, E., Chrzan, R., Eisen, A., et al. (2012). Results of a phase II open-label, non-randomized trial of cisplatin chemotherapy in patients with BRCA1-positive metastatic breast cancer. Breast Cancer Res. BCR *14*, R110.

Canadian Cancer Statistics Advisory Committee (2017). Canadian Cancer Statistics 2017.

Carey, L.A., Rugo, H.S., Marcom, P.K., Mayer, E.L., Esteva, F.J., Ma, C.X., Liu, M.C., Storniolo, A.M., Rimawi, M.F., Forero-Torres, A., et al. (2012). TBCRC 001: randomized phase II study of cetuximab in combination with carboplatin in stage IV triple-negative breast cancer. J. Clin. Oncol. Off. J. Am. Soc. Clin. Oncol. *30*, 2615–2623.

Charafe-Jauffret, E., Ginestier, C., and Birnbaum, D. (2009a). Breast cancer stem cells: tools and models to rely on. BMC Cancer *9*, 202.

Charafe-Jauffret, E., Ginestier, C., Iovino, F., Wicinski, J., Cervera, N., Finetti, P., Hur, M.-H., Diebel, M.E., Monville, F., Dutcher, J., et al. (2009b). Breast cancer cell lines contain functional cancer stem cells with metastatic capacity and a distinct molecular signature. Cancer Res. *69*, 1302–1313.

Charafe-Jauffret, E., Ginestier, C., Iovino F, F., Tarpin, C., Diebel, M., Esterni, B., Houvenaeghel, G., Extra, J.-M., Bertucci, F., Jacquemier, J., et al. (2010). ALDH1-positive cancer stem cells mediate metastasis and poor clinical outcome in inflammatory breast cancer. Clin. Cancer Res. Off. J. Am. Assoc. Cancer Res. *16*, 45–55.

Cheang, M.C.U., Chia, S.K., Voduc, D., Gao, D., Leung, S., Snider, J., Watson, M., Davies, S., Bernard, P.S., Parker, J.S., et al. (2009). Ki67 Index, HER2 Status, and Prognosis of Patients With Luminal B Breast Cancer. JNCI J. Natl. Cancer Inst. *101*, 736.

Chen, J., Li, Y., Yu, T.-S., McKay, R.M., Burns, D.K., Kernie, S.G., and Parada, L.F. (2012). A restricted cell population propagates glioblastoma growth following chemotherapy. Nature *488*, 522–526.

Chen, Y., Thompson, D.C., Koppaka, V., Jester, J.V., and Vasiliou, V. (2013). Ocular Aldehyde Dehydrogenases: Protection against Ultraviolet Damage and Maintenance of Transparency for Vision. Prog. Retin. Eye Res. *33*, 28–39.

Cheng, A., Xiong, W., James E. Ferrell, J., and Solomon, M.J. (2005). Identification and Comparative Analysis of Multiple Mammalian Speedy/Ringo Proteins. Cell Cycle *4*, 155–165.

Clay, M., Tabor, M., Owen, J., Carey, T., Bradford, C., Wolf, G., Wicha, M., and Prince, M. (2010). Single marker identification of head and neck squamous cell carcinoma cancer stem cells with aldehyde dehyrdrogenase. Head Neck *32*, 1195–1201.

Clevers, H. (2011). The cancer stem cell: premises, promises and challenges. Nat. Med. *17*, 313.

Collins, C.A., and Watt, F.M. (2008). Dynamic regulation of retinoic acid-binding proteins in developing, adult and neoplastic skin reveals roles for β-catenin and Notch signalling. Dev. Biol. *324*, 55–67.

Croker, A.K., and Allan, A.L. (2012). Inhibition of aldehyde dehydrogenase (ALDH) activity reduces chemotherapy and radiation resistance of stem-like ALDHhiCD44+ human breast cancer cells. Breast Cancer Res. Treat. *133*, 75–87.

Croker, A.K., Goodale, D., Chu, J., Postenka, C., Hedley, B.D., Hess, D.A., and Allan, A.L. (2009). High aldehyde dehydrogenase and expression of cancer stem cell markers selects for breast cancer cells with enhanced malignant and metastatic ability. J. Cell. Mol. Med. *13*, 2236–2252.

Croker, A.K., Rodriguez-Torres, M., Xia, Y., Pardhan, S., Leong, H.S., Lewis, J.D., and Allan, A.L. (2017). Differential Functional Roles of ALDH1A1 and ALDH1A3 in Mediating Metastatic Behavior and Therapy Resistance of Human Breast Cancer Cells. Int. J. Mol. Sci. *18*.

Curtis, C., Shah, S.P., Chin, S.-F., Turashvili, G., Rueda, O.M., Dunning, M.J., Speed, D., Lynch, A.G., Samarajiwa, S., Yuan, Y., et al. (2012). The genomic and transcriptomic architecture of 2,000 breast tumours reveals novel subgroups. Nature *486*, 346.

Daniel, C.W., De Ome, K.B., Young, J.T., Blair, P.B., and Faulkin, L.J. (1968). The in vivo life span of normal and preneoplastic mouse mammary glands: a serial transplantation study. Proc. Natl. Acad. Sci. U. S. A. *61*, 53–60.

Dean, M. (2009). ABC transporters, drug resistance, and cancer stem cells. J. Mammary Gland Biol. Neoplasia *14*, 3–9.

Deans, A.J., and West, S.C. (2011). DNA interstrand crosslink repair and cancer. Nat. Rev. Cancer *11*, 467–480.

Dent, R., Trudeau, M., Pritchard, K.I., Hanna, W.M., Kahn, H.K., Sawka, C.A., Lickley, L.A., Rawlinson, E., Sun, P., and Narod, S.A. (2007). Triple-negative breast cancer: clinical features and patterns of recurrence. Clin. Cancer Res. Off. J. Am. Assoc. Cancer Res. *13*, 4429–4434.

Diallo-Danebrock, R., Ting, E., Gluz, O., Herr, A., Mohrmann, S., Geddert, H., Rody, A., Schaefer, K.-L., Baldus, S.E., Hartmann, A., et al. (2007). Protein expression profiling in high-risk breast cancer patients treated with high-dose or conventional dose-dense chemotherapy. Clin. Cancer Res. Off. J. Am. Assoc. Cancer Res. *13*, 488–497.

Diehn, M., Cho, R.W., Lobo, N.A., Kalisky, T., Dorie, M.J., Kulp, A.N., Qian, D., Lam, J.S., Ailles, L.E., Wong, M., et al. (2009). Association of Reactive Oxygen Species Levels and Radioresistance in Cancer Stem Cells. Nature *458*, 780–783.

Dontu, G., Al-Hajj, M., Abdallah, W.M., Clarke, M.F., and Wicha, M.S. (2003). Stem cells in normal breast development and breast cancer. Cell Prolif. *36*, 59–72.

Dontu, G., El-Ashry, D., and Wicha, M.S. (2004). Breast cancer, stem/progenitor cells and the estrogen receptor. Trends Endocrinol. Metab. *15*, 193–197.

Dowsett, M., and Haynes, B.P. (2003). Hormonal effects of aromatase inhibitors: focus on premenopausal effects and interaction with tamoxifen. J. Steroid Biochem. Mol. Biol. *86*, 255–263.

Duester, G., Mic, F.A., and Molotkov, A. (2003). Cytosolic retinoid dehydrogenases govern ubiquitous metabolism of retinol to retinaldehyde followed by tissue-specific metabolism to retinoic acid. Chem. Biol. Interact. *143–144*, 201–210.

Duong, H.-Q., Hwang, J.S., Kim, H.J., Kang, H.J., Seong, Y.-S., and Bae, I. (2012). Aldehyde dehydrogenase 1A1 confers intrinsic and acquired resistance to gemcitabine in human pancreatic adenocarcinoma MIA PaCa-2 cells. Int. J. Oncol. *41*, 855–861.

Dylla, S.J., Beviglia, L., Park, I.-K., Chartier, C., Raval, J., Ngan, L., Pickell, K., Aguilar, J., Lazetic, S., Smith-Berdan, S., et al. (2008). Correction: Colorectal Cancer Stem Cells Are Enriched in Xenogeneic Tumors Following Chemotherapy. PLoS ONE *3*.

Edwards, B.K., Noone, A.-M., Mariotto, A.B., Simard, E.P., Boscoe, F.P., Henley, S.J., Jemal, A., Cho, H., Anderson, R.N., Kohler, B.A., et al. (2014). Annual Report to the Nation on the Status of Cancer, 1975-2010, Featuring Prevalence of Comorbidity and Impact on Survival among Persons with Lung, Colorectal, Breast or Prostate Cancer. Cancer *120*, 1290–1314.

Elizondo, G., Corchero, J., Sterneck, E., and Gonzalez, F.J. (2000). Feedback Inhibition of the Retinaldehyde Dehydrogenase GeneALDH1 by Retinoic Acid through Retinoic Acid Receptor α and CCAAT/Enhancer-binding Protein β. J. Biol. Chem. *275*, 39747–39753.

Elizondo, G., Medina-Díaz, I.M., Cruz, R., Gonzalez, F.J., and Vega, L. (2009). Retinoic acid modulates retinaldehyde dehydrogenase 1 gene expression through the induction of GADD153–C/EBPβ interaction. Biochem. Pharmacol. *77*, 248.

Emadi, A., Jones, R.J., and Brodsky, R.A. (2009). Cyclophosphamide and cancer: golden anniversary. Nat. Rev. Clin. Oncol. *6*, 638–647.

Evans, T., Rosenthal, E.T., Youngblom, J., Distel, D., and Hunt, T. (1983). Cyclin: a protein specified by maternal mRNA in sea urchin eggs that is destroyed at each cleavage division. Cell *33*, 389–396.

Fan, C., Oh, D.S., Wessels, L., Weigelt, B., Nuyten, D.S.A., Nobel, A.B., van't Veer, L.J., and Perou, C.M. (2006). Concordance among gene-expression-based predictors for breast cancer. N. Engl. J. Med. *355*, 560–569.

Fenaux, P., Castaigne, S., Dombret, H., Archimbaud, E., Duarte, M., Morel, P., Lamy, T., Tilly, H., Guerci, A., and Maloisel, F. (1992). All-transretinoic acid followed by intensive chemotherapy gives a high complete remission rate and may prolong remissions in newly diagnosed acute promyelocytic leukemia: a pilot study on 26 cases. Blood *80*, 2176–2181.

Ferraiuolo, R.-M., Tubman, J., Sinha, I., Hamm, C., and Porter, L.A. (2017). The cyclin-like protein, SPY1, regulates the ERα and ERK1/2 pathways promoting tamoxifen resistance. Oncotarget *8*, 23337–23352.

Fisher, B., Brown, A.M., Dimitrov, N.V., Poisson, R., Redmond, C., Margolese, R.G., Bowman, D., Wolmark, N., Wickerham, D.L., and Kardinal, C.G. (1990). Two months of doxorubicin-cyclophosphamide with and without interval reinduction therapy compared with 6 months of cyclophosphamide, methotrexate, and fluorouracil in positive-node breast cancer patients with tamoxifen-nonresponsive tumors: results from the National Surgical Adjuvant Breast and Bowel Project B-15. J. Clin. Oncol. Off. J. Am. Soc. Clin. Oncol. *8*, 1483–1496.

Fletcher, J.I., Haber, M., Henderson, M.J., and Norris, M.D. (2010). ABC transporters in cancer: more than just drug efflux pumps. Nat. Rev. Cancer *10*, 147–156.

Friedman, H.S., Colvin, O.M., Kaufmann, S.H., Ludeman, S.M., Bullock, N., Bigner, D.D., and Griffith, O.W. (1992). Cyclophosphamide resistance in medulloblastoma. Cancer Res. *52*, 5373–5378.

Gastwirt, R.F., Slavin, D.A., McAndrew, C.W., and Donoghue, D.J. (2006). Spy1 Expression Prevents Normal Cellular Responses to DNA Damage INHIBITION OF APOPTOSIS AND CHECKPOINT ACTIVATION. J. Biol. Chem. *281*, 35425–35435.

Ghebeh, H., Sleiman, G.M., Manogaran, P.S., Al-Mazrou, A., Barhoush, E., Al-Mohanna, F.H., Tulbah, A., Al-Faqeeh, K., and Adra, C.N. (2013). Profiling of normal and malignant breast tissue show CD44high/CD24low phenotype as a predominant stem/progenitor marker when used in combination with Ep-CAM/CD49f markers. BMC Cancer *13*, 289.

Ginestier, C., Hur, M.H., Charafe-Jauffret, E., Monville, F., Dutcher, J., Brown, M., Jacquemier, J., Viens, P., Kleer, C., Liu, S., et al. (2007). ALDH1 is a marker of normal and malignant human mammary stem cells and a predictor of poor clinical outcome. Cell Stem Cell *1*, 555–567.

Girard, F., Strausfeld, U., Fernandez, A., and Lamb, N.J. (1991). Cyclin A is required for the onset of DNA replication in mammalian fibroblasts. Cell *67*, 1169–1179.

Gluz, O., Nitz, U.A., Harbeck, N., Ting, E., Kates, R., Herr, A., Lindemann, W., Jackisch, C., Berdel, W.E., Kirchner, H., et al. (2008). Triple-negative high-risk breast cancer derives particular benefit from dose intensification of adjuvant chemotherapy: results of WSG AM-01 trial. Ann. Oncol. Off. J. Eur. Soc. Med. Oncol. *19*, 861–870.

Goldhirsch, A., Wood, W.C., Coates, A.S., Gelber, R.D., Thürlimann, B., and Senn, H.-J. (2011). Strategies for subtypes—dealing with the diversity of breast cancer: highlights of the St Gallen International Expert Consensus on the Primary Therapy of Early Breast Cancer 2011. Ann. Oncol. *22*, 1736–1747.

Golipour, A., Myers, D., Seagroves, T., Murphy, D., Evan, G.I., Donoghue, D.J., Moorehead, R.A., and Porter, L.A. (2008). The Spy1/RINGO family represents a novel mechanism regulating mammary growth and tumorigenesis. Cancer Res. *68*, 3591–3600.

Grimshaw, M.J., Cooper, L., Papazisis, K., Coleman, J.A., Bohnenkamp, H.R., Chiapero-Stanke, L., Taylor-Papadimitriou, J., and Burchell, J.M. (2008). Mammosphere culture of metastatic breast cancer cells enriches for tumorigenic breast cancer cells. Breast Cancer Res. *10*, R52.

Gusterson, B. (2009). Do "basal-like" breast cancers really exist? Nat. Rev. Cancer *9*, 128.

Hall, A.G., and Tilby, M.J. (1992). Mechanisms of action of, and modes of resistance to, alkylating agents used in the treatment of haematological malignancies. Blood Rev. *6*, 163–173.

Hamm, C. (2011). SPY-1 Ontario Cancer Trials.

Hayakawa, Y., Ariyama, H., Stancikova, J., Sakitani, K., Asfaha, S., Renz, B.W., Dubeykovskaya, Z.A., Shibata, W., Wang, H., Westphalen, C.B., et al. (2015). Mist1 expressing gastric stem cells maintain the normal and neoplastic gastric epithelium and are supported by a perivascular stem cell niche. Cancer Cell *28*, 800–814.

He, S., Nakada, D., and Morrison, S.J. (2009). Mechanisms of Stem Cell Self-Renewal. Annu. Rev. Cell Dev. Biol. *25*, 377–406.

Heinemann, V., Weikersthal, L.F. von, Decker, T., Kiani, A., Vehling-Kaiser, U., Al-Batran, S.-E., Heintges, T., Lerchenmüller, C., Kahl, C., Seipelt, G., et al. (2014). FOLFIRI plus cetuximab versus FOLFIRI plus bevacizumab as first-line treatment for patients with metastatic colorectal cancer (FIRE-3): a randomised, open-label, phase 3 trial. Lancet Oncol. *15*, 1065–1075.

Hellsten, R., Johansson, M., Dahlman, A., Sterner, O., and Bjartell, A. (2011). Galiellalactone Inhibits Stem Cell-Like ALDH-Positive Prostate Cancer Cells. PLoS ONE *6*.

Henderson, I.C., Berry, D.A., Demetri, G.D., Cirrincione, C.T., Goldstein, L.J., Martino, S., Ingle, J.N., Cooper, M.R., Hayes, D.F., Tkaczuk, K.H., et al. (2003). Improved Outcomes From Adding Sequential Paclitaxel but Not From Escalating Doxorubicin Dose in an Adjuvant Chemotherapy Regimen for Patients With Node-Positive Primary Breast Cancer. J. Clin. Oncol. *21*, 976–983.

Heppner, G.H. (1984). Tumor Heterogeneity. Cancer Res. *44*, 2259–2265.

Hess, D., Meyerrose, T., Wirthlin, L., Craft, T., Herrbrich, P., Creer, M., and Nolta, J. (2004). Functional characterization of highly purified human hematopoietic repopulating cells isolated according to aldehyde dehydrogenase activity. Blood *104*, 1648–1655.

Hess, D.A., Wirthlin, L., Craft, T.P., Herrbrich, P.E., Hohm, S.A., Lahey, R., Eades, W.C., Creer, M.H., and Nolta, J.A. (2006). Selection based on CD133 and high aldehyde dehydrogenase activity isolates long-term reconstituting human hematopoietic stem cells. Blood *107*, 2162–2169.

Hollestelle, A., Nagel, J.H.A., Smid, M., Lam, S., Elstrodt, F., Wasielewski, M., Ng, S.S., French, P.J., Peeters, J.K., Rozendaal, M.J., et al. (2010). Distinct gene mutation profiles among luminal-type and basal-type breast cancer cell lines. Breast Cancer Res. Treat. *121*, 53–64.

Howe, K., Clark, M.D., Torroja, C.F., Torrance, J., Berthelot, C., Muffato, M., Collins, J.E., Humphray, S., McLaren, K., Matthews, L., et al. (2013). The zebrafish reference genome sequence and its relationship to the human genome. Nature *496*, 498–503.

Hurley, J., Reis, I.M., Rodgers, S.E., Gomez-Fernandez, C., Wright, J., Leone, J.P., Larrieu, R., and Pegram, M.D. (2013). The use of neoadjuvant platinum-based chemotherapy in locally advanced breast cancer that is triple negative: retrospective analysis of 144 patients. Breast Cancer Res. Treat. *138*, 783–794.

Ikawa, M., Impraim, C.C., Wang, G., and Yoshida, A. (1983). Isolation and characterization of aldehyde dehydrogenase isozymes from usual and atypical human livers. J. Biol. Chem. *258*, 6282–6287.

Illa-Bochaca, I., Fernandez-Gonzalez, R., Shelton, D.N., Welm, B.E., Ortiz-de-Solorzano, C., and Barcellos-Hoff, M.H. (2010). Limiting-dilution transplantation assays in mammary stem cell studies. Methods Mol. Biol. Clifton NJ *621*, 29–47.

Ishikawa, F., Yoshida, S., Saito, Y., Hijikata, A., Kitamura, H., Tanaka, S., Nakamura, R., Tanaka, T., Tomiyama, H., Saito, N., et al. (2007). Chemotherapy-resistant human AML stem cells home to and engraft within the bone-marrow endosteal region. Nat. Biotechnol. *25*, 1315.

Jatoi, I., Anderson, W.F., Jeong, J.-H., and Redmond, C.K. (2011). Breast cancer adjuvant therapy: time to consider its time-dependent effects. J. Clin. Oncol. Off. J. Am. Soc. Clin. Oncol. *29*, 2301–2304.

Jeffrey, P.D., Russo, A.A., Polyak, K., Gibbs, E., Hurwitz, J., Massagué, J., and Pavletich, N.P. (1995). Mechanism of CDK activation revealed by the structure of a cyclinA-CDK2 complex. Nature *376*, 313–320.

Jeong, Y.-J., Kang, J.S., Lee, S.I., So, D.M., Yun, J., Baek, J.Y., Kim, S.K., Lee, K., and Park, S.-K. (2016). Breast cancer cells evade paclitaxel-induced cell death by developing resistance to dasatinib. Oncol. Lett. *12*, 2153.

Jordan, M.A., and Wilson, L. (2004). Microtubules as a target for anticancer drugs. Nat. Rev. Cancer *4*, 253–265.

Kain, S., Adams, M., Kondepudi, A., Yang, T., W Ward, W., and Kitts, P. (1995). Green fluorescent protein as a reporter of gene expression and protein localization. BioTechniques *19*, 650–655.

Kao, J., Salari, K., Bocanegra, M., Choi, Y.-L., Girard, L., Gandhi, J., Kwei, K.A., Hernandez-Boussard, T., Wang, P., Gazdar, A.F., et al. (2009). Molecular profiling of breast cancer cell lines defines relevant tumor models and provides a resource for cancer gene discovery. PloS One *4*, e6146.

Karaiskou, A., Perez, L.H., Ferby, I., Ozon, R., Jessus, C., and Nebreda, A.R. (2001). Differential Regulation of Cdc2 and Cdk2 by RINGO and Cyclins. J. Biol. Chem. *276*, 36028–36034.

Kennecke, H., Yerushalmi, R., Woods, R., Cheang, M.C.U., Voduc, D., Speers, C.H., Nielsen, T.O., and Gelmon, K. (2010). Metastatic behavior of breast cancer subtypes. J. Clin. Oncol. Off. J. Am. Soc. Clin. Oncol. *28*, 3271–3277.

Khoury, T., Ademuyiwa, F.O., Chandraseekhar, R., Jabbour, M., Deleo, A., Ferrone, S., Wang, Y., and Wang, X. (2012). Aldehyde dehydrogenase 1A1 expression in breast cancer is associated with stage, triple negativity, and outcome to neoadjuvant chemotherapy. Mod. Pathol. Augusta *25*, 388–397.

Kiefer, F.W., Orasanu, G., Nallamshetty, S., Brown, J.D., Wang, H., Luger, P., Qi, N.R., Burant, C.F., Duester, G., and Plutzky, J. (2012). Retinaldehyde Dehydrogenase 1 Coordinates Hepatic Gluconeogenesis and Lipid Metabolism. Endocrinology *153*, 3089–3099.

Kim, W.Y., and Sharpless, N.E. (2006). The Regulation of INK4/ARF in Cancer and Aging. Cell *127*, 265–275.

Kleinsmith, L.J., and Pierce, G.B. (1964). Multipotentiality of Single Embryonal Carcinoma Cells. Cancer Res. *24*, 1544–1551.

Kong, J.N., He, Q., Wang, G., Dasgupta, S., Dinkins, M.B., Zhu, G., Kim, A., Spassieva, S., and Bieberich, E. (2015). Guggulsterone and bexarotene induce secretion of exosome-associated breast cancer resistance protein and reduce doxorubicin resistance in MDA-MB-231 cells. Int. J. Cancer J. Int. Cancer *137*, 1610–1620.

Konopleva, M., Zhao, S., Hu, W., Jiang, S., Snell, V., Weidner, D., Jackson, C.E., Zhang, X., Champlin, R., Estey, E., et al. (2002). The anti-apoptotic genes Bcl-XL and Bcl-2 are over-expressed and contribute to chemoresistance of non-proliferating leukaemic CD34+ cells. Br. J. Haematol. *118*, 521–534.

Krause, D.S., Theise, N.D., Collector, M.I., Henegariu, O., Hwang, S., Gardner, R., Neutzel, S., and Sharkis, S.J. (2001). Multi-organ, multi-lineage engraftment by a single bone marrow-derived stem cell. Cell *105*, 369–377.

Kricker, A., Høyer, A.P., McCredie, M., and Porter, L.A. (1995). Breast cancer in NSW women: a shift in tumour size. Med. J. Aust. *163*, 79–81.

Kumar, P., and Aggarwal, R. (2016). An overview of triple-negative breast cancer. Arch. Gynecol. Obstet. *293*, 247–269.

Lam, S.H., Chua, H.L., Gong, Z., Lam, T.J., and Sin, Y.M. (2004). Development and maturation of the immune system in zebrafish, Danio rerio: a gene expression profiling, in situ hybridization and immunological study. Dev. Comp. Immunol. *28*, 9–28.

Lang, I., Brodowicz, T., Ryvo, L., Kahan, Z., Greil, R., Beslija, S., Stemmer, S.M., Kaufman, B., Zvirbule, Z., Steger, G.G., et al. (2013). Bevacizumab plus paclitaxel versus bevacizumab plus capecitabine as first-line treatment for HER2-negative metastatic breast cancer: interim efficacy results of the randomised, open-label, non-inferiority, phase 3 TURANDOT trial. Lancet Oncol. *14*, 125–133.

Lee, Y.-H., Petkova, A.P., Mottillo, E.P., and Granneman, J.G. (2012). In Vivo Identification of Bipotential Adipocyte Progenitors Recruited by β3-Adrenoceptor Activation and High-Fat Feeding. Cell Metab. *15*, 480–491.

Lenormand, J.-L., Dellinger, R.W., Knudsen, K.E., Subramani, S., and Donoghue, D.J. (1999). Speedy: a novel cell cycle regulator of the G2/M transition. EMBO J. *18*, 1869–1877.

Li, X., Lewis, M.T., Huang, J., Gutierrez, C., Osborne, C.K., Wu, M.-F., Hilsenbeck, S.G., Pavlick, A., Zhang, X., Chamness, G.C., et al. (2008). Intrinsic Resistance of Tumorigenic Breast Cancer Cells to Chemotherapy. J. Natl. Cancer Inst. *100*, 672–679.

Liedtke, C., Mazouni, C., Hess, K.R., André, F., Tordai, A., Mejia, J.A., Symmans, W.F., Gonzalez-Angulo, A.M., Hennessy, B., Green, M., et al. (2008). Response to neoadjuvant therapy and long-term survival in patients with triple-negative breast cancer. J. Clin. Oncol. Off. J. Am. Soc. Clin. Oncol. *26*, 1275–1281.

Lieschke, G.J., and Currie, P.D. (2007). Animal models of human disease: zebrafish swim into view. Nat. Rev. Genet. *8*, 353–367.

Lin, Y., Zhong, Y., Guan, H., Zhang, X., and Sun, Q. (2012). CD44+/CD24- phenotype contributes to malignant relapse following surgical resection and chemotherapy in patients with invasive ductal carcinoma. J. Exp. Clin. Cancer Res. *31*, 59.

Liu, S., Dontu, G., and Wicha, M.S. (2005). Mammary stem cells, self-renewal pathways, and carcinogenesis. Breast Cancer Res. *7*, 86–95.

Liu, X., Feng, D., Liu, D., Wang, S., Yu, X., Dai, E., Wang, J., Wang, L., and Jiang, W. (2016). Dissecting the Origin of Breast Cancer Subtype Stem Cell and the Potential Mechanism of Malignant Transformation. PLoS ONE *11*, 1–16.

Liu, Y., Lv, D., Duan, J., Xu, S., Zhang, J., Yang, X., Zhang, X., Cui, Y., Bian, X., and Yu, S. (2014). ALDH1A1 expression correlates with clinicopathologic features and poor prognosis of breast cancer patients: a systematic review and meta-analysis. BMC Cancer *14*, 444.

Louis, S.A., Rietze, R.L., Deleyrolle, L., Wagey, R.E., Thomas, T.E., Eaves, A.C., and Reynolds, B.A. (2008). Enumeration of neural stem and progenitor cells in the neural colony-forming cell assay. Stem Cells Dayt. Ohio *26*, 988–996.

Lubanska, D., and Porter, L. (2017). Revisiting CDK Inhibitors for Treatment of Glioblastoma Multiforme. Drugs RD *17*, 255–263.

Lubanska, D., Market-Velker, B.A., deCarvalho, A.C., Mikkelsen, T., Fidalgo da Silva, E., and Porter, L.A. (2014). The cyclin-like protein Spy1 regulates growth and division characteristics of the CD133+ population in human glioma. Cancer Cell *25*, 64–76.

Lumachi, F., Brunello, A., Maruzzo, M., Basso, U., and Basso, S.M.M. (2013). Treatment of estrogen receptor-positive breast cancer. Curr. Med. Chem. *20*, 596–604.

Mackey, J.R., Martin, M., Pienkowski, T., Rolski, J., Guastalla, J.-P., Sami, A., Glaspy, J., Juhos, E., Wardley, A., Fornander, T., et al. (2013). Adjuvant docetaxel, doxorubicin, and cyclophosphamide in node-positive breast cancer: 10-year follow-up of the phase 3 randomised BCIRG 001 trial. Lancet Oncol. *14*, 72–80.

Madjd, Z., Zare Mehrjerdi, A., Sharifi, A.M., Molanaei, S., Shahzadi, S.Z., and Asadi-Lari, M. (2009). CD44+ cancer cells express higher levels of the anti-apoptotic protein Bcl-2 in breast tumours. Cancer Immun. J. Acad. Cancer Immunol. *9*.

Magni, M., Shammah, S., Schiro, R., Mellado, W., Dalla-Favera, R., and Gianni, A.M. (1996). Induction of cyclophosphamide-resistance by aldehyde-dehydrogenase gene transfer. Blood *87*, 1097–1103.

Malhotra, G.K., Zhao, X., Band, H., and Band, V. (2010). Histological, molecular and functional subtypes of breast cancers. Cancer Biol. Ther. *10*, 955–960.

Malumbres, M., and Barbacid, M. (2009). Cell cycle, CDKs and cancer: a changing paradigm. Nat. Rev. Cancer *9*, 153–166.

Mamounas, E.P., Bryant, J., Lembersky, B., Fehrenbacher, L., Sedlacek, S.M., Fisher, B., Wickerham, D.L., Yothers, G., Soran, A., and Wolmark, N. (2005). Paclitaxel After

Doxorubicin Plus Cyclophosphamide As Adjuvant Chemotherapy for Node-Positive Breast Cancer: Results From NSABP B-28. J. Clin. Oncol. *23*, 3686–3696.

Manolitsas, T.P., Englefield, P., Eccles, D.M., and Campbell, I.G. (1997). No association of a 306-bp insertion polymorphism in the progesterone receptor gene with ovarian and breast cancer. Br. J. Cancer *75*, 1398–1399.

Marcato, P., Dean, C.A., Pan, D., Araslanova, R., Gillis, M., Joshi, M., Helyer, L., Pan, L., Leidal, A., Gujar, S., et al. (2011a). Aldehyde Dehydrogenase Activity of Breast Cancer Stem Cells Is Primarily Due To Isoform ALDH1A3 and Its Expression Is Predictive of Metastasis. STEM CELLS *29*, 32–45.

Marcato, P., Dean, C.A., Giacomantonio, C.A., and Lee, P.W.K. (2011b). Aldehyde dehydrogenase: Its role as a cancer stem cell marker comes down to the specific isoform. Cell Cycle *10*, 1378–1384.

Marchitti, S.A., Brocker, C., Stagos, D., and Vasiliou, V. (2008). Non-P450 aldehyde oxidizing enzymes: the aldehyde dehydrogenase superfamily. Expert Opin. Drug Metab. Toxicol. *4*, 697–720.

Matsui, W., Huff, C.A., Wang, Q., Malehorn, M.T., Barber, J., Tanhehco, Y., Smith, B.D., Civin, C.I., and Jones, R.J. (2004). Characterization of clonogenic multiple myeloma cells. Blood *103*, 2332–2336.

McDermott, S.P., and Wicha, M.S. (2010). Targeting breast cancer stem cells. Mol. Oncol. *4*, 404–419.

McDonald, E.R., and El-Deiry, W.S. (2000). Cell cycle control as a basis for cancer drug development (Review). Int. J. Oncol. *16*, 871–957.

Migliaccio, A., Piccolo, D., Castoria, G., Di Domenico, M., Bilancio, A., Lombardi, M., Gong, W., Beato, M., and Auricchio, F. (1998). Activation of the Src/p21ras/Erk pathway by progesterone receptor via cross-talk with estrogen receptor. EMBO J. *17*, 2008–2018.

Miller, K., Wang, M., Gralow, J., Dickler, M., Cobleigh, M., Perez, E.A., Shenkier, T., Cella, D., and Davidson, N.E. (2007). Paclitaxel plus bevacizumab versus paclitaxel alone for metastatic breast cancer. N. Engl. J. Med. *357*, 2666–2676.

Minotti, G., Menna, P., Salvatorelli, E., Cairo, G., and Gianni, L. (2004). Anthracyclines: molecular advances and pharmacologic developments in antitumor activity and cardiotoxicity. Pharmacol. Rev. *56*, 185–229.

Moreb, J.S., Gabr, A., Vartikar, G.R., Gowda, S., Zucali, J.R., and Mohuczy, D. (2005). Retinoic Acid Down-Regulates Aldehyde Dehydrogenase and Increases Cytotoxicity of 4-Hydroperoxycyclophosphamide and Acetaldehyde. J. Pharmacol. Exp. Ther. *312*, 339–345.

Moreb, J.S., Baker, H.V., Chang, L.-J., Amaya, M., Lopez, M.C., Ostmark, B., and Chou, W. (2008). ALDH isozymes downregulation affects cell growth, cell motility and gene expression in lung cancer cells. Mol. Cancer *7*, 87.

Morgan, C.A., Parajuli, B., Buchman, C.D., Dria, K., and Hurley, T.D. (2015). N,N-diethylaminobenzaldehyde (DEAB) as a substrate and mechanism-based inhibitor for human ALDH isoenzymes. Chem. Biol. Interact. *234*, 18–28.

Morimoto, K., Kim, S.J., Tanei, T., Shimazu, K., Tanji, Y., Taguchi, T., Tamaki, Y., Terada, N., and Noguchi, S. (2009). Stem cell marker aldehyde dehydrogenase 1-positive breast cancers are characterized by negative estrogen receptor, positive human epidermal growth factor receptor type 2, and high Ki67 expression. Cancer Sci. *100*, 1062–1068.

Morrison, S.J., and Kimble, J. (2006). Asymmetric and symmetric stem-cell divisions in development and cancer. Nature *441*, 1068–1074.

Nebreda, A.R. (2006). CDK activation by non-cyclin proteins. Curr. Opin. Cell Biol. *18*, 192–198.

Neumeister, V., Agarwal, S., Bordeaux, J., Camp, R.L., and Rimm, D.L. (2010). In Situ Identification of Putative Cancer Stem Cells by Multiplexing ALDH1, CD44, and Cytokeratin Identifies Breast Cancer Patients with Poor Prognosis. Am. J. Pathol. *176*, 2131–2138.

Neve, R.M., Chin, K., Fridlyand, J., Yeh, J., Baehner, F.L., Fevr, T., Clark, L., Bayani, N., Coppe, J.-P., Tong, F., et al. (2006). A collection of breast cancer cell lines for the study of functionally distinct cancer subtypes. Cancer Cell *10*, 515–527.

Neville, M.C., Medina, D., Monks, J., and Hovey, R.C. (1998). The Mammary Fat Pad. J. Mammary Gland Biol. Neoplasia *3*, 109–116.

Nguyen, A., Yoshida, M., Goodarzi, H., and Tavazoie, S.F. (2016). Highly variable cancer subpopulations that exhibit enhanced transcriptome variability and metastatic fitness. Nat. Commun. *7*, 11246.

Nie, S., McDermott, S.P., Deol, Y., Tan, Z., Wicha, M.S., and Lubman, D.M. (2015). A quantitative proteomics analysis of MCF7 breast cancer stem and progenitor cell populations. PROTEOMICS *15*, 3772–3783.

Noble, M.E., Endicott, J.A., Brown, N.R., and Johnson, L.N. (1997). The cyclin box fold: protein recognition in cell-cycle and transcription control. Trends Biochem. Sci. *22*, 482–487.

Nurse, P.M. (2002). Nobel Lecture. Cyclin dependent kinases and cell cycle control. Biosci. Rep. *22*, 487–499.

O'Brien, C.A., Kreso, A., and Dick, J.E. (2009). Cancer Stem Cells in Solid Tumors: An Overview. Semin. Radiat. Oncol. *19*, 71–77.

Ohtsubo, M., Theodoras, A.M., Schumacher, J., Roberts, J.M., and Pagano, M. (1995). Human cyclin E, a nuclear protein essential for the G1-to-S phase transition. Mol. Cell. Biol. *15*, 2612–2624.

Paulovich, A.G., and Hartwell, L.H. (1995). A checkpoint regulates the rate of progression through S phase in S. cerevisiae in response to DNA damage. Cell *82*, 841–847.

Perou, C.M., Sørlie, T., Eisen, M.B., Rijn, M. van de, Jeffrey, S.S., Rees, C.A., Pollack, J.R., Ross, D.T., Johnsen, H., Akslen, L.A., et al. (2000). Molecular portraits of human breast tumours. Nature *406*, 747.

Pham, P.V., Phan, N.L., Nguyen, N.T., Truong, N.H., Duong, T.T., Le, D.V., Truong, K.D., and Phan, N.K. (2011). Differentiation of breast cancer stem cells by knockdown of CD44: promising differentiation therapy. J. Transl. Med. *9*, 209.

Phillips, T.M., McBride, W.H., and Pajonk, F. (2006). The Response of CD24 −/low /CD44 + Breast Cancer–Initiating Cells to Radiation. JNCI J. Natl. Cancer Inst. *98*, 1777–1785.

Pines, J., and Hunter, T. (1991). Human cyclins A and B1 are differentially located in the cell and undergo cell cycle-dependent nuclear transport. J. Cell Biol. *115*, 1–17.

Pirker, R., Pereira, J.R., Szczesna, A., von Pawel, J., Krzakowski, M., Ramlau, R., Vynnychenko, I., Park, K., Yu, C.-T., Ganul, V., et al. (2009). Cetuximab plus chemotherapy in patients with advanced non-small-cell lung cancer (FLEX): an open-label randomised phase III trial. Lancet Lond. Engl. *373*, 1525–1531.

Pommier, Y., Leo, E., Zhang, H., and Marchand, C. (2010). DNA topoisomerases and their poisoning by anticancer and antibacterial drugs. Chem. Biol. *17*, 421–433.

Porter, L.A., Dellinger, R.W., Tynan, J.A., Barnes, E.A., Kong, M., Lenormand, J.-L., and Donoghue, D.J. (2002). Human Speedy: a novel cell cycle regulator that enhances proliferation through activation of Cdk2. J. Cell Biol. *157*, 357–366.

Prat, A., Parker, J.S., Karginova, O., Fan, C., Livasy, C., Herschkowitz, J.I., He, X., and Perou, C.M. (2010). Phenotypic and molecular characterization of the claudin-low intrinsic subtype of breast cancer. Breast Cancer Res. BCR *12*, R68.

Prat, A., Ellis, M.J., and Perou, C.M. (2011). Practical implications of gene-expression-based assays for breast oncologists. Nat. Rev. Clin. Oncol. *9*, 48–57.

Prockop, D.J., Gregory, C.A., and Spees, J.L. (2003). One Strategy for Cell and Gene Therapy: Harnessing the Power of Adult Stem Cells to Repair Tissues. Proc. Natl. Acad. Sci. U. S. A. *100*, 11917–11923.

Pruefer, F.G., Lizarraga, F., Maldonado, V., and Melendez-Zajgla, J. (2008). Participation of Omi Htra2 serine-protease activity in the apoptosis induced by cisplatin on SW480 colon cancer cells. J. Chemother. Florence Italy *20*, 348–354.

Raguz, S., and Yagüe, E. (2008). Resistance to chemotherapy: new treatments and novel insights into an old problem. Br. J. Cancer *99*, 387–391.

Resetkova, E., Reis-Filho, J., Jain, R., Mehta, R., Thorat, M., Nakshatri, H., and Badve, S. (2010). Prognostic impact of ALDH1 in breast cancer: a story of stem cells and tumor microenvironment. Breast Cancer Res. Treat. *123*, 97–108.

Rexer, B.N., Zheng, W.L., and Ong, D.E. (2001). Retinoic Acid Biosynthesis by Normal Human Breast Epithelium Is via Aldehyde Dehydrogenase 6, Absent in MCF-7 Cells. Cancer Res. *61*, 7065–7070.

Reya, T., Morrison, S.J., Clarke, M.F., and Weissman, I.L. (2001). Stem cells, cancer, and cancer stem cells. Nature *414*, 105–111.

Reynolds, B.A., and Weiss, S. (1996). Clonal and population analyses demonstrate that an EGF-responsive mammalian embryonic CNS precursor is a stem cell. Dev. Biol. *175*, 1–13.

Ricardo, S., Vieira, A.F., Gerhard, R., Leitão, D., Pinto, R., Cameselle-Teijeiro, J.F., Milanezi, F., Schmitt, F., and Paredes, J. (2011). Breast cancer stem cell markers CD44, CD24 and ALDH1: expression distribution within intrinsic molecular subtype. J. Clin. Pathol. *64*, 937–946.

Rodriguez, S.M., Sarrio, D., Honrado, E., Hardisson, D., Calero, F., Benitez, J., and Palacios, J. (2006). Prognostic significance of basal-like phenotype and fascin expression in node-negative invasive breast carcinomas. Clinc Cancer Res *12*, 1533–1539.

Rojas, M., Xu, J., Woods, C.R., Mora, A.L., and al, et (2005). Bone Marrow-Derived Mesenchymal Stem Cells in Repair of the Injured Lung. Am. J. Respir. Cell Mol. Biol. N. Y. *33*, 145–152.

Rosenberg, B., Vancamp, L., Trosko, J.E., and Mansour, V.H. (1969). Platinum Compounds: a New Class of Potent Antitumour Agents. Nature *222*, 385.

Rouzier, R., Perou, C.M., Symmans, W.F., Ibrahim, N., Cristofanilli, M., Anderson, K., Hess, K.R., Stec, J., Ayers, M., Wagner, P., et al. (2005). Breast cancer molecular subtypes respond differently to preoperative chemotherapy. Clin. Cancer Res. Off. J. Am. Assoc. Cancer Res. *11*, 5678–5685.

Russo, A.A., Jeffrey, P.D., Patten, A.K., Massagué, J., and Pavletich, N.P. (1996). Crystal structure of the p27Kip1 cyclin-dependent-kinase inibitor bound to the cyclin A–Cdk2 complex. Nature *382*, 325.

Sánchez-Muñoz, A., García-Tapiador, A.M., Martínez-Ortega, E., Dueñas-García, R., Jaén-Morago, A., Ortega-Granados, A.L., Fernández-Navarro, M., de la Torre-Cabrera, C., Dueñas, B., Rueda, A.I., et al. (2008). Tumour molecular subtyping according to hormone receptors and HER2 status defines different pathological complete response to neoadjuvant chemotherapy in patients with locally advanced breast cancer. Clin. Transl. Oncol. Off. Publ. Fed. Span. Oncol. Soc. Natl. Cancer Inst. Mex. *10*, 646–653.

Sanz, M.A., and Lo-Coco, F. (2011). Modern Approaches to Treating Acute Promyelocytic Leukemia. J. Clin. Oncol. *29*, 495–503.

Schepers, A.G., Snippert, H.J., Stange, D.E., Born, M. van den, Es, J.H. van, Wetering, M. van de, and Clevers, H. (2012). Lineage Tracing Reveals Lgr5+ Stem Cell Activity in Mouse Intestinal Adenomas. Science *337*, 730–735.

Shackleton, M., Vaillant, F., Simpson, K.J., Stingl, J., Smyth, G.K., Asselin-Labat, M.-L., Wu, L., Lindeman, G.J., and Visvader, J.E. (2006). Generation of a functional mammary gland from a single stem cell. Nature *439*, 84–88.

Sherr, C.J. (1996). Cancer Cell Cycles. Science *274*, 1672–1677.

Sherr, C.J., and Roberts, J.M. (1999). CDK inhibitors: positive and negative regulators of G1-phase progression. Genes Dev. *13*, 1501–1512.

Siddik, Z.H. (2003). Cisplatin: mode of cytotoxic action and molecular basis of resistance. Oncogene *22*, 7265–7279.

Sikov, W.M., Dizon, D.S., Strenger, R., Legare, R.D., Theall, K.P., Graves, T.A., Gass, J.S., Kennedy, T.A., and Fenton, M.A. (2009). Frequent pathologic complete responses in aggressive stages II to III breast cancers with every-4-week carboplatin and weekly paclitaxel with or without trastuzumab: a Brown University Oncology Group Study. J. Clin. Oncol. Off. J. Am. Soc. Clin. Oncol. *27*, 4693–4700.

Simian, M., Hirai, Y., Navre, M., Werb, Z., Lochter, A., and Bissell, M.J. (2001). The interplay of matrix metalloproteinases, morphogens and growth factors is necessary for branching of mammary epithelial cells. Dev. Camb. Engl. *128*, 3117–3131.

Slack, J.M.W. (2008). Origin of Stem Cells in Organogenesis. Science *322*, 1498–1501.

Sleeman, K.E., Kendrick, H., Ashworth, A., Isacke, C.M., and Smalley, M.J. (2006). CD24 staining of mouse mammary gland cells defines luminal epithelial, myoepithelial/basal and non-epithelial cells. Breast Cancer Res. *8*, R7.

Sophos, N.A., and Vasiliou, V. (2003). Aldehyde dehydrogenase gene superfamily: the 2002 update. Chem. Biol. Interact. *143–144*, 5–22.

Sørlie, T., Perou, C.M., Tibshirani, R., Aas, T., Geisler, S., Johnsen, H., Hastie, T., Eisen, M.B., van de Rijn, M., Jeffrey, S.S., et al. (2001). Gene expression patterns of breast

carcinomas distinguish tumor subclasses with clinical implications. Proc. Natl. Acad. Sci. U. S. A. *98*, 10869–10874.

Sotiriou, C., Neo, S.-Y., McShane, L.M., Korn, E.L., Long, P.M., Jazaeri, A., Martiat, P., Fox, S.B., Harris, A.L., and Liu, E.T. (2003). Breast cancer classification and prognosis based on gene expression profiles from a population-based study. Proc. Natl. Acad. Sci. U. S. A. *100*, 10393.

Spangrude, G.J., Heimfeld, S., and Weissman, I.L. (1988). Purification and Characterization of Mouse Hematopoietic Stem Cells. Science *241*, 58–62.

Spector, N.L., Xia, W., Burris, H., Hurwitz, H., Dees, E.C., Dowlati, A., O'Neil, B., Overmoyer, B., Marcom, P.K., Blackwell, K.L., et al. (2005). Study of the biologic effects of lapatinib, a reversible inhibitor of ErbB1 and ErbB2 tyrosine kinases, on tumor growth and survival pathways in patients with advanced malignancies. J. Clin. Oncol. *23*, 2502–2512.

Spike, B.T., Engle, D.D., Lin, J.C., Cheung, S.K., La, J., and Wahl, G.M. (2012). A mammary stem cell population identified and characterized in late embryogenesis reveals similarities to human breast cancer. Cell Stem Cell *10*, 183–197.

Sreerama, L., and Sladek, N.E. (1997). Cellular levels of class 1 and class 3 aldehyde dehydrogenases and certain other drug-metabolizing enzymes in human breast malignancies. Clin. Cancer Res. *3*, 1901–1914.

STEMCELL Technologies (2009). Technical Bulletin: Identification of ALDH-expressing cancer stem cells.

STEMCELL Technologies (2011). Technical Bulletin: ALDEFLUOR Assay Optimization.

Stingl, J., Emerman, J.T., Eaves, C.J., and Kuusk, U. (1998). Phenotypic and functional characterization in vitro of a multipotent epithelial cell present in the normal adult human breast. Differentiation *63*, 201–213.

Stingl, J., Eaves, C.J., Zandieh, I., and Emerman, J.T. (2001). Characterization of bipotent mammary epithelial progenitor cells in normal adult human breast tissue. Breast Cancer Res. Treat. *67*, 93–109.

Stingl, J., Raouf, A., Emerman, J.T., and Eaves, C.J. (2005). Epithelial Progenitors in the Normal Human Mammary Gland. J. Mammary Gland Biol. Neoplasia *10*, 49–59.

Stingl, J., Eirew, P., Ricketson, I., Shackleton, M., Vaillant, F., Choi, D., I Li, H., and J Eaves, C. (2006). Purification and unique properties of mammary epithelial stem cells. Nature *439*, 993–997.

Stockmans, G., Deraedt, K., Wildiers, H., Moerman, P., and Paridaens, R. (2008). Triple-negative breast cancer. Curr. Opin. Oncol. *20*, 614–620.

Storms, R.W., Trujillo, A.P., Springer, J.B., Shah, L., Colvin, O.M., Ludeman, S.M., and Smith, C. (1999). Isolation of primitive human hematopoietic progenitors on the basis of aldehyde dehydrogenase activity. Proc. Natl. Acad. Sci. U. S. A. *96*, 9118–9123.

Sullivan, J.P., Spinola, M., Dodge, M., Raso, M.G., Behrens, C., Gao, B., Schuster, K., Shao, C., Larsen, J.E., Sullivan, L.A., et al. (2010). Aldehyde dehydrogenase activity selects for lung adenocarcinoma stem cells dependent on Notch signaling. Cancer Res. *70*, 9937–9948.

Thiagarajan, P.S., Hitomi, M., Hale, J.S., Alvarado, A.G., Otvos, B., Sinyuk, M., Stoltz, K., Wiechert, A., Mulkearns-Hubert, E., Jarrar, A.M., et al. (2015). Development of a Fluorescent Reporter System to Delineate Cancer Stem Cells in Triple-Negative Breast Cancer. STEM CELLS *33*, 2114–2125.

Townsend, D.M., and Tew, K.D. (2003). The role of glutathione-S-transferase in anti-cancer drug resistance. Oncogene *22*, 7369–7375.

Tu, S.M., Lin, S.H., and Logothetis, C.J. (2002). Stem-cell origin of metastasis and heterogeneity in solid tumours. Lancet Oncol. *3*, 508–513.

Tutt, A., Bertwistle, D., Valentine, J., Gabriel, A., Swift, S., Ross, G., Griffin, C., Thacker, J., and Ashworth, A. (2001). Mutation in Brca2 stimulates error-prone homology-directed repair of DNA double-strand breaks occurring between repeated sequences. EMBO J. *20*, 4704–4716.

Veinotte, C.J., Dellaire, G., and Berman, J.N. (2014). Hooking the big one: the potential of zebrafish xenotransplantation to reform cancer drug screening in the genomic era. Dis. Model. Mech. *7*, 745–754.

Verrier, F., Deniaud, A., LeBras, M., Métivier, D., Kroemer, G., Mignotte, B., Jan, G., and Brenner, C. (2004). Dynamic evolution of the adenine nucleotide translocase interactome during chemotherapy-induced apoptosis. Oncogene *23*, 8049–8064.

Vilella, A.J., Severin, J., Ureta-Vidal, A., Heng, L., Durbin, R., and Birney, E. (2009). EnsemblCompara GeneTrees: Complete, duplication-aware phylogenetic trees in vertebrates. Genome Res. *19*, 327–335.

Villadsen, R., Fridriksdottir, A.J., Rønnov-Jessen, L., Gudjonsson, T., Rank, F., LaBarge, M.A., Bissell, M.J., and Petersen, O.W. (2007). Evidence for a stem cell hierarchy in the adult human breast. J. Cell Biol. *177*, 87–101.

Visvader, J.E. (2009). Keeping abreast of the mammary epithelial hierarchy and breast tumorigenesis. Genes Dev. *23*, 2563–2577.

Visvader, J.E., and Lindeman, G.J. (2006). Mammary Stem Cells and Mammopoiesis. Cancer Res. *66*, 9798–9801.

Visvader, J.E., and Stingl, J. (2014). Mammary stem cells and the differentiation hierarchy: current status and perspectives. Genes Dev. *28*, 1143–1158.

Walker, D.H., and Maller, J.L. (1991). Role for cyclin A in the dependence of mitosis on completion of DMA replication. Nature *354*, 314.

Wang, D., and Lippard, S.J. (2005). Cellular processing of platinum anticancer drugs. Nat. Rev. Drug Discov. *4*, 307–320.

Wang, R., Lv, Q., Meng, W., Tan, Q., Zhang, S., Mo, X., and Yang, X. (2014). Comparison of mammosphere formation from breast cancer cell lines and primary breast tumors. J. Thorac. Dis. *6*, 829.

Weiss, R.B. (1992). The anthracyclines: will we ever find a better doxorubicin? Semin. Oncol. *19*, 670–686.

Weiss, S., Reynolds, B.A., Vescovi, A.L., Morshead, C., Craig, C.G., and van der Kooy, D. (1996). Is there a neural stem cell in the mammalian forebrain? Trends Neurosci. *19*, 387–393.

Welm, B.E., Dijkgraaf, G.J.P., Bledau, A.S., Welm, A.L., and Werb, Z. (2008). Lentiviral transduction of mammary stem cells for analysis of gene function during development and cancer. Cell Stem Cell *2*, 90–102.

White, D.T., Eroglu, A.U., Wang, G., Zhang, L., Sengupta, S., Ding, D., Rajpurohit, S.K., Walker, S.L., Ji, H., Qian, J., et al. (2016). ARQiv-HTS, a versatile whole-organism screening platform enabling in vivo drug discovery at high-throughput rates. Nat. Protoc. *11*, 2432.

White, R., Rose, K., and Zon, L. (2013). Zebrafish cancer: the state of the art and the path forward. Nat. Rev. Cancer *13*, 624–636.

Wicha, M.S., Liu, S., and Dontu, G. (2006). Cancer Stem Cells: An Old Idea—A Paradigm Shift. Cancer Res. *66*, 1883–1890.

Wickström, M., Danielsson, K., Rickardson, L., Gullbo, J., Nygren, P., Isaksson, A., Larsson, R., and Lövborg, H. (2007). Pharmacological profiling of disulfiram using human tumor cell lines and human tumor cells from patients. Biochem. Pharmacol. *73*, 25–33.

Willett, C.E., Cortes, A., Zuasti, A., and Zapata, A.G. (1999). Early hematopoiesis and developing lymphoid organs in the zebrafish. Dev. Dyn. Off. Publ. Am. Assoc. Anat. *214*, 323–336.

Wu, D., Mou, Y.-P., Chen, K., Cai, J.-Q., Zhou, Y.-C., Pan, Y., Xu, X.-W., Zhou, W., Gao, J.-Q., Chen, D.-W., et al. (2016). Aldehyde dehydrogenase 3A1 is robustly upregulated in gastric cancer stem-like cells and associated with tumorigenesis. Int. J. Oncol. *49*, 611–622.

Yardley, D.A., Arrowsmith, E.R., Daniel, B.R., Eakle, J., Brufsky, A., Drosick, D.R., Kudrik, F., Bosserman, L.D., Keaton, M.R., Goble, S.A., et al. (2017). TITAN: phase III study of doxorubicin/cyclophosphamide followed by ixabepilone or paclitaxel in early-stage triple-negative breast cancer. Breast Cancer Res. Treat. *164*, 649–658.

Yui, J., Chiu, C.-P., and Lansdorp, P.M. (1998). Telomerase Activity in Candidate Stem Cells From Fetal Liver and Adult Bone Marrow. Blood *91*, 3255–3262.

Zhang, M., Behbod, F., Atkinson, R.L., Landis, M.D., Kittrell, F., Edwards, D., Medina, D., Tsimelzon, A., Hilsenbeck, S., Green, J.E., et al. (2008). Identification of Tumor-initiating Cells in a p53 Null Mouse Model of Breast Cancer. Cancer Res. *68*, 4674–4682.

Zhong, Y., Shen, S., Zhou, Y., Mao, F., Guan, J., Lin, Y., Xu, Y., and Sun, Q. (2014). ALDH1 is a better clinical indicator for relapse of invasive ductal breast cancer than the CD44+/CD24− phenotype. Med. Oncol. *31*, 1–8.

Zhou, L., Jiang, Y., Yan, T., Di, G., Shen, Z., Shao, Z., and Lu, J. (2010). The prognostic role of cancer stem cells in breast cancer: a meta-analysis of published literatures. Breast Cancer Res. Treat. *122*, 795–801.

Zielske, S.P., Spalding, A.C., Wicha, M.S., and Lawrence, T.S. (2011). Ablation of Breast Cancer Stem Cells with Radiation. Transl. Oncol. *4*, 227–233.

APPENDIX A

Dear Sir/Madam,

Please accept this letter as my authorization for Ms. Ellen Laurie to use the work I conducted in Figures 2 and 3 in her thesis. My contribution to her figures include optimization of drug screening platforms in figure 2, provision of key ideas, *in vivo* drug screening platforms, experimental design, technical assays, and data collection in figure 3. Please do not hesitate to contact me if you require further clarification.

Sincerely,

Rosa-Maria Ferraiuolo, PhD
University of Windsor

APPENDIX B

Dear Sir/Madam,

Please accept this letter as my authorization for Ms. Ellen Laurie to use the work I conducted in Figure 3 in her thesis. My contribution to her figures include technical assays in figure 3. Please do not hesitate to contact me if you require further clarification.

Sincerely,

Annie Semaan
University of Windsor

VITA AUCTORIS

NAME:	Ellen M. Laurie
PLACE OF BIRTH:	Windsor, ON
YEAR OF BIRTH:	1992
EDUCATION:	F.J. Brennan Catholic High School, Windsor, ON, 2010
	University of Windsor, B.Sc., Windsor, ON, 2014